UNIVERSIDADE FEDERAL DE MINAS GERAIS
FACULDADE DE MEDICINA
PROGRAMA DE PÓS-GRADUAÇÃO EM PATOLOGIA

MILENE PEREIRA MOREIRA

ANÁLISE DA HETEROGENEIDADE CELULAR ESTRUTURAL E ULTRAESTRUTURAL, IMUNOFENOTIPAGEM E VIA DE SINALIZAÇÃO *EGFR* EM SUBPOPULAÇÕES DE CÉLULAS-TRONCO DE LINHAGENS DE CÂNCER DE MAMA TRIPLO- NEGATIVO E SUAS IMPLICAÇÕES NO MECANISMO DE RESISTÊNCIA QUIMIOTERÁPICA

Belo Horizonte
2018

UNIVERSIDADE FEDERAL DE MINAS GERAIS
FACULDADE DE MEDICINA
PROGRAMA DE PÓS-GRADUAÇÃO EM PATOLOGIA

MILENE PEREIRA MOREIRA

TESE DE DOUTORADO

ANÁLISE DA HETEROGENEIDADE CELULAR ESTRUTURAL ULTRAESTRUTURAL, IMUNOFENOTIPAGEM E VIA DE SINALIZAÇÃO *EGFR* EM SUBPOPULAÇÕES DE CÉLULAS-TRONCO DE LINHAGENS DE CÂNCER DE MAMA TRIPLO-NEGATIVO E SUAS IMPLICAÇÕES NO MECANISMO DE RESISTÊNCIA QUIMIOTERÁPICA

Belo Horizonte
2018

MILENE PEREIRA MOREIRA

ANÁLISE DA HETEROGENEIDADE CELULAR ESTRUTURAL E ULTRAESTRUTURAL, IMUNOFENOTIPAGEM E VIA DE SINALIZAÇÃO *EGFR* EM SUBPOPULAÇÕES DE CÉLULAS-TRONCO DE LINHAGENS DE CÂNCER DE MAMA TRIPLO NEGATIVO E SUAS IMPLICAÇÕES NO MECANISMO DE RESISTÊNCIA QUIMIOTERÁPICA

Tese apresentada ao Programa de Pós-Graduação em Patologia da Faculdade de Medicina da Universidade Federal de Minas Gerais como parte dos requisitos para a obtenção do título de Doutor.

Área de concentração: Patologia Investigativa.

Orientadora
Dra. Luciana Maria Silva
Coorientadores
Dra. Letícia da Conceição Braga
Dr. Geovanni Dantas Cassali

Belo Horizonte

2018

M838a

Moreira, Milene Pereira.
Análise da heterogeneidade celular estrutural e ultraestrutural, imunofenotipagem e via de sinalização EGFR em subpopulações de células-tronco de linhagens de câncer de mama triplo-negativo e suas implicações no mecanismo de resistência quimioterápica [manuscrito]. / Milene Pereira Moreira. - - Belo Horizonte: 2018.
123f.: il.
Orientador (a): Luciana Maria Silva.
Coorientador (a): Letícia da Conceição Braga
Área de concentração: Patologia Investigativa.
Tese (doutorado): Universidade Federal de Minas Gerais, Faculdade de Medicina.

1. Neoplasias da Mama. 2. Células-Tronco Neoplásicas. 3. Heterogeneidade Genética. 4. Tratamento Farmacológico. 5. Resistência a Medicamentos Antineoplásicos. 6. Dissertações Acadêmicas. I. Silva, Luciana Maria. II. Braga, Letícia da Conceição. III. Universidade Federal de Minas Gerais, Faculdade de Medicina. IV. Título.

NLM: QU 477

Bibliotecário responsável: Fabian Rodrigo dos Santos CRB-6/2697

UNIVERSIDADE FEDERAL DE MINAS GERAIS

PROGRAMA DE PÓS-GRADUAÇÃO EM PATOLOGIA

UFMG

FOLHA DE APROVAÇÃO

Análise da heterogeneidade celular estrutural e ultraestrutural, imunofenotipagem e via de sinalização EGFR em subpopulações de células-tronco de linhagens de câncer de mama triplo- negativo e suas implicações no mecanismo de resistência quimioterápica

MILENE PEREIRA MOREIRA

Tese submetida à Banca Examinadora designada pelo Colegiado do Programa de Pós-Graduação em PATOLOGIA, como requisito para obtenção do grau de Doutor em PATOLOGIA, área de concentração PATOLOGIA INVESTIGATIVA.

Aprovada em 26 de fevereiro de 2018, pela banca constituída pelos membros:

Profa. Luciana Maria Silva - Orientador
FUNED

Profa. Leticia da Conceição Braga
FUNED

Prof. Geovanni Dantas Cassali
UFMG

Prof. Enrrico Bloise
UFMG

Profa. Helen Lima Del Puerto
UFMG

Profa. Rosy Iara Maciel de Azambuja
UFSJ

Prof. Rafael Malagoli Rocha
UNIFESP

Belo Horizonte, 26 de fevereiro de 2018.

UNIVERSIDADE FEDERAL DE MINAS GERAIS

PROGRAMA DE PÓS-GRADUAÇÃO EM PATOLOGIA

UFMG

ATA DA DEFESA DE TESE DA ALUNA

MILENE PEREIRA MOREIRA

Realizou-se, no dia 26 de fevereiro de 2018, às 14:00 horas, ICB, da Universidade Federal de Minas Gerais, a defesa de tese, intitulada *Análise da heterogeneidade celular estrutural e ultraestrutural, imunofenotipagem e via de sinalização EGFR em subpopulações de células-tronco de linhagens de câncer de mama triplo- negativo e suas implicações no mecanismo de resistência quimioterápica*, apresentada por MILENE PEREIRA MOREIRA, número de registro 2013709298, graduada no curso de CIÊNCIAS BIOLÓGICAS, como requisito parcial para a obtenção do grau de Doutora em PATOLOGIA, à seguinte Comissão Examinadora: Profa. Luciana Maria Silva - Orientadora (FUNED), Profa. Leticia da Conceição Braga – Coorientadora (FUNED), Prof. Geovanni Dantas Cassali – Coorientador (UFMG), Prof. Enrico Bloise (UFMG), Profa. Helen Lima Del Puerto (UFMG), Profa. Rosy Iara Maciel de Azambuja (UFSJ), Prof. Rafael Malagoli Rocha (UNIFESP).

A Comissão considerou a tese:

☒ Aprovada

( ) Reprovada

Finalizados os trabalhos, lavrei a presente ata que, lida e aprovada, vai assinada por mim e pelos membros da Comissão.

Belo Horizonte, 26 de fevereiro de 2018.

Profa. Luciana Maria Silva (Doutora)

Profa. Letícia da Conceição Braga (Doutora)

Prof. Geovanni Dantas Cassali (Doutor)

Prof. Enrrico Bloise (Doutor)

Profa. Helen Lima Del Puerto (Doutora)

Profa. Rosy Iara Maciel de Azambuja (Doutora)

Prof. Rafael Malagoli Rocha (Doutor)

Dedico este trabalho ao Marcos, meu marido e grande amigo.

AGRADECIMENTOS

Agradeço a Deus por me conceder força e saúde.

Ao Marcos, pelo amor, companheirismo, dedicação, paciência e confiança.

Aos meus pais e minhas irmãs pelo apoio constante e por sempre acreditarem em mim.

A minha orientadora, Dra. Luciana Maria Silva, pela parceria durante todos esses anos. Por todos os ensinamentos, apoio e amizade. Muito obrigada por confiar em mim!

A minha coorientadora, Dra. Letícia da Conceição Braga, um exemplo de dedicação e determinação. Sou muito grata pela sua amizade, apoio, incentivo e aconselhamentos!

Ao meu coorientador, Prof. Geovanni Cassali, pelo apoio dado a minha entrada na Pós-graduação. Obrigada pela confiança e incentivo!

Aos Dr. Fábio André Brayner e Dr. Luiz Carlos Alves do Laboratório de Biologia Celular e Molecular, Centro de Pesquisa Aggeu Magalhães, Fundação Oswaldo Cruz (CPqAM/FIOCRUZ) pela parceria para realização da microscopia eletrônica. Obrigada pelas belíssimas imagens!

Aos meus colegas do Serviço de Biologia Celular (Funed), Rita, Felipe, Nikole, Karen, Paula, Samuel, Fábio, Cristiane Oliveira, Marco, Diego, Diana, Christiane Contigli, André e a todos que passaram pelo SBC ao longo de todos esses anos pela agradável convivência e trocas de experiência. Em especial, ao Bryan por ter cuidado das minhas células na reta final do doutorado.

A Heloísa pela amizade e carinho.

A Aline pela amizade e ajuda sempre que precisei. Que a nossa parceria seja um sucesso!

As minhas ICs Eliza e Izabela por terem me auxiliado na realização dos experimentos.

A Fundação Ezequiel Dias e todos seus funcionários, pesquisadores, bolsistas e estagiários que me ajudaram de alguma forma.

Aos coordenadores, professores e à secretária do programa de Pós-graduação em Patologia.

Este trabalho foi realizado no Serviço de Biologia Celular, Diretoria de Pesquisa e Desenvolvimento da Fundação Ezequiel dias, com o apoio financeiro da Fundação de Amparo à Pesquisa do Estado de Minas Gerais (FAPEMIG/ Edital 01/2012 - Demanda Universal, Processo n° CBB-APQ-00054-12), Coordenação de Aperfeiçoamento de Pessoal de Nível Superior (CAPES) e Conselho Nacional de Desenvolvimento Científico e Tecnológico (CNPq).

RESUMO

O câncer de mama triplo-negativo (TNBC) caracteriza-se por uma alta heterogeneidade molecular e celular, o que influencia na resposta terapêutica e dificulta a descoberta de alvos efetivos. Essa heterogeneidade é atribuída à presença de células-tronco do câncer (CSCs) de mama, o que determina a resistência à quimioterapia, reduzindo a eficácia do tratamento e, subsequente recorrência da doença e metástase. Neste contexto, este trabalho teve como objetivo avaliar a heterogeneidade celular morfológica e fenotípica e a expressão de genes da via de sinalização do *EGFR* em subpopulações celulares obtidas de linhagens de TNBC, bem como suas implicações na resistência à quimioterapia. Para isso as linhagens de câncer de mama BT-549 e Hs 578T e a linhagem de tumor benigno de mama HMT-3522 S1 foram cultivadas em monocamada e em cultura de enriquecimento de CSCs (ensaio de tumoresferas-TS). Em seguida, BT-549 and Hs 578T foram caracterizadas por microscopia de fluorescência e eletrônica e citometria de fluxo. Além disso, as células foram tratadas com paclitaxel (PTX) e doxorrubicina (DOX). Para o estudo de expressão de genes associados à via *EGFR* foi utilizado a BT-549 TS antes e após o tratamento com DOX. Os resultados mostraram que a BT-549 TS após enriquecimento de CSCs, identificada pelo fenótipo $CD44^+/CD24^-$ e $ALDH^+$ apresentou subexpressão da maioria dos genes avaliados (64 genes) e apenas 3 genes foram superexpressos. Entre os genes superexpressos (*MAPK3*, *PRKCZ* e *STAT3)*, *STAT3* apresentou o maior nível de expressão. A análise da BT-549 e Hs 578T demonstrou grande heterogeneidade celular entre as linhagens, bem como entre as subpopulações celulares que as compõem, tanto em termos morfológicos quanto fenotípicos e de resposta a PTX e DOX. Para BT-549, sugere-se que a plasticidade das células tumorais híbridas $CD44^+/CD24^+/CD146^+$, caracterizadas por apresentar um fenótipo mesenquimal e epitelial, e das células tumorais epiteliais $CD44^-/CD24^+/ CD146^+$ originou a CSCs EMT-*like* $CD44^+/CD24^-/CD146^-$, através da conversão fenotípica induzida por transição epitélio-mesenquimal (EMT). Além disso, estas células podem gerar CSCs identificadas como $ALDH^+$ epitelial-*like*. As CSCs podem se autorrenovar e diferenciar em células tumorais ($CD44^-/CD24^-/CD146^-$). Esta plasticidade fenotípica não foi observada para a Hs 578T e HMT-3522S1. Os dados de citotoxicidade mostraram que a BT-549 foi mais resistente ao PTX, o que parece estar associado ao fenótipo $CD24^+$. Em contraste, a BT-549 TS foi extremamente resistente a DOX, devido ao enriquecimento de CSCs ($CD44^+/CD24^-/CD146^-$ e $ALDH^+$). Esses resultados mostram a alta heterogeneidade e plasticidade associada à EMT da BT-549, sendo esta capaz de alterar completamente o fenótipo das subpopulações celulares sob cultura de enriquecimento de CSCs. Esse achado parece desempenhar um papel importante na resistência de TNBC ao tratamento com DOX. Além disso, *STAT3* destacou-se como uma assinatura molecular de TNBC relacionada à resistência a DOX e como possível alvo terapêutico.

Palavras-chave: câncer de mama, célula-tronco do câncer, heterogeneidade celular, quimioterapia, resistência

ABSTRACT

Triple negative breast cancer (TNBC) is characterized by high molecular and cellular heterogeneity, which influences the therapeutic response and it makes difficult the discovery of effective targets. This heterogeneity is attributed to the presence of breast cancer stem cells (BCSCs), which determines resistance to chemotherapy and subsequently disease recurrence and metastasis. In this context, this work aimed to evaluate the morphological and phenotypic cellular heterogeneity and the EGFR signaling pathway gene expression in cell subpopulations obtained from TNBC cell lines, as well as determined their implications in chemotherapy resistance. The BT-549 and Hs 578T TNBC cell lines and HMT-3522 S, a non-malignant breast cell line, were cultured in monolayer and in BCSCs enrichment culture (tumorspheres-TS assay). Furthermore, the BT-549 and Hs578T were characterized by fluorescence and electron microscopy and flow cytometry. In addition, the cell lines cultured in two models were treated with paclitaxel (PTX) and doxorubicin (DOX). BT-549 TS was used to evaluate EGFR-associated gene expression before and after DOX treatment. The results showed that BT-549 TS after BCSCs enrichment, identified by the $CD44^+/CD24^-$ and $ALDH^+$ phenotype, showed subexpression a majority of the evaluated genes (64 genes) and only 3 genes were overexpressed. Among the overexpressed genes (MAPK3, PRKCZ and STAT3), STAT3 had the highest expression level. The BT-549 and Hs 578T analysis demonstrated large morphological and phenotypic heterogeneity between these cell lines, as well as between the cell subpopulations that compose them, as well as in PTX and DOX response. For BT-549, it is suggested that the plasticity of $CD44^+/CD24^+/CD146^+$ hybrid tumor cells, characterized by a mesenchymal and epithelial phenotype, and $CD44^-/CD24^+/CD146^+$ epithelial tumor cells originated $CD44^+/CD24^-/CD146^-$ BCSCs EMT-like, through the phenotypic conversion induced by epithelial-mesenchymal transition (EMT). In addition, these cells could originate BCSCs identified $ALDH^+$ epithelial-like. BCSCs can self-renewal and differentiate into $CD44^-/CD24^-/CD146^-$ tumor cells. Same phenotypic plasticity was not observed for Hs 578T and HMT-3522 S1. Cytotoxicity data showed that BT-549 was more resistant to PTX, which appears to be associated with the $CD24^+$ phenotype. In contrast, BT-549 TS was extremely resistant to DOX probably due to the enrichment of BCSCs ($CD44^+/CD24^-/CD146^-$ and $ALDH^+$ cells). These results showed the high BT-549 EMT-associated heterogeneity and plasticity, being able to completely altered the phenotype of the cellular subpopulations under CSC enrichment culture. This finding appears to play an important role in TNBC resistance to DOX treatment. In addition, STAT3 was highlighted as DOX-resistance related TNBC molecular signature and as a possible therapeutic target.

Keywords: breast cancer, cancer stem cell, cell heterogeneity, chemotherapy, resistance

LISTA DE SIGLAS

ALDH - Aldeído desidrogenase

BCSCs - Células-tronco do câncer de mama

BRCA - Proteína de susceptibilidade ao câncer de mama

CD - Grupamento de diferenciação (*cluster of differentiation*)

cDNA - DNA complementar

CSCs - Células-tronco do câncer

DNA - Ácido Desoxirribonucleico

DOX - Doxorrubicina

EGFR - Receptor do fator de crescimento epidérmico

EMT - Transição epitélio-mesenquimal

EPCAM - Molécula de adesão celular epitelial

ESR1 - Receptor de estrógeno (gene)

ERBB2 - Fator de crescimento epidérmico tipo 2 (gene)

HER-2 - Fator de crescimento epidérmico tipo 2 (proteína)

IARC - Agência Internacional para Pesquisa em Câncer (*International Agency for Research on Cancer*)

IMC - Índice de Massa Corporal

IC - Concentração máxima que inibe 50% do crescimento celular *(Half maximal inhibitory concentration)*

IS - Índice de seletividade

MET - Transição mesenquimal-epitelial

MET - Microscopia eletrônica de transmissão

MEV - Microscopia eletrônica de varredura

PGR - Receptor de progesterona (gene)

PTX - Paclitaxel

QT - Quimioterapia

TNBC - Câncer de mama triplo-negativo (*Triple-negative breast cancer*)

TP53 - Proteína de tumor

TS - Tumoresfera

RNA - Ácido ribonucleico

SERMs - Moduladores seletivos de receptor de estrogênio

STAT3 - Fator de transdutor de sinal e ativador de transcrição 3

WCRF - Fundo Mundial para Pesquisa em Câncer (*World Cancer Research Fund International*)

WHO - Organização Mundial de Saúde (*World Health Organization*)

2D - Bidimensional

3D - Tridimensional

LISTA DE FIGURAS

LISTA DE TABELAS

SUMÁRIO

1 INTRODUÇÃO

O câncer é uma doença genética que se caracteriza por um crescimento celular desordenado que pode invadir tecidos adjacentes e disseminar para outros órgãos do corpo (WHO, 2017). Segundo o proposto por HANAHAN e WEINBERG (2011), a malignização celular se manifesta à medida que oito essenciais habilidades são adquiridas: 1) autossuficiência em sinais proliferativos; 2) escape aos mecanismos inibitórios do crescimento celular; 3) perda de senescência celular; 4) evasão à apoptose; 5) indução da angiogênese; 6) capacidade de invasão e metástase; 7) reprogramação do metabolismo energético; 8) evasão tumoral ao sistema imune (HANAHAN; WEINBERG, 2011).

A Organização Mundial de Saúde (WHO) classifica o câncer no grupo de doenças não transmissíveis ou crônicas juntamente com doenças cardíacas, doenças respiratórias crônicas e diabetes. Esse grupo é responsável por 70% dos casos de morte no mundo por ano (WHO, 2017). O câncer representa a segunda causa de morte no mundo, sendo responsável por 8,8 milhões de mortes em 2015. Os tipos de cânceres mais letais no mundo em 2015, em ordem de frequência, foram pulmão, fígado, colorretal, estômago e mama (WHO, 2018).

No Brasil, as neoplasias malignas constituem a segunda causa de morte, sendo estimados para o biênio 2018/2019, 600 mil novos casos de câncer. Os tipos mais incidentes de câncer serão próstata (31,7%), pulmão (8,7%), intestino (8,1%), estômago (6,3%) e cavidade oral (5,2%) para o sexo masculino e, mama (29,5%), intestino (9,4%), colo do útero (8,1%), pulmão (6,2%) e tireoide (4,0%) para o sexo feminino (INCA, 2018).

O câncer de mama é a neoplasia maligna mais frequente em mulheres em todo o mundo tanto em países em desenvolvimento quanto em países desenvolvidos (SIEGEL et al., 2011). Segundo estatísticas do GLOBOCAN para 2012 cerca de 1,7 milhão de mulheres foram diagnosticadas com câncer de mama naquele ano e 522 mil mulheres morreram em decorrência desta doença (HOWELL et al., 2014), o que representa um aumento na incidência e mortalidade relacionada ao câncer de mama em relação a 2008 (DESANTIS et al., 2013). HORTOBAGYI e colaboradores (2005) estimam que a incidência mundial do câncer de mama feminino atinja cerca de 3,2 milhões de novos casos por ano em 2050 (HORTOBAGYI et al., 2005). Desta forma, a magnitude da incidência do câncer de mama, seu efeito na sociedade mundial e a necessidade de urgência para medidas preventivas e de tratamento destaca esta condição como importante problema de saúde pública (HOWELL et al., 2014).

No Brasil, o câncer de mama está entre os dez tipos de câncer mais incidentes no Brasil, exceto pele não melanoma, sendo esperados 59.700 novos casos (INCA, 2016). Apesar de ser considerado um câncer de relativamente bom prognóstico se diagnosticado e tratado oportunamente, as taxas de mortalidade por câncer de mama continuam elevadas no Brasil (13,68 óbitos a cada 100 mil mulheres em 2015).

1.1 Câncer de mama

O câncer de mama é uma doença genética complexa, caracterizada pelo acúmulo de alterações moleculares múltiplas, tais como: mutações pontuais, amplificações cromossômicas, deleções, rearranjos, translocações e duplicações (VOGELSTEIN et al., 2013). Ele constitui um grupo heterogêneo de neoplasias, constituído por vários tipos histológicos, que diferem nas manifestações clínicas, evolução e resposta terapêutica. Em termos de etiologia e características patológicas, alguns casos apresentam crescimento lento com excelente prognóstico, enquanto que outros casos apresentam um curso clínico altamente agressivo (VERMA et al., 2012). Isso reflete efeitos sobre a sociedade no mundo todo e ressalta a necessidade urgente de medidas preventivas e de tratamento mais eficazes.

Devido à sua etiologia multifatorial, o risco de desenvolver câncer de mama sofre influência de vários aspectos. Um fator de risco proeminente para o início do câncer de mama é a idade. No entanto, fatores ligados ao estilo de vida, fatores reprodutivos, familiares e pessoais, dieta, entre outros (HASHEMI; KARIMI; MAHBOOBI, 2014; HOWELL et al., 2014). O hábito de fumar é sabidamente conhecido como um fator de risco, não apenas para o câncer de mama, mas para a maioria dos tipos de câncer. No que diz respeito ao câncer de mama, vários estudos foram realizados. Em 2012, a *International Agency for Research on Cancer* (IARC) confirmou a associação positiva entre tabagismo e câncer de mama e o relatório de 2014 da *US Surgeron General*, revisou sua declaração de 2004, para reportar um risco estimado de 10% de mulheres com história de tabagismo desenvolver câncer de mama (DIETERICH et al., 2014). Outro fator importante relacionado ao estilo de vida se refere ao consumo de álcool. Segundo recomendação da *World Cancer Research Found* (WCRF) em 2007, um consumo máximo de álcool equivalente a 10 g de etanol por dia reduz o risco de câncer de mama. Contudo, estudos recentes sugerem que o consumo de álcool mesmo abaixo de 10 g de etanol por dia pode estar associado a um risco aumentado de câncer de mama (BAGNARDI et al., 2013). O Índice de Massa Corporal (IMC) acima de 25 kg/m^2 e gordura abdominal estão associados a um risco aumentado de desenvolver câncer de mama pós-menopausa (THOMSON et al., 2014). Inclusive o alto nível socioeconômico

está associado a um risco aumentado de câncer de mama. Vários fatores desempenham um papel nesta associação. Embora, mulheres com alto nível socioeconômico realizem consultas médicas mais frequentes e exames físicos que contribuem para o diagnóstico precoce do câncer de mama, o menor número de gestações e uso de anticoncepcional está associado com o aumento do risco de câncer de mama (HASHEMI; KARIMI; MAHBOOBI, 2014).

Dentre os fatores de risco, os fatores genéticos incluem alterações hereditárias decorrentes de mutações na linhagem germinativa que são responsáveis por cerca de 10-30% dos casos, definindo-se estas situações como "câncer de mama hereditário". Refere-se com um padrão de herança autossômica dominante nas famílias que resulta em uma probabilidade elevada de câncer em mulheres predispostas. O principal fator de risco considerado são mulheres que têm parente de primeiro grau com história de câncer de mama antes dos 40 anos, câncer de ovário, câncer de mama bilateral e câncer de mama masculino. Embora, apenas 5% a 10% dos casos de câncer de mama são identificados com um forte componente hereditário, apenas uma pequena fração desses casos (4% - 5%) é explicada por mutações patogênicas nos genes *BRCA1* (*BReast-CAncer susceptibility gene 1*) e *BRCA2*, transmitidos de forma autossômica dominante com alta penetrância (APOSTOLOU; FOSTIRA, 2013). Ambos os genes são importantes supressores tumorais que contribuem para o reparo do DNA e regulação transcricional em resposta a danos no DNA. Por volta de 70% dos tumores de mama decorrem de mutações somáticas que surgem de maneira esporádica e aleatória como consequência da interação do genoma com o meio. Mutações ou desregulação da expressão de certos genes, tais como *HER2, PIK3CA, TP53, MDM2 e TPRB* e outros desempenham papéis importantes no câncer de mama esporádico, bem como podem desempenhar papéis nas respostas terapêuticas do câncer de mama (DAVIS et al., 2014).

Contudo, durante a última década, as pesquisas sobre o câncer de mama se concentraram em aprofundar os conhecimentos sobre a biologia molecular desta doença. Os avanços tecnológicos, em particular nas abordagens de *high throughput*, tais como sequenciamento de última geração, microarranjos de DNA e hibridização genômica comparativa, permitiram que os pesquisadores investigassem a natureza do câncer de mama. Estes estudos têm revelado que a doença requer a interação de várias vias de sinalização, além do microambiente celular e das características inatas do paciente, que influenciam a patofisiologia da doença, os desfechos clínicos e resposta ao tratamento. Assim, pode-se afirmar que o câncer de mama não é apenas uma doença, mas muitas, e que cada paciente envolve um caso particular em que a medicina personalizada, através da análise simultânea de genes de alta a intermediária penetrância que predispõem à essa doença pode

desempenhar um papel crucial na expectativa e qualidade de vida dos pacientes (DAVIS et al., 2014; EROLES et al., 2012).

1.1.1 Subtipos moleculares do câncer de mama

A classificação do perfil molecular do câncer de mama permitiu sua divisão em subtipos intrínsecos conhecidos como luminal A e B, basal e HER-2 enriquecido (PEROU et al., 2000; SORLIE et al., 2001). Em 2007, HERSCHKOWITZ e colaboradores, identificaram um novo subtipo molecular conhecido como claudina-baixo (HERSCHKOWITZ et al., 2007). A Tabela 1 descreve as principais características de cada subtipo.

Tabela 1- Principais características dos subtipos moleculares do câncer de mama

Subtipos moleculares	**Características**
Luminal A e B	Alta expressão de genes luminais: receptores de estrógeno (*ESR1*), receptores de progesterona (*PGR*) e citoqueratinas 8/18; Ausência de expressão do gene do fator de crescimento epidérmico tipo 2 (*HER-2/ERBB2*); Luminal A - maior expressão de ESR1 em relação ao Luminal B; Luminal B - maior taxa de proliferação celular em relação ao Luminal A; Luminal A e B apresentam incidência de 30,6% e 18,2, respectivamente.
HER-2 enriquecido	Superexpressão do gene *HER-2*/*ERBB2*; Expressão intermediária de genes luminais (*ESR1* e *PGR*); Expressão baixa de genes basais (citoqueratina 5) Incidência de 10,3%.
Basal	Alta expressão de genes basais (citoqueratinas 5, 6, e 17 e, laminina); Expressão intermediária de genes relacionados à *HER-2/ERBB2*; Muito baixa/ausência de expressão de genes luminais; Incidência de 32,7%.
Claudina-baixo	Baixa/ausência expressão de genes epiteliais (E-caderina e claudinas 3, 4 e 7) e luminais (CD24 e EPCAM); Baixa expressão do gene *HER-2/ERBB2;* Alta expressão de genes mesenquimais (vimentina), genes relacionados a células-tronco e resposta imune; Baixa taxa de proliferação celular; Incidência de 7-14%.

Fonte: (HERSCHKOWITZ et al., 2007; PEROU et al., 2000; PRAT et al., 2010a, 2015; SORLIE et al., 2001)

O subtipo luminal, de forma geral, apresenta melhor prognóstico quando comparado aos demais subtipos (PRAT et al., 2015). SORLIE e colaboradores (2001;2003) demonstraram que o subtipo luminal A possui a maior sobrevida livre de doença e sobrevida global, enquanto o subtipo basal e HER-2 enriquecido (sem terapia anti-HER-2) apresentam a menor sobrevida (SORLIE et al., 2001, 2003). Além disso, o subtipo Luminal apresenta a menor incidência de mutação do gene *TP53* em relação aos demais subtipos. Adicionalmente, tumores basais apresentam mutações no gene *BRCA1* (PRAT et al., 2015; SORLIE et al., 2001, 2003).

Embora exista essa classificação molecular, na prática clínica o câncer de mama tem sido estratificado em apenas três grupos baseado na expressão proteica dos receptores hormonais estrógeno (RE), progesterona (RP) e o receptor do fator de crescimento epidérmico humano tipo 2 (HER-2) denominados RE/RP positivo, HER-2 positivo e triplo-negativo (ALLRED, 2010). O termo triplo-negativo é frequentemente usado como sinônimo do subtipo basal. Entretanto, o subtipo basal é caracterizado por certas características que incluem o fenótipo triplo-negativo, porém eles não são sinônimos (BOSCH et al., 2010)(BOSCH et al., 2010).

Os RE/RP e HER-2 possuem valor prognóstico/preditivo validado para uso clínico rotineiro no tratamento das pacientes com câncer de mama. Os fatores prognósticos definidos por características clínicas, patológicas e biológicas que permitem prever a evolução clínica da doença ou sobrevida das pacientes no momento do diagnóstico. Em contraste, fatores preditivos são utilizados para estimar a probabilidade de resposta a um tipo particular de terapia adjuvante (ALLRED, 2010). A expressão de receptores hormonais é indicador de terapia hormonal (hormonioterapia), como opção terapêutica adicional a quimioterapia, melhorando a sobrevida das pacientes (PAYNE et al., 2008). A hormonioterapia visa bloquear a ação do estrógeno com o uso de moduladores seletivos de receptor de estrogênio (SERMs), como o tamoxifeno ou impedir sua produção com o uso de inibidores da aromatase (RIGGS; HARTMANN, 2003; SMITH; DOWSETT, 2003). No entanto, pacientes com tumores HER-2-positivo se beneficiam da terapia biológica que impede a ação do receptor com o uso, por exemplo, do anticorpo monoclonal humanizado anti-HER2 (Trastuzumabe/Herceptin®) (SLAMON et al., 2001). Entretanto, para os tumores triplo-negativos não existe uma terapia específica, sendo a única opção de tratamento sistêmico a quimioterapia (QT) (DE LAURENTIIS et al., 2010)(DE LAURENTIIS et al., 2010). A QT utiliza drogas citotóxicas, que tem como alvo células de rápida divisão celular, capazes de induzir morte celular (LIND, 2011; MALHOTRA; PERRY, 2003).

1.1.2 Quimioterapia

As drogas quimioterápicas amplamente utilizadas no tratamento do câncer de mama em estágio inicial e avançado incluem as antraciclinas (doxorrubicina e epirrubicina) e os taxanos (paclitaxel e docetaxel) (BRAUNSTEIN et al., 2016; COATES et al., 2015). O mecanismo principal de ação das antraciclinas está relacionado à inibição da topoisomerase II, devido à intercalação da droga entre os pares de bases adjacentes do DNA, e geração de espécies de oxigênio reativas resultando em apoptose (GONZALEZ-ANGULO; MORALES-VASQUEZ; HORTOBAGYI, 2007). Os taxanos têm como principal mecanismo de ação inibição da mitose (SYMMANS et al., 2000), pois se ligam aos microtúbulos estabilizando-os promovendo a parada do ciclo celular na fase G2/M e levando, consequentemente, a célula a apoptose (HORWITZ 1992; ROWINSKY e DONEHOWER, 1995).

Paclitaxel (Taxol®/PTX), um dos mais importantes quimioterápicos, foi originalmente identificado em 1971 na planta *Taxus brevifolia* por Wani e colaboradores. PTX possui ação antimitótica através da sua interação com os microtúbulos das células (WEAVER, 2014). Os microtúbulos são formados por estruturas proteicas compostas por dímeros de α-tubulina e β-tubulina polimerizadas formando os protofilamentos. Os filamentos de tubulinas são instáveis, por isso, estão em constante polimerização/despolimerização de suas extremidades (CHIEN et al. 2008). Eles estão envolvidos em uma variedade de funções celulares, como na manutenção da morfologia celular, na motilidade celular, no transporte intracelular de substâncias e no deslocamento de cromossomos durante a divisão celular (CHIEN et al. 2008). O PTX se liga reversivelmente aos microtúbulos estabilizando as tubulinas alterando, assim o balanço polimerização/despolimerização destas estruturas. Como consequência, a proliferação celular é inibida, conduzindo a uma parada do ciclo celular na transição metáfase/anáfase e potencialmente a morte celular por apoptose.

Além de induzir a parada do ciclo celular, PTX também atua sobre membros antiapoptóticos da subfamília BCL-2 (BCL-2, BCL-XL, BCL-W, MCL1 e BFL1/A1) que atuam prevenindo a liberação de citocromo *c* pela mitocôndria. PTX induz a fosforilação de BCL-2 com consequente diminuição dos heterodímeros BCL-2/BAX, com isso a ativação de BAX e BAK resulta em sua homo-oligomerização com a membrana externa da mitocôndria e subsequente liberação de proteínas pró-apoptóticas que induzem a ativação da caspase 9, favorecendo a morte celular. (SAKAMAKI et al., 2015). Adicionalmente, PTX pode induzir a geração de espécies de oxigênio reativo (ROS) (ALEXANDRE et al., 2006, 2007) contribuindo para potencializar seu papel antitumoral. Há relatos ainda do papel de PTX na inibição da angiogênese tumoral, por afetar tanto as células endoteliais maduras quanto as progenitoras (BELOTTI et al., 1996; MUTA et al., 2009).

Doxorrubicina (Adriamicina®/DOX) foi isolado na década de 70 de uma bactéria do solo, *Streptomyces peucetius* (GUILFOILE; HUTCHINSON, 1991). Um vasto número de mecanismos tem sido proposto para descrever a morte celular desencadeada por DOX, tais como: inibição da toposoimerase II resultando em quebra do DNA por impedir a restauração da quebra da dupla fita durante o mecanismo de replicação (LIU, 1989); formação de adutos de DNA (CUTTS et al., 1996; SWIFT et al., 2006); geração de espécies de oxigênio reativo (ROS) pela redução da quinona a um radical semi-quinona pela NADPH oxidoredutase. Esses radicais reagem com oxigênio formando superóxidos e peróxido de hidrogênio (BERLIN; HASELTINE, 1981; GAJEWSKI et al., 2007; GEWIRTZ, 1999). Além disso, a DOX leva a acúmulo de ferro nas mitocôndrias e aumento dos níveis de ROS (ICHIKAWA et al., 2014); superprodução de ceramida (DELPY et al., 1999; KAWASE et al., 2002; LUCCI et al., 1999), molécula lipídica envolvida na proliferação (SASAKI; HAZEKI; HAZEKI, 1995), diferenciação celular (OKAZAKI et al., 1990; OKAZAKI; BELL; HANNUN, 1989) e apoptose (KOLESNICK; KRÖNKE, 1998). Uma limitação no uso da DOX é a cardiotoxicidade irreversível e potencialmente fatal desenvolvida pelas pacientes após o tratamento (ICHIKAWA et al., 2014; VAVROVA et al., 2013).

Observa-se que muitos tumores apresentam-se intrinsicamente resistentes aos quimioterápicos, sendo este o principal motivo para falha terapêutica (DENG et al., 2017; MALLINI et al., 2014). Aproximadamente 40% das pacientes com câncer de mama apresentam recidiva da doença. Destas, 60-70% desenvolvem metástases (SMALLEY; PIGGOTT; CLARKSON, 2013) culminando na baixa sobrevida das pacientes afetadas. Entre os tipos de câncer de mama, tumores triplo-negativo apresentam-se quimiorresistentes em cerca de 90% dos casos e, a ausência de terapias-alvo, fazem deste um tipo de câncer de mama particularmente agressivo.

1.2 Câncer de mama triplo-negativo

O câncer de mama triplo-negativo (TNBC - *Triple-negative Breast Cancer*) constitui cerca de 10-20% de todos os casos de câncer de mama no mundo (SCHETTINI et al., 2016). Apresentam uma alta incidência em mulheres jovens e exibem maior chance de recidiva e morte dentro de 3-5 anos após o diagnóstico comparado aos outros subtipos de câncer de mama (DENT et al., 2007; LIEDTKE et al., 2008). Um estudo conduzido no Brasil mostra uma incidência de 27% de mulheres com TNBC dentre os tumores de mama e estas apresentaram menor sobrevida em 10 anos quando comparado com pacientes com outros subtipos de câncer de mama (EISENBERG; PINTO; KOIFMAN, 2013).

Como dito anteriormente o câncer de mama pode ser classificado em subtipos distintos de acordo com seu perfil genético e a análise de expressão de genes permitiu a identificação de subgrupos moleculares de TNBC. LEHMANN e colaboradores (2011;2016) identificaram quatro subgrupos de TNBC cada um com características biológicas únicas: Basal caracterizado por alta proliferação celular, sendo subdivido em (1) Basal 1: enriquecido de genes relacionados com reparo ao dano no DNA e (2) Basal 2: enriquecido de genes relacionados à via de fatores de crescimento, (3) Mesenquimal: possui expressão de genes associados a células-tronco e perda de gene de adesão epitelial e (4) receptor de androgênio luminal: regulado por vias hormonais com expressão de receptor andrógeno (receptor hormonal nuclear) (LEHMANN et al., 2016, 2011). Esses subtipos exibem significativas diferenças na resposta ao tratamento quimioterápico baseado em antraciclinas/taxanos, sendo que o subgrupo basal 1 exibe maior sensibilidade após a QT neoadjuvante enquanto o basal 2 e o receptor de androgênio luminal são os que apresentam pior resposta ao tratamento (LEHMANN et al., 2016; MASUDA et al., 2013).

TNBC são um desafio na medicina, pois ainda que apresentem características clínicas e patológicas semelhantes aos demais tipos de câncer de mama, seu prognóstico difere entre as pacientes, sendo umas mais responsivas do que outras (BOSCH et al., 2010). Inicialmente, são sensíveis a QT prévia a cirurgia, no entanto apresentam evolução clínica agressiva culminando em baixa sobrevida das pacientes afetadas (CAREY et al., 2007; DENT et al., 2007; O'REILLY et al., 2015). Neste contexto, o TNBC constitui uma doença heterogênea composta por subgrupos com perfil genético distinto culminando em heterogeneidade tumoral. Esta tem um impacto significativo no sucesso ou falha do tratamento quimioterápico (LEHMANN et al., 2016; PALMA et al., 2015; SMITH et al., 2017).

1.3 Heterogeneidade tumoral

A grande diversidade de subtipos tumorais traduz a variabilidade molecular, histológica e celular observada no câncer (TELLEZ-GABRIEL et al., 2016). A heterogeneidade molecular observada em tumores individuais demonstra que não há uma via de sinalização que seja predominantemente desregulada. Vários substratos envolvidos na regulação das funções celulares de progressão, proliferação, sobrevivência e crescimento celular são fosforilados e sua ativação em cascata promove a carcinogênese (HONG; LEE; NAM, 2015). A heterogeneidade celular tumoral pode ocorrer entre as células presentes em um único tumor (intratumoral) ou entre subtipos tumorais (intertumoral) conferindo as essas células um perfil fenotípico distinto relacionado à morfologia,

proliferação, metabolismo e potencial metastático (TELLEZ-GABRIEL et al., 2016). A Figura 1 ilustra de forma simplificada os modelos de heterogeneidade celular intertumoral e intratumoral.

FIGURA 1 - Modelos de heterogeneidade celular tumoral

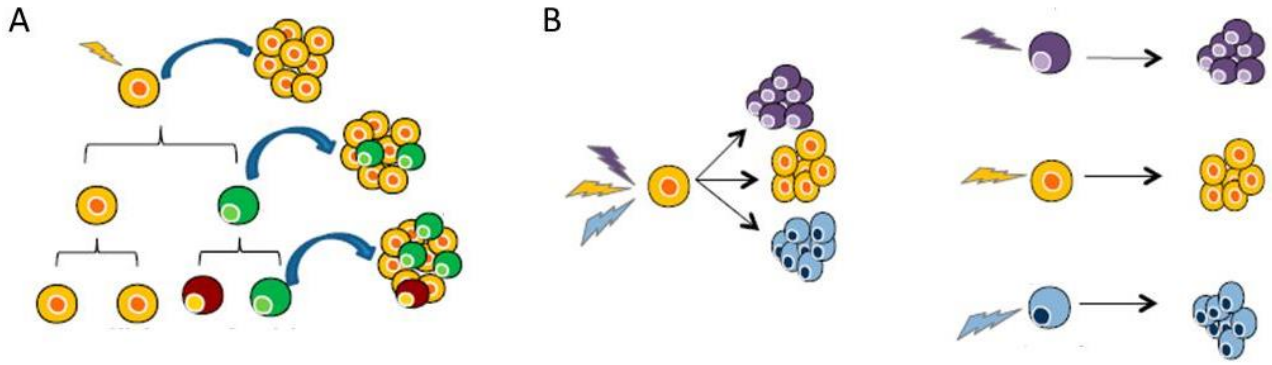

A) Heterogeneidade intratumoral: células tumorais podem sofrer sucessivas mutações genéticas e/ou epigenéticas resultando no desenvolvimento de diferentes subpopulações celulares em um mesmo tumor. B) Heterogeneidade intertumoral: uma célula ou células distintas podem sofrer diferentes mutações genéticas e/ou epigenéticas resultando no desenvolvimento de subtipos tumorais diferentes. Fonte: Adaptado de TELLEZ-GABRIEL et al. (2016).

A heterogeneidade tumoral, por exemplo, retratada na variedade de subgrupos encontrados nos tumores TNBC é um influenciador importante na diferença de resposta terapêutica observada nas pacientes afetadas (BOSCH et al., 2010; TELLEZ-GABRIEL et al., 2016). Além disso, dificulta a identificação de marcadores moleculares necessários para o desenvolvimento de terapias-alvo para esse subtipo de câncer de mama (PALMA et al., 2015). Células tumorais residuais resistentes a QT neoadjuvante estão presentes em 70% dos tumores TNBC (YU et al., 2013). A quimiorresistência apresentada pelos tumores TNBC sugere a existência de uma subpopulação celular inerentemente resistente ao tratamento (LEHMANN et al., 2016), sendo estas responsáveis pela recorrência da doença e desenvolvimento de metástases (CAREY et al., 2007; DENG et al., 2017).

A heterogeneidade celular intratumoral pode ser atribuída à presença de células tumorais com características de células-tronco, conhecidas como células-tronco do câncer (CSCs). A teoria da CSC propõe uma organização hierárquica de células dentro do tumor, onde essa pequena subpopulação celular é responsável por sustentar o crescimento do tumor (VISVADER; LINDEMAN, 2008). Elas podem se originar de células-tronco mutadas ou células adultas diferenciadas que retornam a um estágio indiferenciado através do mecanismo conhecido como transição epitélio-mesenquimal (EMT) (CARNERO et al., 2016; VISVADER, 2011) (Figura 2). As CSCs possuem capacidade de autorrenovação e diferenciação dando origem a novas CSCs e células não-tumorigênicas (não-CSCs) (CLARKE et al., 2006; SCHATTON; FRANK; FRANK, 2010).

FIGURA 2 - Origem das células-tronco do câncer (CSCs)

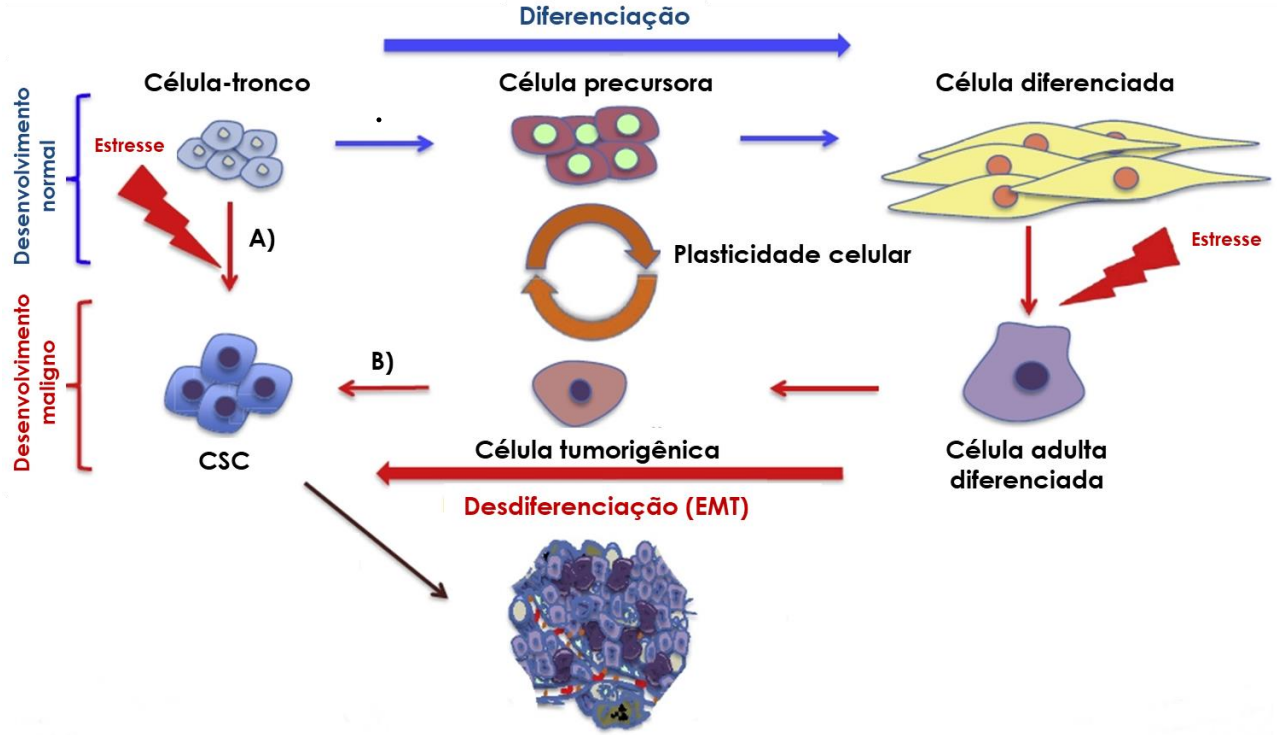

As CSCs podem se originar de: A) Células-tronco que sofrem transformações como resultado de ativação oncogênica, de mutações e/ou influência de fatores extrínsecos (estresse). B) Desdiferenciação (reprogramação ou indução de "*stemness*") a partir de uma célula adulta diferenciada através do processo de transição epitélio-mesenquimal (EMT). Fonte: Adapatado de CARNERO et al. (2016).

CSCs foram identificadas pela primeira vez na década de 1990, na leucemia mielóide aguda e estudos posteriores descreveram a existência de CSC em diversos tipos de tumores malignos incluindo o de mama, endométrio, ovário, pâncreas, próstata, pulmão, cólon e glioblastoma (SAVAGE, 2016).

Devido ao potencial de autorrenovação, as CSCs são, portanto, capazes de regenerar tumores através de um quadro assimétrico de divisão (BU et al. 2013), contribuindo para recidiva de tumores. As CSCs empregam uma série de mecanismos de defesa contra a ação dos agentes quimioterápicos, entre eles: quiescência, uma vez que a terapia citotóxica tem como alvo células de divisão celular rápida; efluxo da droga, através da atividade de transportadores de membrana ABC; capacidade de reparo do dano ao DNA e evasão a apoptose, capacidade de migração e crescimento independente de ancoragem (DONTU et al., 2003; ZHAO, 2016). Assim, a resistência ao tratamento quimioterápico atribuída a presença de CSCs nos tumores acarreta na recorrência da doença, no desenvolvimento de metástases, e consequentemente, em um pior prognóstico da doença (CHARAFE-JAUFFRET et al., 2009; ZHAO, 2016).

1.4 Transição epitélio-mesenquimal

Durante o processo de disseminação celular, as células se desprendem do tumor primário devido à perda de moléculas de adesão epitelial, alteração da polaridade celular, reorganização do citoesqueleto e resistência a *anoikis* (morte celular desencadeada pela interação inapropriada célula/matriz extracelular) (DRASIN; ROBIN; FORD, 2011; LAMOUILLE; XU; DERYNCK, 2014) culminando na migração das células tumorais através do sistema sanguíneo e/ou linfático para órgãos distantes (YAN et al., 2017). O mecanismo chave ativado no câncer durante o processo de invasão e metástase é chamado transição epitélio-mesenquimal (EMT) (CHARAFE-JAUFFRET et al., 2009; IMBERT et al., 2012). A EMT é definida como um processo reversível de transição celular entre fenótipo epitelial com a perda de adesão entre as células (perda de expressão de E-caderina) e aquisição de um fenótipo mesenquimal (expressão de vimentina e N-caderina) (LAMOUILLE; XU; DERYNCK, 2014). A EMT está intimamente associada à geração das CSCs, resistência ao tratamento e aumento do potencial metastático das células tumorais (CARNERO et al., 2016; DAVE et al., 2012; MANI et al., 2008). A doença metastática é a principal causa de morte entre as pacientes com câncer de mama (MALLINI et al., 2014).

A conversão fenotípica epitélio-mesenquimal é orquestrada por vias de sinalização de transdução de sinal ativadas por TGFB, Notch, Wnt, entre outros, bem como por componentes da matriz extracelular (colágeno e ácido hialurônico) e, fatores de transcrição indutores de EMT (Snail, Twist, Zeb, entre outros) e microRNAs que induzem alteração na expressão de genes envolvidos na adesão celular, diferenciação e motilidade (BURGER; DANEN; BELTMAN, 2017; POLYAK; WEINBERG, 2009)

ZENG e colaboradores (2012) mostraram o papel de uma molécula de adesão, chamada CD146, na indução de EMT em linhagens de câncer de mama (ZENG et al., 2012). CD146 é uma molécula da adesão célula-célula e célula-matriz extracelular que pertence à superfamília de Imunoglobulinas (WANG; YAN, 2013). Esta molécula foi relacionada ao fenótipo mesenquimal (perda de adesão celular, capacidade de migração), aumento da resistência à morte induzida por doxorrubicina e docetaxel e com desenvolvimento de metástases (IMBERT et al., 2012; ZABOUO et al., 2009; ZENG et al., 2012).

O processo reverso a EMT é conhecido como transição mesenquimal-epitelial (MET) que acredita-se acionar a cessação da migração celular, com repressão dos fatores de transcrição indutores de EMT induzindo adesão celular e proliferação dessas células no sítio secundário para colonização

metastática (NIETO, 2013). Assim, EMT e MET atuam como reguladores da plasticidade celular, resultando em um conjunto de estados transitórios e múltiplos entre o fenótipo epitelial, parcial/intermediário e mesenquimal contribuindo para heterogeneidade tumoral (NIETO et al., 2016).

LIU e colaboradores (2014) relatam que as CSCs de mama existem em dois estados fenotípicos, o estado mesenquimal, caracterizado por células quiescentes e localizadas na periferia do tumor, e o estado epitelial, caracterizado por células proliferativas e localizadas mais no centro do tumor. Desse modo, as CSCs conseguem invadir, disseminar e proliferar no sítio metastático (LIU et al., 2014).

1.5 Células-tronco do câncer de mama

As CSCs do câncer de mama foram identificadas como $CD44^{+}/CD24^{-/low}$ por AL-HAJJ e colaboradores (2003). Neste trabalho, foi observada a formação de novos tumores com a mesma heterogeneidade fenotípica do tumor original quando essa subpopulação celular ($CD44^{+}/CD24^{-/low}$), isolada de tumores de mama humana, foi inoculada em camundongos imunocomprometidos. No entanto, células fenotipicamente distintas não foram capazes de induzir o desenvolvimento tumoral. Assim, as células $CD44^{+}/CD24^{-/low}$ são as únicas células tumorais com potencial tumorigênico e com capacidade de autorrenovação e diferenciação celular (AL-HAJJ et al., 2003a). GINESTIER e colaboradores (2007) demonstraram que as CSCs de mama possuem atividade aumentada da enzima aldeído desidrogenase tipo 1(ALDH1) (GINESTIER et al., 2007).

ALDH (Aldeído desidrogenase) é uma enzima responsável pela oxidação de aldeídos intracelulares e acredita-se que tem um importante papel na diferenciação das células-tronco através da oxidação do retinol a ácido retinóico (CHUTE et al., 2006; SOPHOS; VASILIOU, 2003). ALDH1, através da sua função no metabolismo do ácido retinóico, regula a proliferação e diferenciação em células progenitoras mamárias (HONETH et al., 2014). Além disso, GINESTIER e colaboradores (2009) mostraram que o bloqueio da atividade enzimática de ALDH1 induz autorrenovação das CSCs e, a ativação da via do ácido retinóico reduz a subpopulação de CSCs por promover a diferenciação celular (GINESTIER et al., 2009). Vários trabalhos indicam que ALDH1 medeia desenvolvimento de metástases e quimiorresistência (CHARAFE-JAUFFRET et al., 2009; CROKER et al., 2017; CROKER; ALLAN, 2012).

As moléculas de adesão CD44 e CD24 são vastamente utilizadas para identificar e isolar as CSCs de mama. CD44 é uma glicoproteína transmembrana que atua como receptor para várias moléculas da matriz extracelular, como ácido hialurônico, colágeno, fibronectina, laminina, osteopontina (CHANMEE et al., 2015). Essa molécula pode atuar também como coreceptor para fatores de crescimento (EFG, FGF, VEGF), citocinas (TFGB) e metaloproteases estimulando autorrenovação CSCs e promovendo invasão e metástase (YAN; ZUO; WEI, 2015). Diversos trabalhos demonstraram o seu papel na regulação de migração e invasão celular (BOURGUIGNON et al., 2010; LI et al., 2012; MONTGOMERY et al., 2012; NAM et al., 2015; UCHINO et al., 2010), bem como na resistência a morte celular induzida por PTX e DOX em linhagem de mama (BOURGUIGNON et al., 2009; CHEN; BOURGUIGNON, 2014). Além disso, em um estudo de meta-análise (XU et al., 2016) correlacionaram a expressão de CD44 com fenótipo EMT e CSC em câncer de mama.

CD24 é um glicoproteína de membrana do tipo mucina expressa em células hematopoiéticas e não hematopoiéticas (FANG et al., 2010). SCHABATH (2006) demonstraram que células com baixo nível de expressão de CD24 tem maior potencial tumorigênico em relação as células com alta expressão de CD24 devido a regulação negativa dessa molécula sobre o receptor de quimiocina CXCR4, que medeia migração celular (SCHABATH, 2006).

Vários autores demonstraram que após o término da terapia quimioterápica em pacientes com câncer de mama, o tumor residual se mostraram enriquecidas de CSCs, assumindo um fenótipo mais agressivo (CREIGHTON et al., 2009);LEE et al., 2011; LI et al., 2008). Estes estudos fornecem a evidência clínica que as CSCs do câncer de mama são resistentes ao tratamento antitumoral e, assim estão associadas à progressão do tumor. Neste contexto, nota-se a necessidade de desenvolver novas abordagens terapêuticas que visem à eliminação dessa subpopulação celular. Essa terapia-alvo CSCs combinada ao tratamento convencional permitirá eliminar de forma mais efetiva toda a massa tumoral.

1.5.1 Vias de sinalização celular

O nicho de CSCs de mama representa um sistema complexo, onde múltiplas vias de sinalização regulam o comportamento celular, como autorrenovação, quiescência, diferenciação ou apoptose (SEHL et al., 2015). O nicho das CSCs compreende o microambiente onde elas residem favorecendo comunicação célula-célula ou célula-matriz extracelular e sinalização química (citocinas e fatores de crescimento), processos mediados pelas células tumorais, bem como células

endoteliais, fibroblastos, macrófagos e células imunes que compõem o microambiente tumoral (CARNERO et al., 2016; LUO; BROOKE; WICHA, 2015).

Analogamente às células-tronco normais, as CSCs de mama têm uma relação intrínseca com vias de sinalização Wnt/β-catenina, Hedgehog e Notch que regulam autorrenovação e diferenciação (PIRES et al., 2016). As vias de sinalização relacionadas à inflamação, como por exemplo, NFKB (fator nuclear *kappa* B) e STAT3 (transdutor de sinal e ativador de transcrição 3) contribuem para fenótipo CSCs (HINOHARA; GOTOH, 2010; PIRES et al., 2016), bem como a sinalização do receptor do fator de crescimento epidérmico (EGFR), requerida para autorrenovação (ABHOLD et al., 2012). Tumores que superexpressam EGF/EGFR também contribuem para o fenótipo CSCs, aumentando suas propriedades de autorrenovação, influenciando a patofisiologia da doença, os desfechos clínicos, a resposta terapêutica e possibilitando o desenvolvimento de novas terapias direcionadas para moléculas específicas desta via, que promovem o crescimento e a sobrevivência do tumor (ABHOLD et al., 2012); MA e ZHANG et al. 2013).

A família EGFR compreende 4 membros intimamente relacionados EGFR (ErbB1, HER1), ErbB2 (HER2/neu), ErbB3 (HER3) e ErbB4 (HER4). Esses receptores são glicoproteínas transmembrana contendo três domínios: um domínio de ligação extracelular, um domínio transmembranar e um domínio tirosina quinase intracelular. O domínio extracelular é ativado por meio de ligantes que ativam uma sinalização intracelular. O domínio transmembranar envolve homodimerização entre receptores HER1 e/ou heterodimerização com HER2, que é o ligante preferido para a dimerização em câncer de mama. O domínio intracelular tirosina quinase tem uma cauda carboxyl-terminal contendo sítios de autofosforilação de tirosina. A fosforilação de resíduos de tirosina ativa o receptor e cria sitios de ligação para proteínas adaptadoras que em cascata ativam uma série de outras moléculas transdutoras de sinal, tais como as proteínas quinase B (PKB ou AKT), tirosina quinase Src, c-Jun quinase estresse-ativada, ativadores transcricionais (STATs) e subsequente estimulação de vias de sinalização, como PI3K/Akt, Ras-Raf-MAPK-Erk, PLCγ 1/PKC e STAT. A ativação dessas cascatas de sinalização pode levar a uma variedade de respostas celulares como proliferação, sobrevivência, diferenciação e motilidade celular (ALANAZI; KHAN, 2016; FITZGERALD et al., 2015) alterando a adesão e motilidade, protegendo contra a apoptose e promovendo a invasão e angiogênese (ECCLES, 2011; MASUDA; ZHANG, 2012). Em cultura tridimensional, WANG e colaboradores (1998) demonstraram que a ativação de membros da família EGFR promove, em linhagens celulares de câncer de mama, a perda de polarização celular e

outros aspectos da diferenciação epitelial fatores que favorecem a dispersão e invasão de tumores (WANG et al., 1998).

Em relação ao câncer de mama, a via EGF/EGFR desempenha papéis distintos no câncer de mama como um importante fator oncogênico. Desde a descoberta do EGF na década de 1960 e seu receptor nos anos 80, nossa compreensão da via EGF/EGFR avançou significativamente e, esta via tornou-se alvo terapêutico atraente neste tipo de tumor (LO; HSU; HUNG, 2006). A sinalização EGFR induzida pelo seu ligante é necessária para que CSCs derivadas de cultura primária de carcinoma ductal *in situ* formem colônias em meio semi-sólido (FOLEY et al., 2010). Além disso, a superexpressão de HER-2, membro da família EGFR, em células de linhagens de células de câncer de mama SUM159, SUM149 e MCF7 induz o aumento da atividade de ALDH, conforme determinado pelo ensaio de Aldefluor (KORKAYA et al., 2008). Portanto, essas células exibem características de células de tronco/progenitoras, refletindo o aumento da fração de células que exibem propriedades semelhantes a CSC em um ensaio de formação de mamosferas *in vitro* (KORKAYA et al., 2008). Esses achados sugerem que a sinalização de EGFR deve desempenhar um papel substancial no estabelecimento e manutenção de CSCs de mama. Além disso, EGFR é altamente envolvido na EMT. A ativação da via de Ras-Erk mostrou também regular a EMT durante a mestástase, uma vez que esta via é conhecida por induzir a motilidade mesenquimal e a invasão das células cancerosas (MASUDA; ZHANG, 2012)

As vias de sinalização NFKB e STAT3, bem como as vias MAPK e PI3K/AKT, atuam na regulação de EMT e CSCs de mama (KOTIYAL; BHATTACHARYA, 2014). A nível transcricional NFkB e STAT3 podem induzir a superexpressão de TWIST, em resposta a ativação das vias WNT, TGFB, integrinas e receptores tirosina-quinase, que poderá mediar a indução de EMT, via AKT e ERK (TANG et al., 2016; ZHANG et al., 2015; ZHAO et al., 2015). Desta maneira, devido à íntima relação entre as CSCs e EMT, o bloqueio dessas vias pode reduzir ou suprimir as CSCs, como é mostrado em vários trabalhos com linhagens celulares de câncer de mama. A inibição combinada das vias Notch e Ras/MAPK suprimiu as CSCs de mama e bloqueou o crescimento tumoral (MITTAL et al., 2014). (XU et al., 2015) obtiveram resultados similares após a inibição das vias Ras/NF-kB e Ras/MAPK/ERK. ERK, uma molécula da via MAPK, que segundo (JUNG et al., 2016) tem papel direto na sobrevivência das CSCs de mama.

Em um trabalho para avaliar mecanismos de resistência a drogas, TSOU e colaboradores (2015) induziram resistência a DOX em linhagem celular de câncer de mama MCF-7. Foi observado que a resistência a DOX foi acompanhada por superexpressão de genes EMT e da proteína ABCB1

(Transportador ABC), bem como aumento das CSCs de mama. Além disso, o uso de um inibidor da via PI3K/AKT suprimiu parcialmente os genes EMT (TSOU et al., 2015). Desta forma, a ativação das vias de sinalização que regulam EMT e CSCs também pode contribuir para resistência ao tratamento e recorrência do câncer (ISLAM et al., 2015).

1.6 Modelos de cultura in vitro tridimensional

Modelos de cultura tridimensional (3D) que promovem o enriquecimento *in vitro* de células-tronco/progenitoras são vastamente utilizadas no estudo das CSCs, permitindo o crescimento dessas células como esferas multicelulares não-aderentes (tumoresferas) (WEISWALD; BELLET; DANGLES-MARIE, 2015). O uso de modelos esferoides com características de células-tronco derivados de tumores pode fornecer indícios inestimáveis na terapia oncológica (ISHIGURO et al., 2017).

As linhagens celulares de câncer são frequentemente utilizadas como modelo para estudo da biologia do câncer. Modelos de cultura 3D, chamados esferoide, são capazes de reproduzir características *in vivo* dos tumores recapitulando as interações células-células e células-microambiente de forma mais fidedigna do que os modelos convencionais de cultura bidimensional (2D) (LAURENT et al., 2013; RIFFLE et al., 2017; RIFFLE; HEGDE, 2017). Neste contexto, a transposição dos achados *in vitro* em modelos 3D para a prática clínica potencializa o sucesso do tratamento anticâncer (LEE et al., 2016; TELLEZ-GABRIEL et al., 2016). Além disso, são menos onerosos comparados aos modelos *in vivo* e atenuam as questões éticas envolvidas nestes estudos (HUBER et al., 2016).

Modelos esferoides mimetizam vários parâmetros presentes nos tumores envolvidos na resistência das células tumorais ao tratamento agregando valor aos estudos de desenvolvimento e eficácia de novas drogas. O crescimento dos tumores sólidos é acompanhado pelo desenvolvimento de regiões de baixo aporte de oxigênio (hipóxia) que favorecem a resistência celular ao tratamento, aumento do potencial metastático e instabilidade genômica (RIFFLE et al., 2017). Modelos esferoides demonstram a existência de um gradiente de proliferação celular constituído por células proliferativas na periferia, células quiescentes mais internamente e um centro necrótico/apoptótico, semelhante ao observado em tumores sólidos, provavelmente devido à diminuição da disponibilidade de nutrientes e oxigênio (LAURENT et al., 2013). Além disso, o microambiente tumoral hipóxico induz a ativação de vias de reparo do DNA e acúmulo de glicogênio favorecendo a proliferação e sobrevida das células tumorais (RIFFLE et al., 2017).

(WEISWALD; BELLET; DANGLES-MARIE, 2015) classificaram os modelos 3D de cultura esferoide em: 1) Esfera multicelular tumoral: células provenientes de suspensão celular de linhagens celulares cancerosas; 2) Tumoresfera: diferencia-se do modelo anterior por favorecer o enriquecimento de CSCs; 3) Tumoresfera-derivada de tumor: composto por células tumorais sem a presença de células não tumorais derivadas da dissociação mecânica parcial de tecidos tumorais; 4) Esfera multicelular organotípica: utiliza fragmentos de tecido tumoral, composto por todos os tipos celulares que residem no tecido incluindo as células do estroma, permitindo que ele se estruture em um arranjo arredondado. Todos os modelos esferoides são estabelecidos em condição de cultivo não aderente e cada um deles possui propriedades próprias. Os modelos 1, 3 e 4 proporcionam de forma crescente uma maior acurácia no estabelecimento *in vitro* das características *in vivo* do tumor (WEISWALD e BELLET *et al*., 2015).

1.8 JUSTIFICATIVA

O TNBC é o único subtipo de câncer de mama que não possui uma terapia-alvo, o que resulta no prognóstico ruim da doença. Além disso, a QT é altamente agressiva e tóxica, o que leva a deterioração da qualidade de vida das pacientes. Um grande obstáculo para a identificação de alvos efetivos para o tratamento do TNBC é a vasta heterogeneidade intra e intertumoral da doença. Neste contexto, existe claramente uma grande necessidade de entender melhor a base molecular do TNBC, bem como o papel das subpopulações celulares que compõem o tumor para o desenvolvimento de novas estratégias terapêuticas. Desta forma, o presente trabalho utilizou linhagens celulares de TNBC para análise da heterogeneidade celular e da participação da via de sinalização do *EGFR* no mecanismo de resistência aos quimioterápicos DOX e PTX, no intuito de descobrir biomarcadores ou subtipos celulares que possam ter valor preditivo no tratamento dessa doença.

2 OBJETIVOS

2.1 Objetivo principal

Analisar a heterogeneidade celular estrutural, ultraestrutural e imunofenotípica e a via de sinalização do *EGFR* em subpopulações celulares obtidas de linhagens celulares de câncer de mama triplo-negativo e suas implicações na resistência quimioterápica.

2.2 Objetivos secundários

- Obter tumoresferas (modelo de enriquecimento de CSCs) a partir das linhagens celulares humanas de câncer de mama triplo-negativo e mama não-maligna;

- Caracterizar estruturalmente as linhagens celulares e as tumoresferas;

- Caracterizar ultraestruturalmente as linhagens celulares e tumoresferas;

- Obter o perfil fenotípico das linhagens celulares de câncer de mama e suas tumoresferas utilizando marcadores de CSCs de mama (CD44, CD24 e ALDH) e EMT (CD146);

- Avaliar citotoxicidade e obter IC50 dos quimioterápicos PTX e DOX nas linhagens celulares e nas tumoresferas;

- Avaliar a expressão de genes associados à via de sinalização do *EGFR* por PCR quantitativa em tempo-real;

- Analisar os dados obtidos por meio de ferramentas estatísticas apropriadas.

3 METODOLOGIA

3.1 Cultivo celular

Os ensaios foram realizados utilizando dois modelos de cultura celular: I) Cultura em monocamada (bidimensional/2D); II) Cultura de tumoresferas (tridimensional/3D), conforme descrito abaixo:

3.1.1 Linhagens celulares humanas

As linhagens celulares humanas, carcinoma ductal de mama BT-549 (cat. # HTB-122™) e carcinoma de mama Hs 578T (cat. # HTB-126™), adquiridas do *American Type Culture Collection* (ATCC), foram cultivadas, respectivamente, em meio RPMI 1640 (Sigma, cat. # R6504) com 10% de soro fetal bovino/SFB (Sigma, cat. # F6178) e 0,10μg/mL de insulina bovina (Sigma, cat. # I1882); DMEM (Sigma, cat. # D7777) com 10% de SFB (Sigma, cat. # F6178) e 0,01mg/mL de insulina bovina (Sigma, cat. # I1882). A linhagem de tumor benigno de mama HMT-3522 S1 (ECACC, Cat. # 98102210) foi cultivada em meio DMEM/F-12 com 250 ng/mL de insulina bovina (Sigma, cat. # I1882), 10 μg/ml de transferrina (Sigma, cat. # T8158), 10^{E-10M} de 17 beta-estradiol (Sigma, cat. #E2758), 0.5 μg/mL de hidrocortisona (Sigma, cat. # H0135), 5 μg/mL de prolactina (Sigma, cat. #L6520) e 10 ng/ml de EGF (Sigma, cat. # E1257). As linhagens celulares foram incubadas em estufa úmida contendo 5% de CO_2 à 37 ºC.

3.1.2 Tumoresferas

As linhagens celulares foram tripsinizadas e a suspensão celular (1 x 10^5 células/mL) foi semeada em meio de enriquecimento de células-tronco/progenitoras DMEM/F-12 (Sigma, cat. # D0547) suplementado com 20ng/mL de EGF (Sigma, cat. # E1257), 10μg/mL de insulina bovina (Sigma, cat. # I1882), 2% de soro de cavalo inativado (Sigma, cat. # H1270) e 0,5μg/mL de hidrocortisona (Sigma, cat. # H0135) por sete dias para obtenção das tumoresferas. No quarto dia de cultivo metade do volume do meio de cultura foi trocado.

3.2 Caracterização celular por microscopia

3.2.1 Microscopia óptica

3.2.1.1 Fluorescência

Foi utilizado o kit *Image-iT™ LIVE Plasma Membrane and Nuclear Labeling* (Invitrogen, Cat. # I34406) para marcação na membrana plasmática/núcleo e os marcadores Faloidina Alexa Fluor® 488 (Molecular Probes, Cat. # A12379) para marcação dos filamentos de actina do citoesqueleto e o núcleo foi contracorado com *4,6-diaminidino-2-phenylindole* - DAPI (Molecular Probes, Cat. #

D13061), segundo recomendações dos fabricantes. As células marcadas foram visualizadas no microscópio invertido de fluorescência AxioVert 200 (Zeiss)

3.2.1.2 Imunofluorescência

As células foram fixadas com formaldeído 4% por 1h, em temperatura ambiente (TA), lavadas 3 vezes com PBS 1X e, em seguida incubadas com tampão de bloqueio (10% de soro fetal bovino (SFB), 1% albumina bovina (BSA) em PBS 1X) por 1h (TA). Após serem lavadas 3 vezes com PBS 1X, as células foram incubadas por 45 min (TA) com o anticorpo E-caderina (BD, Cat. # 810182) diluído em tampão de bloqueio na concentração indicada pelo fabricante. Em seguida as células foram lavadas 3 vezes com PBS 1X e incubadas com o anticorpo secundário anti-mouse IgG (Fab específico) - FITC (Sigma, Cat. # F5262) diluído 1:40 em 1% BSA/PBS 1X por 30 min. (TA). As células foram lavadas 3 vezes com PBS 1X e o núcleo celular foi contra-corado com DAPI (Molecular Probes, Cat. # D13061) na concentração de 300nM por 5min. (TA). As células marcadas foram visualizadas no microscópio invertido de fluorescência AxioVert 200 (Zeiss).

3.2.2 Microscopia eletrônica

Realizada em parceria com os pesquisadores Dr. Fábio André Brayner e Dr. Luiz Carlos Alves no Laboratório de Biologia Celular e Molecular, Centro de Pesquisa Aggeu Magalhães, Fundação Oswaldo Cruz (CPqAM/FIOCRUZ) utilizando as células em suspensão BT-549 e Hs 578T e suas tumoresferas.

3.2.2.1 Microscopia eletrônica de varredura (MEV)

As células foram fixadas com 2,5% de glutaraldeído em 0,1M de tampão Cacodilato ph 6,8 contendo 7% de sucrose. Em seguida, as células foram tratadas com solução de 2% de tetróxido de ósmio e 1,6% ferrocianeto de potássio por 3h. Após desidratação com concentrações crescentes de acetona (30-100%), as células foram secas na câmera de ponto crítico com CO_2. As células foram montadas no suporte porta-amostra do MEV ("*stub*") e cobertas com partículas de ouro através de um sistema de evaporação conhecido como "*sputtering*" (Silva et al., 2008). As imagens foram analisadas no JEOL 5600 SEM.

3.2.2.2 Microscopia eletrônica de transmissão (MET)

As células foram fixadas e desidratadas como descrito acima. Em seguida foram embebidas em Epon 812 (Silva et al., 2008). Cortes ultra-finos foram obtidos com faca de diamante no micrótomo

Reichert Ultracut, constrastado com acetado de uranil e citrato de chumbo para ser analisado no microscópio Zeiss EM 109.

3.3 Caracterização celular por citometria de fluxo

A imunofenotipagem das linhagens celulares de trabalho cultivadas sob recomendações da ATCC (modelo monocamada) bem como nas tumoresferas (modelo de enriquecimento de CSC) obtidas das linhagens celulares foi realizada por citometria de fluxo. As células foram lavadas com PBS 1X e ressuspendidas em tampão de marcação (PBS 1X + 0,1% de azida sódica + 1% SFB). Em seguida, foram adicionados os anticorpos anti-humano conjugados com fluorocromo e seus respectivos controles de isotipos (Tabela 2) e incubados protegidos da luz por 20 min. a 4°C. As células marcadas foram lavadas com tampão de marcação e ressuspendidas em 0,5 mL do mesmo tampão e, em seguida analisadas no equipamento FACSCanto II (BD Bioscience) utilizando o programa FACSDiva 6.1.3.

Para identificação das células $ALDH^+$ foi utilizado o kit *ALDEFLUOR Stem Cell Identification* (Stem Cell Technologies, cat. # 01700) de acordo com as instruções do fabricante.

Tabela 2 - Anticorpos utilizados na citometria de fluxo.

Anticorpos	Isotipo	Marca	Catálogo
FITC mouse anti-humano CD24	Ms IgG1	Invitrogen	MHCD240
APC rat anti-humano CD44	Rat IgG2b	ImmunoTools	21850446
PE mouse anti-humano CD146	Ms IgG1κ	BD Bioscience	5501315
FITC mouse IgG1 controle isotipo	Ms IgG1	Invitrogen	MG101
APC rat IgG2b controle isotipo	Rat IgG2b	ImmunoTools	22255036
PE mouse IgG1κ controle isotipo	Ms IgG1κ	BD Bioscience	555749

3.4 Análise de viabilidade celular por MTT

Para avaliar a citotoxicidade provocada por PTX e DOX nas células foi utilizado o ensaio colorimétrico MTT (*Thiazolyl Blue Tetrazolium Bromide*). O ensaio de MTT é um método colorimétrico sensível e quantitativo, que mensura a viabilidade, proliferação e estado de ativação das células. Este ensaio baseia-se na capacidade de enzimas desidrogenases, presentes na mitocôndria de células viáveis, em reduzir o substrato dimetiltiazol (MTT), solúvel em água, no

cristal de formazan, insolúvel em água (CARMICHAEL *et al.*, 1987). A quantidade de cristais produzidos é diretamente proporcional ao número de células viáveis.

Para determinar a concentração de IC50 (concentração que inibe 50% do crescimento celular), as células foram expostas a 10 diferentes concentrações dos quimioterápicos paclitaxel (Ontax®, Libbs, lote 15d0236) e cloridrato de doxorrubicina (Fauldoxo, Libbs, lote 13G0025). Utilizou-se de 0,02µM a 10 µM para paclitaxel (PTX) e de 0,16 a 80uM para doxorubicina (DOX), dobrando a concentração em cada ponto.

As linhagens celulares foram plaqueadas nas concentrações celulares: BT-549 ($2{,}0x10^4$ células/poço), Hs 578T ($1x10^4$ células/poço) e HMT-3522 S1 ($4x10^4$ células/poço) em placas de cultivo celular de 96 poços (CORNING) e incubadas em estufa úmida contendo 5% de CO_2 à 37 ºC por 24 horas. Em seguida foram lavadas com PBS 1X e incubadas com as drogas. Após 48h de incubação, as células foram lavadas com PBS 1X e incubadas com 0,5 mg/mL de MTT (*Thiazolyl blue formazan*, Sigma, Cat # M2003), exceto Hs 578T (1,5 mg/mL de MTT), por 3h a 37ºC (5% CO_2). O formazan formado foi precipitado a 1.000RPM por 10 minutos e solubilizado em DMSO (Merck, Cat # K35781952610).

Para as tumoresferas, obtidas conforme descrito no item 4.2 Cultivo Celular, após 48h de incubação com os quimioterápicos foi adicionado o MTT e o formazan obtido foi solubilizado em isopropanol/0,04 N HCL sob agitação por 1h.

A quantificação colorimétrica foi realizada por espectrofometria a 550nm, utilizando-se o equipamento SpectraMax M5e (Molecular Devices). O valor de IC50 foi estimado utilizando o programa DR FIT (Di Veroli 2015)

O Índice de Seletividade (IS) é capaz de demonstrar a seletividade de um composto comparando os resultados entre uma linhagem tumoral e uma não- maligna. Neste estudo, o IS dos quimioterápicos foi avaliado por meio da razão entre o IC50 estimado para as linhagens celulares não-maligna HMT-3522 S1 e IC50 das linhagens de câncer de mama (BT-549 e Hs 578T). O valor de IS indica a seletividade de DOX e PTX frente BT-549 e Hs 578T. IS maiores que 3 foram considerados com tendo alta seletividade (Mahavorasirikul e Viyanant et al., 2010).

3.5 Análise da expressão de genes da via de sinalização do EGFR

O RNA total da tumoresfera BT-549 não-tratada e tratada com DOX na concentração de IC50 foi extraído utilizando o TRIzol (Life Technologies, cat # 15596026) de acordo com as instruções do fabricante. A concentração do RNA total foi mensurada no espectrofotômetro NanoVue (GE Healthcare) em relação a absorbância 260/280 e a sua integridade foi avaliada em gel de agarose 1%. Em seguida, uma possível contaminação com DNA genônico foi eliminada utilizando RNase-free DNase Set (Qiagen, cat # 79254) de acordo com as instruções do fabricante. O cDNA foi sintetizado utilizando M-MLV Reverse transcriptase (Promega, cat # M170A) conforme orientações do fabricante. Para análise gênica foi utilizado o ensaio Taqman® Array Human EGF Pathway 96-well Plate (Applied Biosystems, cat. #4414129) no equipamento 7500 Real-Time PCR System (Applied Biosystems). Esse ensaio permite a análise simultânea de 92 genes associados à via de sinalização do *EGFR* e 4 genes endógenos.

Uma análise de expressão independente de *STAT3* foi realizada usando PrimeTime® Gene Expression Master Mix (IDT) de acordo com as instruções do fabricante. Foram utilizados *STAT3* PrimeTime® qPCR assay (IDT) e o *RNU6B* Taqman® assay (Applied Biosystems) como gene endógeno. Sequência de primers e probe do gene *STAT3*: Primer 1: 5'-TTCTGGGCACAAACACAAAAG-3'; Primer 2: 5'-TCAGTCACAATCAGGGAAGC-3'; e Probe: 5'-/56-FAM/ AGGGAGCAG/ZEN/ AGATGTGGGAATGG/3IABkFQ/-3'.

3.6 Análise estatística

Os dados de expressão gênica foram avaliados no Cloud (Thermo Fisher Scientific) a fim de determinar o valor de expressão gênica relativa para cada um dos alvos estudados e, em seguida, foram analisados pelos programas REST 2009 (Qiagen) para determinar os genes diferencialmente expressos ($p<0,05$) entre os grupos não-tratado e tratado. A análise de agrupamento dos genes avaliados foi feita no programa Bionumerics (Applied Maths).

Para análise estatística utilizou-se o programa SPSS Statistics 18 (IBM) sendo valor de p menor que 0.05 considerado estatisticamente significativo.

4 RESULTADOS E DISCUSSÃO

Essa sessão será apresentada sob a forma de três artigos científicos

ARTIGO 1

***STAT3* as a promising chemoresistance biomarker associated with the CD44$^{+/high}$/CD24$^{-/low}$/ALDH^{+} BCSCs-like subset of the triple-negative breast cancer (TNBC) cell line**

Experimental Cell Research 363 (2018) 283–290

Contents lists available at ScienceDirect

Experimental Cell Research

journal homepage: www.elsevier.com/locate/yexcr

STAT3 as a promising chemoresistance biomarker associated with the $CD44^{+/high}/CD24^{-/low}/ALDH^{+}$ BCSCs-like subset of the triple-negative breast cancer (TNBC) cell line

Milene Pereira Moreira[a,d], Letícia da Conceição Braga[b,c], Geovanni Dantas Cassali[d], Luciana Maria Silva[a,*]

[a] Serviço de Biologia Celular, Diretoria de Pesquisa e Desenvolvimento, Fundação Ezequiel Dias - Rua Conde Pereira Carneiro, 80, Gameleira, Belo Horizonte 30510-010, Minas Gerais, Brazil
[b] Departamento de Ginecologia e Obstetrícia, Faculdade de Medicina, Universidade Federal de Minas Gerais - Av. Prof. Alfredo Balena, 190, Santa Efigênia, Belo Horizonte 30130-100, Minas Gerais, Brazil
[c] Instituto de Ciências Biológicas e Saúde, Centro Universitário UNA - Rua dos Guajajaras, 175, Centro, Belo Horizonte 30180-100, Minas Gerais, Brazil
[d] Laboratório de Patologia Comparada, Departamento de Patologia Geral, Instituto de Ciências Biológicas, Universidade Federal de Minas Gerais - Avenida Presidente Antônio Carlos, 6627 - Pampulha, Belo Horizonte 31270-901, Minas Gerais, Brazil

ARTICLE INFO

Keywords:
Breast cancer
Cancer stem cell
Chemoresistance
Doxorubicin

ABSTRACT

The cancer stem cell (CSC) concept is currently employed to explain the mechanism of multidrug resistance that is implicated in the reduced efficacy of many chemotherapeutic agents, consequently leading to metastatic spread and disease relapse. We searched for potential predictive markers of doxorubicin (DOX) resistance in breast cancer stem cells (BCSCs) of the BT-549 human triple-negative breast cancer (TNBC) cell line classified as a claudin-low subtype. In this study, we show that BT-549 presents a BCSCs-like subset determined by a $CD44^{+/high}/CD24^{-/low}/ALDH1^{+}$ phenotype. The $CD44^{+/high}/CD24^{-/low}/ALDH^{+}$ BCSCs-like subset presented the downregulation of a majority of the genes analyzed (64 genes), and only 3 genes were upregulated after DOX treatment. Among the upregulated genes, *MAPK3*, *PRKCZ* and *STAT3*, *STAT3* presented a higher level of up-regulation in the DOX-treated $CD44^{+/high}/CD24^{-/low}/ALDH^{+}$ BCSCs-like subset. The identification of biomarkers that predict antitumor responses is at the top of cancer research priorities. *STAT3* was highlighted as a molecular signature in the $CD44^{+/high}/CD24^{-/low}/ALDH1^{+}$ BCSCs-like subset obtained from the TNBC BT-549 cell line related to DOX resistance. A majority of the evaluated genes in the EGF pathway appear to be not associated with DOX resistance, as observed in the $CD44^{+/high}/CD24^{-/low}/ALDH1^{+}$ BCSCs-like subset.

1. Introduction

Breast cancer (BC) is the most prevalent cancer diagnosed among women worldwide. In the United States, 40,610 women will die of breast cancer in 2017 [1]. A major obstacle to breast cancer eradication is disease recurrence. Approximately 40% of all breast cancer patients will relapse, with 60–70% of relapse cases due to distant metastasis [2]. Residual BC cell populations are enriched for breast cancer stem cells (BCSCs) after chemotherapy, exhibiting a more aggressive phenotype [3–5]. These cells are hierarchically organized, displaying stem cell-like features, and they are also responsible for chemotherapy resistance, metastatic spread and disease relapse in many solid tumors, such as breast cancer [6,7].

The cancer stem cell (CSC) concept currently explains the mechanism of multidrug resistance implicated in the reduced efficacy of many chemotherapeutic agents [8] because chemotherapy drugs only affect differentiated cells from the tumor bulk leaving behind the CSCs [6]. CSCs possess multiple defense features, such as quiescence,

Abbreviations: AKT1, AKT serine/threonine kinase 1; AKT2, AKT serine/threonine kinase 1; BC, breast cancer; BCSCs, breast cancer stem cells; CAV2, caveolin 2; CSCs, cancer stem cells; DOX, doxorubicin; EGF, epidermal growth factor; EGFR, epidermal growth factor receptor; EMT, epithelial-mesenchymal transition; HER-2, human epidermal growth factor receptor 2; IC50, half maximal inhibitory concentration; MAPK3, mitogen-activated protein kinase 3; MUC1, mucin 1, cell surface associated; PLCG1, phospholipase C gamma 1; PPI, protein-protein interactions; PRKCZ, protein kinase C zeta; RRAS, related RAS viral (r-ras) oncogene homolog; RHOA, ras homolog family member A; RHOC, ras homolog family member C; RT-qPCR, real-time quantitative reverse transcription; STAT3, signal transducer and activator of transcription 3; TS, tumorspheres; TNBC, triple-negative breast cancer

* Corresponding author.
E-mail addresses: mipmoreira@gmail.com (M.P. Moreira), braga.ltc@gmail.com (L. da Conceição Braga), geovanni.cassali@gmail.com (G.D. Cassali), luciana.silva@funed.mg.gov.br (L.M. Silva).

https://doi.org/10.1016/j.yexcr.2018.01.018
Received 2 August 2017; Received in revised form 2 January 2018; Accepted 12 January 2018
Available online 17 January 2018

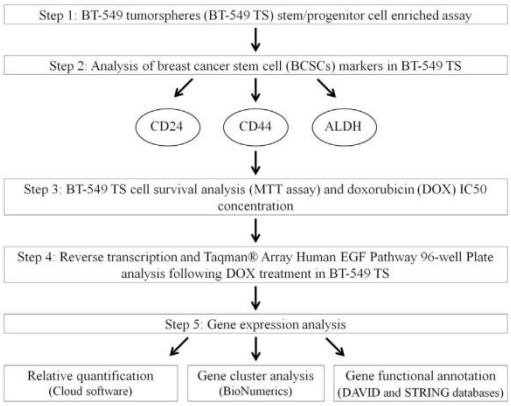

Fig. 1. Workflow of the analysis performed in this study.

apoptosis evasion, drug efflux mechanisms, DNA repair, self-renewal, and a hypoxic and inflammatory microenvironment, to survive cytotoxic chemotherapy [7]. Therefore, a new approach combining conventional chemotherapy and BCSC-target therapy may lead to a better clinical outcome and prevent BC relapse.

An important pathway implicated in regulating the proliferation, differentiation and survival of epithelial cells is epidermal growth factor receptor (EGFR) signaling [9]. EGFR and its downstream pathway have been linked to cancer cell migration and invasion [10], as well as BCSC enrichment [11].

In the present study, we evaluated data based on the expression of EGF pathway-associated genes in a BCSC-like population and identified $CD44^{+/high}/CD24^{-/low}/ALDH^{+}$ markers by flow cytometry following doxorubicin (DOX) treatment. We intended to understand the effect of DOX treatment on a set of genes in a BCSC-like population ($CD44^{+/high}/CD24^{-/low}/ALDH^{+}$) obtained from BT-549 cells, an established triple-negative breast cancer (TNBC) cell line. The potential identification of the BT-549 BCSCs-like subset and their EGF pathway gene expression profiling could be used in further research for targeting and eliminating cancer cells. Fig. 1 shows the workflow of the research performed in this study.

2. Materials and methods

2.1. Tumorsphere cultures

Our study was performed using BT-549 cells, a human TNBC cell line obtained from the American Type Culture Collection (ATCC, Manassas, USA) propagated in a monolayer according to the manufacturer's instructions. For BT-549 tumorspheres (BT-549 TS) culture, stem/progenitor cell-enriched assay was performed. The cells in the monolayer were replicated, and the suspension cells (1×10^5 cells/mL) were plated on low-attachment plates (Corning, New York, USA) using DMEM/F-12 medium for TS selection with 20 ng/mL of EGF, 10 μg/mL of bovine insulin, 2% inactivated horse serum and 0.5 μg/mL of hydrocortisone, all obtained from Sigma (St. Louis, MO, USA). To establish the BT-549 TS, the cells were incubated for seven days in a 5% CO_2 incubator at 37 °C.

2.2. Flow cytometry analysis

After seven days of suspension culture, the BT-549 TS were collected, washed with PBS and incubated with Trypsin-EDTA (0.25%/0.5 mM) for two minutes at 37 °C to dissociate the cells. The cells were resuspended in labeling buffer (PBS, 0.1% sodium azide and 1% fetal bovine serum) and incubated with anti-human antibodies against CD44 (APC-H7; BD Biosciences, San Jose, CA, USA) and CD24 (FITC; Invitrogen, Carlsbad, CA, EUA), as markers of the BCSCs-like subset, at concentrations recommended by the manufacturer. The antibodies were incubated on ice protected from light for 20 min at 4 °C. Isotype controls were used to set the threshold for positivity.

ALDEFLUOR™ stem cell identification (Stem Cell Technologies, Vancouver, BC, Canada) was performed to identify $ALDH^{+}$ cells. A total of 1×10^6 cells/mL was incubated for 40 min at 37 °C according to the manufacturer's instructions.

The experiments were performed on the FACSCanto II flow cytometer (BD Bioscience, San Jose, CA, USA) with cell acquisition and data analysis using FACSDiva 6.1.3 software (BD Bioscience, San Jose, CA, USA).

2.3. Cell survival analysis

The effect of DOX on cell viability was evaluated by MTT (Thiazolyl Blue Tetrazolium Bromide) colorimetric assay. To titrate the half maximal inhibitory concentration (IC50) of DOX (Fauldoxo®, Libbs, Embu das Artes, SP, MG), BT-549 TS and BT-549 cell propagated in a monolayer were exposed to a range of drug concentrations (0.0781–80.0 μM), increasing the concentration by 2-fold between each point. Untreated cells served as controls. The drug was prepared freshly for each experiment and incubated for 48 h. The formazan crystals, the MTT product formed in the mitochondria of viable cells, were solubilized with 100 μL of isopropanol/0.04 M HCl (Merck, Darmstadt, Germany) at room temperature for one hour under agitation. The colorimetric reaction was measured using the SpectraMax M5e Microplate Reader (Molecular Devices, Sunnyvale, CA, USA) at 550 nm. The assays were performed in triplicate in three independent experiments. The IC50 was estimated using the cell survival average of three independent experiments.

2.4. Reverse transcription and epidermal growth factor (EGF) pathway arrays analysis

Total RNA from control and BT-549 TS treated with DOX at the calculated IC50 was isolated using TRIzol® (Invitrogen, Carlsbad, CA, USA) according to the manufacturer's instructions. The concentration of total RNA and the 260/280 absorbance ratio were measured using the NanoVue spectrophotometer (GE Healthcare, Little Chalfont, United Kingdom). Total RNA was treated with RNase-free DNase Set (Qiagen, Hilden, Germany). The cDNA was synthesized using M-MLV Reverse transcriptase (Promega, Madison, Wisconsin, USA) according to the manufacturer's recommendations. The Taqman® Array Human EGF Pathway 96-well Plate (Applied Biosystems, Foster City, CA, USA) was performed according to the manufacturer's instructions on the 7500 Real-Time PCR System (Applied Biosystems, Foster City, CA, USA).

2.5. Validation of STAT3 expression

An independent RT-qPCR for *STAT3* expression was performed using the PrimeTime® Gene Expression Master Mix (IDT, Coralville, Iowa, USA) according to the manufacturer's instructions. The *RNU6B* gene provided in the Taqman® assay (Applied Biosystems, Foster City, CA, USA) was utilized as an endogenous gene. For the *STAT3* PrimeTime® qPCR assay (IDT, Coralville, Iowa, USA), the following primers and probe were used: Primer 1: 5'-TTCTGGGCACAAACACAA AAG-3'; Primer 2: 5'-TCAGTCACAATCAGGGAAGC-3'; and Probe: 5'-/56-FAM/ AGGGAGCAG/ZEN/ AGATGTGGGAATGG/3IABkFQ/ – 3'.

2.6. Gene functional and network pathway analysis

The differentially expressed genes were classified according to the Database for Annotation, Visualization and Integrated Discovery

(DAVID) version 6.8 [12,13] into Gene Ontology (GO) categories in terms of their associated Biological Processes (BP). For the pathway analysis of gene-associated proteins, the Kyoto Encyclopedia of Genes and Genomes (KEGG) was investigated by using STRING database, version 10.5 [14]. STRING was also used to evaluate protein-protein interactions (PPI) among the associated genes.

2.7. Data analysis

IC50 DOX concentration was estimated by Dr Fit, version 1.042 [15], and statistical analysis was performed in SPSS software, version 18.0 (SPSS Inc., Chicago, Illinois, USA).

The p-value computation was performed by Relative Expression Software Toll (REST© 2009), version 2.0.13 [16] (Qiagen, Hilden, Alemanha) to identify differentially expressed genes. The statistical significance was assessed at $p < 0.05$. The relative quantification (Rq) values for the statistical significance of overall genes was calculated by using the 2(-Delta Delta C(T)) method on Cloud software, version 1.0 (Thermo Fisher, Waltham, MA USA). The data were plotted by using SPSS software. A clustering analysis was performed using the UPGMA (Unweighted Pair Group Method using Arithmetic averages) method and Euclidian distance by BioNumerics software, version 7.5 (Applied Maths, Sint-Martens-Latem, Belgium).

3. Results

3.1. Flow cytometry analysis identify BCSCs markers in BT-549 TS

FACS analysis showed that BT-549 TS presents the BCSCs-like subset determined by $CD44^{+/high}/CD24^{-/low}$ (Fig. 2A-B) and $ALDH1^{+}$ phenotype (Fig. 2C-D), as described by AL-HAJJ *et al.* [17]; GINESTIER *et al.* [18].

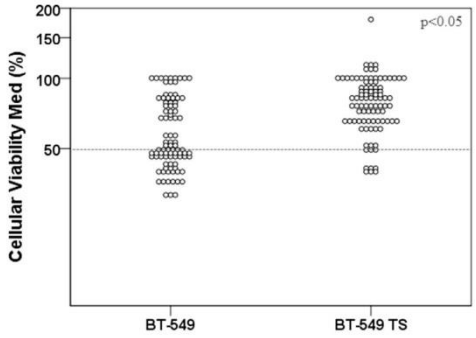

Fig. 3. Effect of DOX on BT-549 propagated in a monolayer and as tumorspheres. The cells were treated with DOX at a range of concentrations from 0.0781 to 80.0 μM, increasing the concentration by 2-fold between each point. Cell viability was assessed by MTT assay, and the results are presented as the cellular viability median (%). Each dot represents the cell viability value at each concentration tested in three independent experiments performed in triplicate. The $CD44^{+/high}/CD24^{-/low}/ALDH1^{+}$ BCSCs-like subset presented high cell viability values for the most drug concentrations tested. The opposite result was observed in the monolayer culture. Statistical significance was indicated by $p < 0.05$ using non-parametric tests Mann-Whitney for independent samples.

3.2. $CD44^{+/high}/CD24^{-/low}/ALDH1^{+}$ BCSCs-like subset of BT-549 presents high resistance to DOX treatment

To identify changes in gene expression in BCSCs that correlate with the resistance to DOX, the sensitivity of the $CD44^{+/high}/CD24^{-/low}/ALDH1^{+}$ BCSCs-like subset of BT-549 was evaluated. Fig. 3 illustrates the high-level resistance of the $CD44^{+/high}/CD24^{-/low}/ALDH1^{+}$ BCSCs-like subset of BT-549 to DOX when compared with BT-549 cells in monolayer culture. The $CD44^{+/high}/CD24^{-/low}/ALDH1^{+}$ BCSCs-like

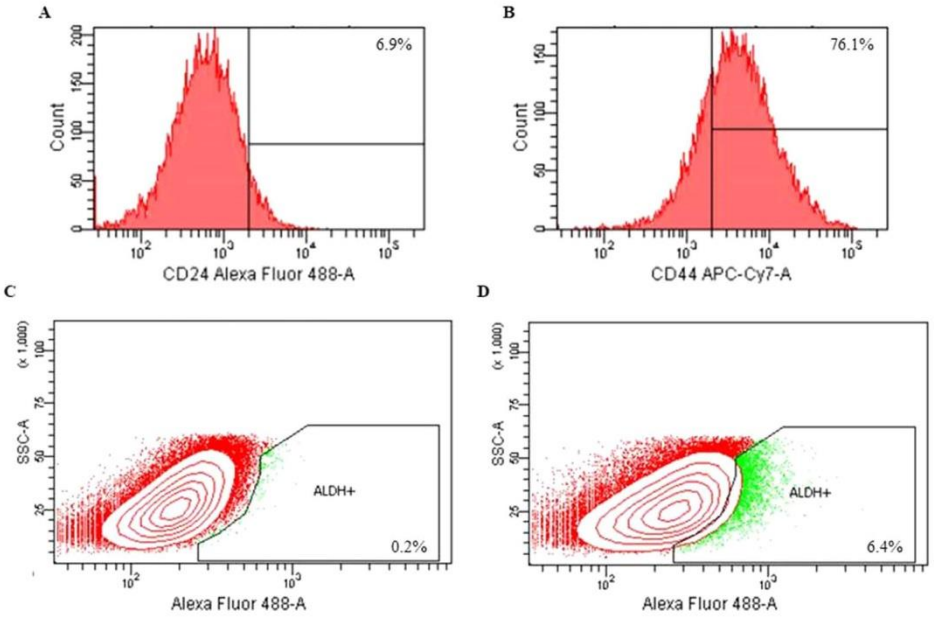

Fig. 2. Representative FACS plot of the BCSCs marker analysis on BT-549 TS. A-B: BT-549 TS labeling with CD24 and CD44 antibodies, respectively. Histograms showing the percentage of positive cells. Isotype controls were used to set the threshold for positivity. C: The cells were incubated with both ALDEFLUOR™ substrate (BAAA) and DEAB, a specific inhibitor of ALDH, to establish the baseline fluorescence (R1) and define the ALDEFLUOR-positive region (R2) D: Cells incubated with ALDEFLUOR substrate alone. Dot plot showing the percentage of ALDH-positive cells.

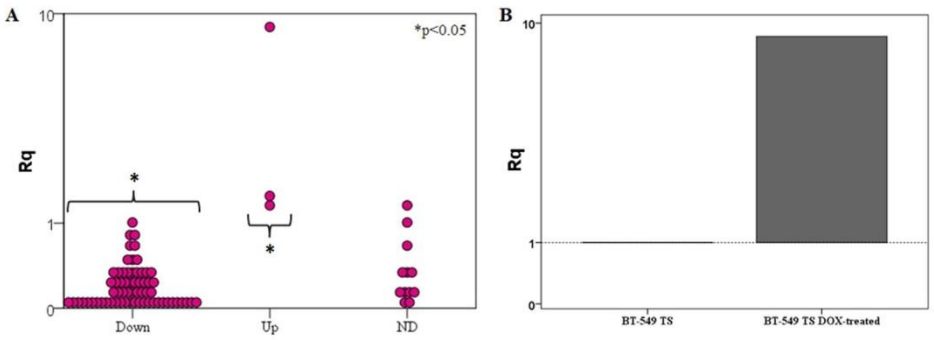

Fig. 4. Relative quantification analysis of EGF pathway-associated genes in the CD44$^{+/high}$/CD24$^{-/low}$/ALDH1^{+} BCSCs-like subset. Gene expression was assessed by Taqman® assay, and the results are presented as a relative quantification (Rq). A. After DOX treatment with 55.7 μM, we observed 64 genes downregulated and 3 genes upregulated, determined by REST© 2009 software. Among the upregulated genes *MAPK3*, *PRKCZ* and *STAT3*, *STAT3* presented higher Rq values. Twelve genes were not significantly different from control (ND - no difference). *Significant differences of each point compared with the control. Statistical significance was indicated by $p < 0.05$ using Kruskal-Wallis non-parametric test. B. *STAT3* expression was validated by qRT-qPCR assay, showed an 8.7-fold expression change after DOX treatment, confirming the array results.

subset demonstrated an IC50 value of 55.7 μM of DOX, which was 97.4× higher than that of the BT-549 monolayer, with an estimated IC50 of 0.572 μM of DOX.

3.3. *STAT3* is associated with the chemoresistance of the CD44$^{+/high}$/CD24$^{-/low}$/ALDH1^{+} BCSCs-like subset of BT-549 cells

To identify predictive markers associated with DOX-resistance in the BCSCs-like subset, a gene expression profiling analysis was performed using RT-qPCR array. We divided the obtained gene expression profiles into the following two subsets: the DOX-treated CD44$^{+/high}$/CD24$^{-/low}$/ALDH1^{+} BCSCs-like subset and the untreated CD44$^{+/high}$/CD24$^{-/low}$/ALDH1^{+} BCSCs-like subset as a control. REST© 2009 software was used to filter out differentially expressed genes. The expression analysis revealed changes in 67 (85%) out of the 79 genes examined in the DOX-treated CD44$^{+/high}$/CD24$^{-/low}$/ALDH1^{+} BCSCs-like subset compared to the control. The majority of these genes (64 genes − 95.5%) were downregulated and 3 genes, *MAPK3*, *PRKCZ* and *STAT3*, were upregulated (4.5%) (Fig. 4). A complete list of the analyzed genes, relative quantification values and up/downregulation status was submitted as Supplementary Material (Table S1).

We performed a cluster analysis on the array data relative to the 67 differentially expressed genes in the DOX- treated CD44$^{+/high}$/CD24$^{-/low}$/ALDH1^{+} BCSCs-like subset. The genes are clustered in the branches of the dendrogram based on overall similarity in patterns of relative quantification data according to the Euclidian distance. The genes were clustered into the following two main groups (Fig. 5A): cluster 1 formed by the most upregulated gene, *STAT3*, and cluster 2 formed by two upregulated genes, *MAPK3* and *PRKCZ* (branch named as 2 A), and all downregulated genes (branch named as 2B). Additionally, the downregulated genes *CAV2, RHOA* and *RRAS* (branch named as a); *AKT1, AKT2, MUC1, RHOC* and *PLCG1* (branch named as b) exhibited more accentuate differences in the Rq value than the other downregulated genes and were categorized into close branches (branch named as 2B.1). The clustering dendrogram shows the other 56 downregulated genes categorized into close branches (branch named as 2B.2). *STAT3* were not clustered into single branches with the other upregulated genes because the Rq value for this gene was approximately 6-fold higher than the Rq values for *MAPK3* and *PRKCZ* (Fig. 4 and Table S1), highlighting a role for *STAT3* in the DOX-treated CD44$^{+/high}$/CD24$^{-/low}$/ALDH1^{+} BCSCs-like subset.

We performed an independent *STAT3* RT-qPCR to validate the obtained results and observed *STAT3* upregulation (8.7-fold) in the DOX-treated BT-549 TS. These data confirmed the array results, showing a 8.89-fold increase in *STAT3* expression in the CD44$^{+/high}$/CD24$^{-/low}$/ALDH1^{+} BCSCs-like subset after DOX treatment (Supplementary material - Table S1).

3.4. Gene ontology and network pathway analysis

The gene ontology categories were evaluated to further explore the biological processes and functional pathways related to the upregulated and downregulated genes categorized in the close branches (cluster 2B.1), and the results are shown in Table 1. The data demonstrate that DOX treatment could lead to overall changes in the patterns of gene expression, including proliferation, apoptosis and other important pathways associated with carcinogenesis. The PPI among the associated genes are shown in Fig. 5B.

4. Discussion

The development of metastatic disease is the primary cause of mortality in BC patients. Approximately 30% of early breast cancer patients eventually develop metastasis, and in 90% of patients, multidrug resistance occurs [19]. Several lines of evidence have shown BCSCs as the main players in chemoresistance, metastasis and disease recurrence [20]. Based on these findings, we aimed to identify molecular targets that could be used as markers of BCSCs DOX resistance.

Tumorsphere assays can be useful for investigating the features of BCSCs, as these cells typically contain undifferentiated stem/progenitor cells [21]. Since CD44$^{+/high}$/CD24$^{-/low}$/ALDH1^{+} cells have been widely used in BCSC characterization [17,18], our results suggest that BT-549 TS are enriched by this subpopulation.

According to the Genomics of Drug Sensitivity in Cancer (GDSC) database [22], the IC50 concentration of DOX (a common chemotherapeutic agent used in the treatment of BC) in a panel of BC cell lines ranged from 14.6 to 0.00969 μM. Our results showed the estimated IC50 value of monolayer BT-549 cells across the range of GDSC. However, the CD44$^{+/high}$/CD24$^{-/low}$/ALDH1^{+} BCSCs-like subset was 97.4× more resistant to DOX-induced cell death compared to BT-549 cells cultured in a monolayer. These data on the CD44$^{+/high}$/CD24$^{-/low}$/ALDH1^{+} subset reinforce the role of BCSCs as drivers of chemoresistance. The role of BCSCs in chemoresistance has been extensively described in the literature. Jia *et al.* [4] demonstrated that individual chemotherapeutic treatment with 5-fluorouracil, doxorubicin and paclitaxel markedly enriched the CD44$^{+/high}$/CD24$^{-/low}$ BCSCs subpopulation and increased ALDH expression. Furthermore, stemness genes were upregulated after drug treatment. A BCSC phenotype

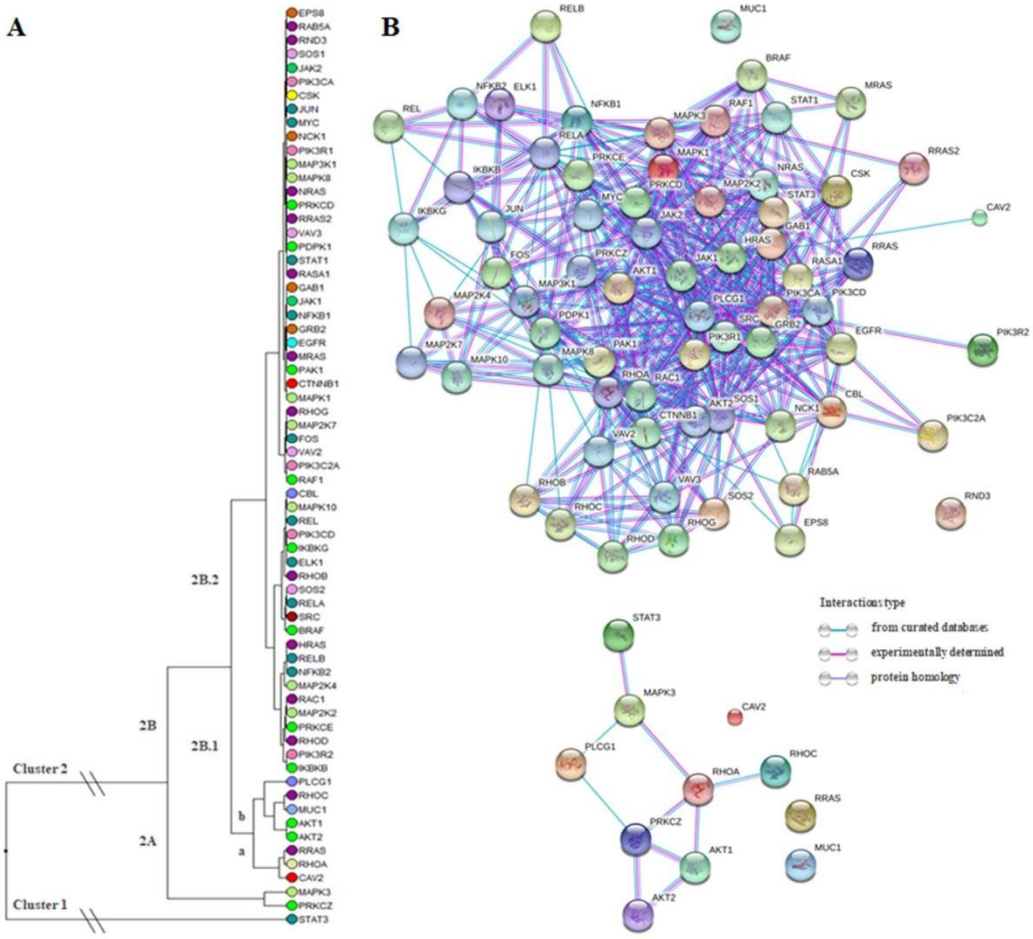

Fig. 5. Gene cluster and PPI network among the associated genes analysis in the DOX-treated $CD44^{+/high}/CD24^{-/low}/ALDH1^{+}$ BCSCs-like subset. A. The mRNA expression of 67 genes associated with the DOX-treated $CD44^{+/high}/CD24^{-/low}/ALDH1^{+}$ BCSCs-like subset using hierarchical cluster. The relationships among analyzed genes are represented by trees whose branch lengths represent the degree of similarity based on relative quantification (Rq) data. B. The confidence view of the protein-protein interactions (PPI) among the associated genes provided by STRING. The data were extracted form curated databases (blue line) and experimentally determined (purple line). The light blue line represents protein homology. A small node size denotes proteins of unknown 3D structure, and a large node size indicates that some 3D structure is known or predicted.

Table 1
Functional annotation analysis of *STAT3*-associated genes.

Category	Term	Genes
GOTERM_BP_DIRECT	GO.0043066~Negative regulation of apoptotic process	AKT1,AKT2,MUC1,PRKCZ, **STAT3**
GOTERM_BP_DIRECT	GO.0060397~JAK-STAT cascade involved in growth hormone signaling pathway	MAPK3,**STAT3**
GOTERM_BP_DIRECT	GO:0071407~Cellular response to organic cyclic compound	AKT1,**STAT3**
KEEG pathway	Hsa05205: Proteoglycans in cancer	AKT1,AKT2,CAV2,MAPK3, PLCG1,RHOA,RRAS,**STAT3**
KEEG pathway	Hsa04066: HIF－1 signaling pathway	AKT1,AKT2,MAPK3,PLCG1, **STAT3**
KEEG pathway	Hsa05200: Pathways in cancer	AKT1,AKT2,MAPK3,PLCG1,RHOA,**STAT3**
KEEG pathway	Hsa04062: Chemokine signaling pathway	AKT1,AKT2,MAPK3,RHOA, **STAT3**
KEEG pathway	Hsa04068: Foxo signaling pathway	AKT1,AKT2,MAPK3,**STAT3**
KEEG pathway	Hsa05206: MicroRNAs in cancer	PLCG1,RHOA,**STAT3**
KEEG pathway	Hsa04630: Jak-STAT signaling pathway	AKT1,AKT2,**STAT3**

Note: Functional annotation analysis performed in DAVID and STRING databases.

($CD44^{+/high}/CD24^{-/low}$) was also induced in the DOX-resistant BC cell line after treatment [8]. Our study model, BT-549 TS, was used by our group to evaluate the antitumor properties of new 3-alkylpyridine marine alkaloid analogs [23]. The results showed that one of the 3-alkylpyridine marine alkaloid analogs performed differently in monolayer and tumorsphere models. In monolayer model, the compound has no action, but in the tumorsphere model, both cell populations (BCSCs and non-BCSCs) were decreased after treatment. The test compound induced $CD44^{+/high}/CD24^{-/low}$ BCSCs-like subset death, emerging as a promising class for the development of anticancer agents.

TNBC, an aggressive subtype of breast carcinoma, is defined by a lack of estrogen and progesterone receptor expression and a lack of HER-2 amplification/overexpression, thus cytotoxic chemotherapy is the mainstream anticancer therapy available [24]. Because of the high rate of EGFR overexpression, approximately 50% of these tumors, EGFR inhibitors are among the targeted agents being developed for TNBC treatment [10]. These inhibitors enhance TNBC cell sensitivity to cytotoxic therapy [25]. The primary goal of performing the EGF gene expression array was to select genes as predictive biomarkers associated with chemoresistance in the $CD44^{+/high}/CD24^{-/low}/ALDH1^{+}$ BCSCs-like subset of the TNBC cell line. Our results showed that *EGFR* expression was downregulated in the $CD44^{+/high}/CD24^{-/low}/ALDH1^{+}$ BCSCs-like subset after DOX treatment. Additionally, *ERBB2* expression was low (data not shown because these results were not statistically significant when the difference of expression before and after DOX treatment was analyzed - Supplementary material 1: Table S1). BT-549, the cell line utilized in our study, is classified as a claudin-low subtype [26]. Clinically defined as TNBC, this subtype is characterized by a low-level of ERBB2 expression and is highly enriched with epithelial-mesenchymal transition (EMT) markers and cancer stem cell-like features [26]. Therefore, EGFR inhibitors may not have effects on the $CD44^{+/high}/CD24^{-/low}/ALDH1^{+}$ BCSCs-like subset as adjuvants in DOX treatment. This finding demonstrates the extreme importance of predicted markers of chemoresistance.

We identified a total of 11 genes associated with DOX-resistance. *PRKCZ*, *MAPK3* and *STAT3* genes were upregulated and *AKT1*, *AKT2*, *CAV2*, *MUC1*, *PLCG1*, *RHOA*, *RHOC* and *RRAS* were downregulated following DOX treatment.

STAT3 expression was approximately 6-fold higher than that of the other upregulated genes, which suggests that this gene is a predictive biomarker of anti-apoptotic *STAT3* signaling, decreasing DOX-induced cell death and promoting chemoresistance in the $CD44^{+/high}/CD24^{-/low}/ALDH1^{+}$ BCSCs-like subset. The other upregulated genes, *PRKCZ* and *MAPK3,* encoded proteins that are upstream activators of the STAT3 signaling pathway [27–29]. Thus, these activators may enhance STAT3 activation in the $CD44^{+/high}/CD24^{-/low}/ALDH1^{+}$ BCSCs-like subset following DOX treatment.

In addition, the upregulated genes are critical regulators of the EMT phenotype, which involves the shift of an epithelial state to a mesenchymal state [27,30–32]. EMT, a key mechanism implicated in metastasis, endows epithelial cells with stem cell characteristics, providing an association between EMT, CSCs and drug resistance [6,33]. Since most tumors are carcinomas arising from epithelial cells, EMT in cancer cells has been established as a crucial event because the resistance-mediated therapy is observed in many types of cancer.

MAPK3 and *STAT3* were directly associated with BCSCs enrichment [34–38], and several authors have suggested these genes are correlated with DOX-resistance in BC cell lines [39–41]. The role of PRKCZ in DOX-resistance was reported in a cervical cell line [42]. Therefore, *PRKCZ*, *MAPK3* and *STAT3* upregulation following DOX treatment in the $CD44^{+/high}/CD24^{-/low}/ALDH1^{+}$ BCSCs-like subset may contribute to the chemoresistance observed in our study. To the best of our knowledge, there is no described link between *PRKCZ* and the BCSC subpopulation, as observed for other PRKC isoenzymes [43–45].

RRAS, a member of the Ras superfamily, is involved in the RAS/RAF/MAPK pathway [38]. Nonetheless, the *RRAS* downregulation demonstrated in our study may not affect MAPK3 signaling, as Valkova *et al.* [46] demonstrated that PRKCZ activates this protein in a manner independent of RAS.

Several authors have recently reported that *AKT1*, *AKT2*, *CAV2*, *MUC1*, *PLCG1*, *RHOA*, and *RHOC* also trigger the EMT phenotype, and some of these genes (*AKT, RHOC* and *MUC1*) are related to drug resistance [8,47–54]. These findings suggested that the downregulated genes, although related to EMT and chemoresistance, observed in our study model have no or little effect on the DOX resistance of the $CD44^{+/high}/CD24^{-/low}/ALDH1^{+}$ BCSCs-like subset.

Functional annotation in terms of the biological processes of *STAT3*-associated genes revealed their function in cell proliferation and anti-apoptotic signaling. Moreover, these genes are associated with important pathways implicated in cancer. STAT3 is a central signaling node enabling cross-talk with signaling pathways related to cancer development and progression, such as metastasis, immune suppression, angiogenesis, inflammation and BCSCs regulation [55,56]. We highlighted the strong relationship between inflammation and BCSC. IL (interleukin) − 6, an inflammatory cytokine, has previously been described as the most potent inducer of STAT3, in an EGFR-independent manner; conversely, STAT3 can also activate IL-6 [35,57]. IL-6/STAT3 signaling is involved in the self-renewal, survival and invasive phenotype of BCSCs [58,59].

The role of the STAT3 signaling pathway in TNBC cell growth and invasiveness [60–63], as well as is implication in the growth of BCSC subsets [64,65], is well-known. In addition, numerous reports have demonstrated the association of STAT3 activation with chemoresistance and STAT3 inhibition can restore the efficacy of chemotherapeutic agents [66–68]. Thus, our findings are consistent with prior STAT3 knowledge. This study includes only one cell line and chemotherapeutic, but our study involved an extensive gene expression analysis of 67 genes associated with the EGF signaling pathway in a specific cell population, the $CD44^{+/high}/CD24^{-/low}/ALDH1^{+}$ BCSCs-like subset to screen putative molecular markers. Therefore, we proposed *STAT3* upregulation as a molecular signature in the $CD44^{+/high}/CD24^{-/low}/ALDH1^{+}$ BCSCs-like subset related to DOX-resistance, and these data were validated by qRT-PCR.

STAT3 is constitutively activated in many types of cancers and tumor cell lines. This protein activates proliferation and inhibits apoptosis, thereby stimulating malignant transformation. STAT3 overexpression has been observed in chemoresistance as an indirect effect of the negative regulation of the cell death pathway [69]. Our study indicates a strong relationship of STAT3 with DOX treatment resistance in the $CD44^{+/high}/CD24^{-/low}/ALDH1^{+}$ BCSCs-like subset, highlighting this protein as a potential therapeutic target in TNBC, the only major type of breast cancer without a specific targeted therapy. STAT3 inhibition may increase the efficacy of chemotherapy and improve TNBC patient outcomes. Further clinical studies are needed to further understand the underlying mechanism of the STAT3 signal pathway in chemotherapy resistance.

5. Conclusions

Tumor biology can be determined from studies of specialized cell types and the microenvironment that tumors construct during the course of tumorigenesis. The genetic and molecular heterogeneity of tumors has been the greatest obstacle to chemotherapy, as these tissues produce varied responses to drugs. Our study may provide clues about the failures of certain chemotherapeutics on triple-negative tumors. Strategies using commercial cancer cell lines may be particularly useful to predict chemotherapeutic responses and determine the biological mechanisms of drug action. Thus, when we reach the validation phase with clinical patient samples we will carry out targeted tests, since promising biomarkers have previously been identified in models of immortalized cells. Notably, the drug sensitivity data derived from previously phenotyped sphere culture models show clinically and

faithfully more relevant responses than that from standard monolayer culture. Our results indicated that the $CD44^{+/high}/CD24^{-/low}/ALDH1^{+}$ BCSCs-like subset obtained from the TNBC BT549 cell line are STAT3-expressing cells, which likely contributes to their resistance to DOX treatment. Additionally, a majority of the evaluated genes in EGF pathway appear to be not associated with the DOX resistance presented in our $CD44^{+/high}/CD24^{-/low}/ALDH1^{+}$ BCSCs-like subset. The identification of biomarkers that predict antitumor responses is at the top of cancer research priorities.

Conflicts of interest

None

Funding

This work was financially supported through grants from Fundação de Amparo à Pesquisa do Estado de Minas Gerais (FAPEMIG) [grant number CBB-APQ-00054-12], Coordenação de Aperfeiçoamento de Pessoal de Nível Superior (CAPES) and Conselho Nacional de Desenvolvimento Científico e Tecnológico (CNPq).

Acknowledgments

Not applicable

Appendix A. Supplementary material

Supplementary data associated with this article can be found in the online version at http://dx.doi.org/10.1016/j.yexcr.2018.01.018.

References

[1] R.L. Siegel, K.D. Miller, A. Jemal, Cancer Statistics, 2017, Ca Cancer J. Clin. 67 (2017) 7–30.
[2] M. Smalley, L. Piggott, R. Clarkson, Breast cancer stem cells: obstacles to therapy, Cancer Lett. 338 (2013) 57–62.
[3] C.J. Creighton, X. Lia, M. Landis, J.M. Dixon, V.M. Neumeister, A. Sjolund, D.L. Rimm, H. Wong, et al., Residual breast cancers after conventional therapy display mesenchymal as well as tumor-initiating features, PNAS 106 (33) (2009) 13820–13825.
[4] D. Jia, Y. Tan, H. Liu, S. Ooi, L. Li, K. Wright, S. Bennett, C.L. Addison, L. Wang, Cardamonin reduces chemotherapy-enriched breast cancer stem-like cells in vitro and in vivo, Oncotarget 7 (1) (2015) 771–785.
[5] R. Sun, S. Shen, Y.-J. Zhang, C.-F. Xu, Z.-T. Cao, L.-P. Wen, J. Wang, Nanoparticle-facilitated autophagy inhibition promotes the efficacy of chemotherapeutics against breast cancer stem cells, Biomaterials 103 (2016) 44–55.
[6] A. Carnero, Y. Garcia-Mayea, C. Mir, J. Lorente, I.T. Rubio, M.E. LLeonart, The cancer stem-cell signaling network and resistance to therapy, Cancer Treat. Rev. 49 (2016) 25–36.
[7] J. Zhao, Cancer stem cells and chemoresistance: the smartest survives the raid, Pharmacol. Ther. 160 (2016) 145–158.
[8] S.-H. Tsou, T.-M. Chen, H.-T. Hsiao, Y.-H. Chen, Critical dose of doxorubicin is required to alter the gene expression profiles in MCF-7 cells acquiring multidrug resistance, Plos One 10 (1) (2015) 1–24.
[9] L. Ma, G. Zhang, X.-B. Miao, X.-B. Deng, Y. Wu, Y. Liu, Z.-R. Jin, X.-Q. Li, Q.-Z. Liu, et al., Cancer stem-like cell properties are regulated by EGFR/AKT/β-catenin signaling and preferentially inhibited by gefitinib in nasopharyngeal carcinoma, FEBS J. 280 (9) (2013) 1–20.
[10] H. Masuda, D. Zhang, C. Bartholomeusz, H. Doihara, G.N. Hortobagyi, N.T. Ueno, Role of epidermal growth factor receptor in breast cancer, Breast Cancer Res Treat. 136 (2) (2012) 1–21.
[11] H. Korkaya, A. Paulson, E. Charafe-Jauffret, C. Ginestier, M. Brown, J. Dutcher, S.G. Clouthier, M.S. Wicha, Regulation of mammary stem/progenitor cells by PTEN/Akt/b-Catenin signaling, PLoS Biol. 7 (6) (2009) e1000121.
[12] D.W. Huang, B.T. Sherman, R.A. Lempicki, Systematic and integrative analysis of large gene lists using DAVID Bioinformatics Resources, Nat. Protoc. 4 (1) (2009) 44–57.
[13] D.W. Huang, B.T. Sherman, R.A. Lempicki, Bioinformatics enrichment tools: paths toward the comprehensive functional analysis of large gene lists, Nucleic Acids Res. 37 (1) (2009) 1–13.
[14] D. Szklarczyk, A. Franceschini, S. Wyder, K. Forslund, D. Heller, J. Huerta-Cepas, M. Simonovic, A. Roth, A. Santos, et al., STRING v10: protein-protein interaction networks, integrated over the tree of life, Nucleic Acids Res. 43 (2015) D447–D452 Database issue.
[15] G.Y. Di Veroli, C. Fornari, I. Goldlust, G. Mills, S.B. Koh, J.L. Bramhall, F.M. Richards, D.I. Jodrell, An automated fitting procedure and software for dose-response curves with multiphasic features, Sci. Rep. 5 (2015) 14701.
[16] M.W. Pfaffl, G.W. Horgan, L. Dempfle, Relative expression software tool (REST) for group-wise comparison and statistical analysis of relative expression results in real-time PCR, Nucl. Acids Res. 30 (9) (2002) 1–10.
[17] M. Al-Hajj, M.S. Wicha, A. Benito-Hernandez, S.J. Morrison, M.F. Clarke, Prospective identification of tumorigenic breast cancer cells, PNAS 100 (7) (2003) 3983–3988.
[18] C. Ginestier, M.H. Hur, E. Charafe-Jauffret, F. Monville, J. Dutcher, M. Brown, J. Jacquemier, P. Viens, C. Kleer, et al., ALDH1 is a marker of normal and malignant human mammary stem cells and a predictor of poor clinical outcome, Cell Stem Cell 1 (5) (2007) 555–567.
[19] P. Mallini, T. Lennard, J. Kirby, A. Meeson, Epithelial-to-mesenchymal transition: what is the impact on breast cancer stem cells and drug resistance, Cancer Treat. Rev. 40 (2014) 341–348.
[20] M. Luo, M. Brooke, M.S. Wicha, Epithelial-mesenchymal plasticity of breast cancer stem cells: implications for metastasis and therapeutic resistance, Curr. Pharm. Des. 21 (10) (2015) 1301–1310.
[21] D. Ponti, A. Costa, N. Zaffaroni, G. Pratesi, G. Petrangolini, D. Coradini, S. Pilotti, M.A. Pierotti, M.G. Daidone, Isolation and in vitro propagation of tumorigenic breast cancer cells with stem/progenitor cell properties, Cancer Res. 65 (13) (2005) 5506–5511.
[22] W. Yang, J. Soares, P. Greninger, E.J. Edelman, H. Lightfoot, S. Forbes, N. Bindal, D. Beare, J.A. Smith, et al., Genomics of drug sensitivity in cancer (GDSC): a re-source for therapeutic biomarker discovery in cancer cells, Nucleic Acids Res. 41 (2013) D955–D961 Database issue.
[23] A.B. Lima, C.S. Barbosa, A.M.M.N. Gonçalves, F.V. Santos, G.H.R. Viana, F.P. Varotti, L.M. Silva, New 3-alkylpyridine marine alkaloid analogues as promisor antitumor agents against $CD44^{+/high}/CD24^{-/low}$ subset of triple-negative breast cancer (TNBC) cell line, Chem. Biol. Drug Des. 90 (1) (2017) 5–11.
[24] B.D. Lehmann, J.A. Pietenpol, Clinical implications of molecular heterogeneity in triple negative breast cancer, Breast 24 (02) (2015) S36–S40.
[25] Y.-T. Li, X.-J. Qian, Y. Yu, Z.-H. Li, R.-Y. Wu, J. Ji, L. Jiao, X. Li, P.-F. Kong, et al., EGFR tyrosine kinase inhibitors promote pro-caspase-8 dimerization that sensitizes cancer cells to DNA-damaging therapy, Oncotarget 6 (19) (2015) 17491–17500.
[26] A. Prat, J.S. Parker, O. Karginova, C. Fan, C. Livasy, J.I. Herschkowitz, X. He, C.M. Perou, Phenotypic and molecular characterization of the claudin-low intrinsic subtype of breast cancer, Breast Cancer Res. 12 (R68) (2010) 1–18.
[27] L.M. McCaffrey, J. Montalbano, C. Mihai, I.G. Macara. Loss of the Par3 polarity protein promotes breast tumorigenesis and metastasis. Cancer Cell 22 (2102) 601-614.
[28] A.M. Butler, M.L.S. Buzhardt, S. Li, K.E. Smith, A.P. Fields, N.R. Murray, Protein kinase C Zeta regulates human pancreatic cancer cell transformed growth and in-vasion through a STAT3-dependent mechanism, Plos One 8 (8) (2013) e72061.
[29] D.J. Gough, L. Koetz, D.E. Levy, The MEK-ERK pathway is necessary for serine phosphorylation of mitochondrial STAT3 and Ras-mediated transformation, Plos One 8 (11) (2013) e83395.
[30] Y.-Q. Zhang, X.-L. Wei, Y.-K. Liang, W.L. Chen, F. Zhang, J.W. Bai, S.-Q. Qiu, C.-W. Du, W.H. Huang, G.-J. Zhang, Over-expressed Twist associates with markers of epithelial mesenchymal transition and predicts poor prognosis in breast cancers via ERK and Akt activation, Plos One 10 (8) (2015) e0135851.
[31] D. Zhao, A.H. Besser, S.A. Wander, J. Sun, W. Zhou, B. Wang, T. Ince, M.A. Durante, W. Guo, et al., Cytoplasmic p27 promotes epithelial–mesenchymal transition and tumor metastasis via STAT3-mediated Twist1 upregulation, Oncogene 34 (2015) 5447–5459.
[32] C. Rejon, M. Al-Masri, L. McCaffrey, Cell polarity proteins in breast cancer pro-gression, J. Cell Biochem. 117 (2016) 2215–2223.
[33] S.A. Mani, W. Guo, M.-J. Liao, E.N. Eaton, A. Ayyanan, A.Y. Zhou, N. Brooks, F. Reinhard, C.C. Zhang, et al., The epithelial-mesenchymal transition generates cells with properties of stem cells, Cell 133 (2008) 704–715.
[34] L. Lin, B. Hutzen, H.-F. Lee, Z. Peng, W. Wang, C. Zhao, H.-J. Lin, D. Sun, P.K. Li, et al., Evaluation of STAT3 signaling in $ALDH^{+}$ and $ALDH^{+}/CD44^{+}/CD24^{-}$ sub-populations of breast cancer cells, Plos One 8 (12) (2013) e82821.
[35] L. Yang, S. Han, Y. Sun, An IL6-STAT3 loop mediates resistance to PI3K inhibitors by inducing epithelial–mesenchymal transition and cancer stem cell expansion in human breast cancer cells, Biochem Biophys. Res Commun. 453 (2014) 582–587.
[36] H. An, J.Y. Kim, E. Oh, N. Lee, Y. Cho, J.H. Seo, Salinomycin promotes anoikis and decreases the $CD44^{+}/CD24^{-}$ stem-like population via inhibition of STAT3 activa-tion in MDA-MB-231 cells, Plos One 10 (11) (2015) e0141919.
[37] S. Mittal, A. Sharma, S.A. Balaji, M.C. Gowda, R.R. Dighe, R.V. Kumar, A. Rangarajan, Coordinate hyperactivation of Notch1 and Ras/MAPK pathways correlates with poor patient survival: novel therapeutic strategy for aggressive breast cancers, Mol. Cancer Ther. 13 (12) (2014) 3198–3209.
[38] Y.-C. Jung, S. Han, L. Hua, Y.-H. Ahn, H. Cho, C.-J. Lee, H. Lee, Y.-Y. Cho, J.-H. Ryu, et al., Kazinol-E is a specific inhibitor of ERK that suppresses the enrichment of a breast cancer stem-like cell population, Biochem Biophys. Res Commun. 470 (2016) 294–299.
[39] R.H. Kolb, P.M. Greer, P.T. Cao, K.H. Cowan, Y. Yan, ERK1/2 signaling plays an important role in topoisomerase II poison-induced G2/M checkpoint activation, Plos One 7 (11) (2012) e50281.
[40] J.-H. Kim, S.C. Lee, J. Ro, H.S. Kang, H.S. Kim, S. Yoon, Jnk signaling pathway-mediated regulation of Stat3 activation is linked to the development of doxorubicin resistance in cancer cell lines, Biochem Pharmacol. 79 (2010) 373–380.
[41] A. Liu, Y. Liu, Z. Jin, Q. Hu, L. Lin, D. Jou, J. Yang, Z. Xu, H. Wang, et al., XZH-5 inhibits STAT3 phosphorylation and enhances the cytotoxicity of chemotherapeutic

drugs in human breast and pancreatic cancer cells, Plos One 7 (10) (2012) e46624.
[42] A. Rimessi, E. Zecchini, R. Siviero, C. Giorgi, S. Leo, R. Rizzuto, P. Pinton, The selective inhibition of nuclear PKCζ restores the effectiveness of chemotherapeutic agents in chemoresistant cells, Cell Cycle 11 (5) (2012) 1040–1048.
[43] Z. Chen, L.W. Forman, R.M. Williams, D.V. Faller, Protein kinase C-delta inactivation inhibits the proliferation and survival of cancer stem cells in culture and in vivo, BMC Cancer 14 (90) (2014) 1–15.
[44] A. Zafar, K. Hardy, F. Wu, J. Li, S. Rao, The role of protein kinase-C theta in control of epithelial to mesenchymal transition and cancer stem cell formation, Genom. Data. 3 (2015) 28–32.
[45] D.E. Berardi, C. Flumian, C.E. Rodriguez, M.I.D. Bessone, S.M. Cirigliano, E.D.B.K. Joff, G.L. Fiszman, A.J. Urtreger, L.B. Todaro, PKC delta inhibition impairs mammary cancer proliferative capacity but selects cancer stem cells, involving autophagy, J. Cell Biochem. 117 (2016) 730–740.
[46] C. Valkova, C. Mertens, S. Weisheit, S. Imhof, C. Liebmann. Activation by tyrosine phosphorylation as a prerequisite for protein kinase Cζ to mediate epidermal growth factor receptor signaling to ERK. Mol Cancer Res. 8 (5) (20100 783-797.
[47] H. Tang, D. Massi, B.A. Hemmings, M. Mandalà, Z. Hu, A. Wicki, G. Xue, AKT-ions with a TWIST between EMT and MET, Oncotarget 7 (38) (2016) 62767–62777.
[48] H. Kawata, T. Kamiakito, Y. Omoto, C. Miyazaki, Y. Hozumi, A. Tanaka, RhoC upregulation is correlated with reduced E-cadherin in human breast cancer specimens after chemotherapy and in human breast cancer MCF-7 cells, Horm. Canc. 5 (2014) 414–423.
[49] J. Shankar, I.R. Nabi, Actin cytoskeleton regulation of epithelial mesenchymal transition in metastatic cancer cells, Plos One 10 (3) (2015) e0119954.
[50] E. Leung, J.M. Hung, D. Barker, J. Reynisson, The effect of a thieno[2,3-b]pyridine PLC-g inhibitor on the proliferation, morphology, migration and cell cycle of breast cancer cells, Med Chem. Commun. 5 (99) (2014) 99–106.
[51] A.-M. Dragoi, R. Swiss, B. Gao, H. Agaisse, Novel strategies to enforce an epithelial phenotype in mesenchymal cells, Cancer Res. 74 (14) (2014) 3659–3672.
[52] H. Rajabi, M. Alam, H. Takahashi, A. Kharbanda, M. Guha, R. Ahmad, D. Kufe, MUC1-C oncoprotein activates the ZEB1/miR-200c regulatory loop and epithelial-mesenchymal transition, Oncogene 33 (13) (2014) 1680–1689.
[53] Y. Uchida, D. Raina, S. Kharbanda, D. Kufe, Inhibition of the MUC1-C oncoprotein is synergistic with cytotoxic agents in the treatment of breast cancer cells, Cancer Biol. Ther. 14 (2) (2013) 127–134.
[54] C.G. Kleer, K.A. Griffith, M.S. Sabel, G. Gallagher, K.L. van Golen, Z.-F. Wu, S.D. Merajver, RhoC-GTPase is a novel tissue biomarker associated with biologically aggressive carcinomas of the breast, Breast Cancer Res Treat. 93 (2005) 101–110.
[55] J. Yuan, F. Zhang, R. Niu, Multiple regulation pathways and pivotal biological functions of STAT3 in cancer, Sci. Rep. 5 (2015) 17663.
[56] J. Huynh, N. Etemadi, F. Hollande, M. Ernst, M. Buchert, The JAK/STAT3 axis: a comprehensive drug target for solid malignancies, Semin. Cancer Biol. 45 (2017) 13–22.
[57] V. Sriuranpong, J.I. Park, P. Amornphimoltham, V. Patel, B.D. Nelkin, J.S. Gutkind, Epidermal growth factor receptor-independent constitutive activation of STAT3 in head and neck squamous cell carcinoma is mediated by the autocrine/paracrine stimulation of the interleukin 6/gp130 cytokine system, Cancer Res. 63 (2003) 2948–2956.
[58] P. Sansone, G. Storci, S. Tavolari, T. Guarnieri, C. Giovannini, M. Taffurelli, C. Ceccarelli, D. Santini, P. Paterini, et al., IL-6 triggers malignant features in mammospheres from human ductal breast carcinoma and normal mammary gland, J. Clin. Invest. 117 (2007) 3988–4002.
[59] H. Korkaya, G.-il Kim, A. Davis, F. Malik, N.L. Henry, S. Ithimakin, A.A. Quraishi, N. Tawakkol, R. D'Angelo, et al., Activation of an IL6 Inflammatory Loop Mediates Trastuzumab Resistance in HER2+ Breast Cancer by Expanding the Cancer Stem Cell Population, Mol. Cell 47 (2012) 570–584.
[60] R. Mehta, H. Katta, F. Alimirah, R. Patel, G. Murillo, X. Peng, M. Muzzio, R.G. Mehta, Deguelin action involves c-Met and EGFR signaling pathways in triple negative breast cancer cells, Plos One 8 (6) (2013) e65113.
[61] X. Liu, Q. Xiao, X. Bai, Z. Yu, M. Sun, H. Zhao, X. Mi, E. Wang, W. Yao, et al., Activation of STAT3 is involved in malignancy mediated by CXCL12-CXCR4 signaling in human breast cancer, Oncol. Rep. 32 (2014) 2760–2768.
[62] N. Uddin, R.-K. Kim, K.-C. Yoo, Y.-H. Kim, Y.-H. Cui, I.-G. Kim, Y. Suh, S.-J. Lee, Persistent activation of STAT3 by PIM2-driven positive feedback loop for epithelial-mesenchymal transition in breast cancer, Cancer Sci. 106 (2015) 718–725.
[63] J.M. McDaniel, K.E. Varley, J. Gertz, D.S. Savic, B.S. Roberts, S.K. Baile, L.A. Shevde, R.C. Ramaker, B.N. Lasseigne, et al., Genomic regulation of invasion by STAT3 in triple negative breast cancer, Oncotarget 8 (5) (2017) 8226–8238.
[64] L.L.C. Marotta, V. Almendro, A. Marusyk, M. Shipitsin, J. Schemme, S.R. Walker, N. Bloushtain-Qimron, J.J. Kim, S.A. Choudhury, et al., The JAK2/STAT3 signaling pathway is required for growth of CD44$^+$CD24$^-$ stem cell–like breast cancer cells in human tumors, J. Clin. Invest 121 (7) (2011) 2723–2735.
[65] B. Dave, M.D. Landis, L.E. Dobrolecki, M.-F. Wu, X. Zhang, T.F. Westbrook, S.G. Hilsenbeck, D. Liu, M.T. Lewis, et al., Selective small molecule Stat3 inhibitor reduces breast cancer tumor-initiating cells and improves recurrence free survival in a human-xenograft model, Plos One 7 (8) (2012) e30207.
[66] J.T. Sims, S.S. Ganguly, H. Bennett, J.W. Friend, J. Tepe, Imatinib reverses doxorubicin resistance by affecting activation of STAT3-dependent NF-κB and HSP27/p38/AKT pathways and by inhibiting ABCB1, Plos One 8 (1) (2013) e55509.
[67] C. Zhao, H. Li, H.-J. Lin, S. Yang, J. Lin, G. Liang, Feedback activation of STAT3 as a cancer drug-resistance mechanism, Trends Pharmacol. Sci. 37 (1) (2016) 47–61.
[68] T. Feng, W. Cao, W. Shen, L. Zhang, X. Gu, Y. Guo, H-i Tsai, X. Liu, J. Li, et al., Arctigenin inhibits STAT3 and exhibits anticancer potential in human triple-negative breast cancer therapy, Oncotarget 8 (1) (2017) 329–344.
[69] B. Barré, A. Vigneron, N. Perkins, I.B. Roninson, E. Gamelin, O. Coqueret, The STAT3 oncogene as a predictive marker of drug resistance, Trends Mol. Med. 13 (1) (2006) 4–11.

Supplementary material

Table S1 - Taqman® Array Human EGF Pathway-associated genes (Applied Biosystems®, Cat. 4414129) and relative quantification values

GENE	NAME	TYPE	ASSAY ID	Rq	STATUS
18S	RNA, 18S ribosomal	REF*	Hs99999901_s1	-	-
GAPDH	glyceraldehyde-3-phosphate dehydrogenase	REF	Hs99999905_m1	-	-
HPRT1	hypoxanthine phosphoribosyltransferase 1	REF	Hs99999909_m1	-	-
GUSB	glucuronidase beta	REF*	Hs99999908_m1	-	-
ABI1	abl-interactor 1	TRG	Hs00178550_m1	NA	NA
AKT1	AKT serine/threonine kinase 1	TRG	Hs00178289_m1	0.81	DOWN
AKT2	AKT serine/threonine kinase 2	TRG	Hs01086102_m1	0.82	DOWN
AKT3	AKT serine/threonine kinase 3	TRG	Hs00178533_m1	NA	NA
ARAF	A-Raf proto-oncogene, serine/threonine kinase	TRG	Hs00176427_m1	NA	NA
BRAF	B-Raf proto-oncogene	TRG	Hs00269944_m1	0.23	DOWN
CAV1	caveolin 1	TRG	Hs00971716_m1	NA	NA
CAV2	caveolin 2	TRG	Hs00184597_m1	0.53	DOWN
CBL	Cbl proto-oncogene	TRG	Hs00231981_m1	0.19	DOWN
CDH1	cadherin 1	TRG	Hs01023894_m1	0.62	ND
CHUK	conserved helix-loop-helix ubiquitous kinase	TRG	Hs00175141_m1	0.06	ND
CSK	c-src tyrosine kinase	TRG	Hs00177843_m1	0.03	DOWN
CTNNB1	catenin beta 1	TRG	Hs00355045_m1	0.09	DOWN
DIRAS3	DIRAS family GTPase 3	TRG	Hs00190723_m1	0.14	ND
DOK2	docking protein 2	TRG	Hs00182758_m1	NA	NA
EGF	epidermal growth factor	TRG	Hs01099999_m1	NA	NA
EGFR	epidermal growth factor receptor	TRG	Hs01076078_m1	0.08	DOWN
ELK1	ELK1, ETS transcription factor	TRG	Hs00428286_g1	0.20	DOWN
EPS8	epidermal growth factor receptor pathway substrate 8	TRG	Hs00610286_m1	0.02	DOWN

GENE	NAME	TYPE	ASSAY ID	Rq	STATUS
ERBB2	erb-b2 receptor tyrosine kinase 2	TRG	Hs01001580_m1	0.29	ND
FOS	Fos proto-oncogene, AP-1 transcription factor subunit	TRG	Hs00170630_m1	0.12	DOWN
GAB1	GRB2 associated binding protein 1	TRG	Hs00157646_m1	0.06	DOWN
GRB2	growth factor receptor bound protein 2	TRG	Hs00157817_m1	0.08	DOWN
HRAS	HRas proto-oncogene, GTPase	TRG	Hs00610483_m1	0.36	DOWN
IKBKB	inhibitor of kappa light polypeptide gene enhancer in B-cells, kinase beta	TRG	Hs00233287_m1	0.33	DOWN
IKBKE	inhibitor of kappa light polypeptide gene enhancer in B-cells, kinase epsilon	TRG	Hs01063858_m1	0.32	ND
IKBKG	inhibitor of kappa light polypeptide gene enhancer in B-cells, kinase gamma	TRG	Hs00415849_m1	0.20	DOWN
JAK1	Janus kinase 1	TRG	Hs01026983_m1	0.07	DOWN
JAK2	Janus kinase 2	TRG	Hs01078136_m1	0.03	DOWN
JUN	Jun proto-oncogene, AP-1 transcription factor subunit	TRG	Hs99999141_s1	0.01	DOWN
KRAS	KRAS proto-oncogene, GTPase	TRG	Hs00364282_m1	0.03	ND
MAP2K1	mitogen-activated protein kinase kinase 1	TRG	Hs00605615_mH	NA	NA
MAP2K2	mitogen-activated protein kinase kinase 2	TRG	Hs00360961_m1	0.30	DOWN
MAP2K4	mitogen-activated protein kinase kinase 4	TRG	Hs00387426_m1	0.39	DOWN
MAP2K7	mitogen-activated protein kinase kinase 7	TRG	Hs00178198_m1	0.12	DOWN
MAP3K1	mitogen-activated protein kinase kinase kinase 1	TRG	Hs00394890_m1	0.04	DOWN
MAPK1	mitogen-activated protein kinase 1	TRG	Hs01046830_m1	0.10	DOWN
MAPK10	mitogen-activated protein kinase 10	TRG	Hs00373461_m1	0.19	DOWN
MAPK3	mitogen-activated protein kinase 3	TRG	Hs00385075_m1	1.46	UP
MAPK8	mitogen-activated protein kinase 8	TRG	Hs01548508_m1	0.04	DOWN
MAPK9	mitogen-activated protein kinase 9	TRG	Hs00177102_m1	0.10	ND
MRAS	muscle RAS oncogene homolog	TRG	Hs00171926_m1	0.07	DOWN
MUC1	mucin 1, cell surface associated	TRG	Hs00159357_m1	0.71	DOWN
MYC	v-myc avian myelocytomatosis viral oncogene homolog	TRG	Hs99999003_m1	0.01	DOWN
NCK1	NCK adaptor protein 1	TRG	Hs00237216_m1	0.04	DOWN

GENE	NAME	TYPE	ASSAY ID	Rq	STATUS
NFKB1	nuclear factor kappa B subunit 1	TRG	Hs00765730_m1	0.07	DOWN
NFKB2	nuclear factor kappa B subunit 2	TRG	Hs00174517_m1	0.36	DOWN
NRAS	neuroblastoma RAS viral oncogene homolog	TRG	Hs00180035_m1	0.05	DOWN
PAK1	p21 (RAC1) activated kinase 1	TRG	Hs00176815_m1	0.07	DOWN
PDPK1	3-phosphoinositide dependent protein kinase 1	TRG	Hs00176884_m1	0.05	DOWN
PIK3C2A	phosphatidylinositol-4-phosphate 3-kinase catalytic subunit type 2 alpha	TRG	Hs00153223_m1	0.13	DOWN
PIK3C2B	phosphatidylinositol-4-phosphate 3-kinase catalytic subunit type 2 beta	TRG	Hs00153248_m1	0.37	ND
PIK3CA	phosphatidylinositol-4,5-bisphosphate 3-kinase catalytic subunit alpha	TRG	Hs00180679_m1	0.03	DOWN
PIK3CB	phosphatidylinositol-4,5-bisphosphate 3-kinase catalytic subunit beta	TRG	Hs00927728_m1	NA	NA
PIK3CD	phosphatidylinositol-4,5-bisphosphate 3-kinase catalytic subunit delta	TRG	Hs00192399_m1	0.20	DOWN
PIK3R1	phosphoinositide-3-kinase regulatory subunit 1	TRG	Hs00381459_m1	0.04	DOWN
PIK3R2	phosphoinositide-3-kinase regulatory subunit 2	TRG	Hs00178181_m1	0.33	DOWN
PLCG1	phospholipase C gamma 1	TRG	Hs00234046_m1	0.97	DOWN
PRKCA	protein kinase C alpha	TRG	Hs00176973_m1	0.15	ND
PRKCB	protein kinase C beta	TRG	Hs00176998_m1	NA	NA
PRKCD	protein kinase C delta	TRG	Hs01090047_m1	0.05	DOWN
PRKCE	protein kinase C epsilon	TRG	Hs00178455_m1	0.29	DOWN
PRKCG	protein kinase C gamma	TRG	Hs00177010_m1	NA	NA
PRKCQ	protein kinase C theta	TRG	Hs00989970_m1	NA	NA
PRKCZ	protein kinase C zeta	TRG	Hs00177051_m1	1.24	UP
PTK2	protein tyrosine kinase 2	TRG	Hs00178587_m1	0.10	ND
PXN	paxillin	TRG	Hs00236064_m1	1.38	ND
RAB5A	RAB5A, member RAS oncogene family	TRG	Hs00991290_m1	0.02	DOWN
RAC1	ras-related C3 botulinum toxin substrate 1 (rho family, small GTP binding protein Rac1)	TRG	Hs01025984_m1	0.31	DOWN
RAF1	Raf-1 proto-oncogene, serine/threonine kinase	TRG	Hs00234119_m1	0.14	DOWN
RASA1	RAS p21 protein activator 1	TRG	Hs00243115_m1	0.06	DOWN

GENE	NAME	TYPE	ASSAY ID	Rq	STATUS
REL	REL proto-oncogene, NF-kB subunit	TRG	Hs00968436_m1	0.18	DOWN
RELA	RELA proto-oncogene, NF-kB subunit	TRG	Hs00153294_m1	0.25	DOWN
RELB	RELB proto-oncogene, NF-kB subunit	TRG	Hs00232399_m1	0.36	DOWN
RHOA	ras homolog family member A	TRG	Hs00357608_m1	0.44	DOWN
RHOB	ras homolog family member B	TRG	Hs00269660_s1	0.17	DOWN
RHOC	ras homolog family member C	TRG	Hs00237129_m1	0.67	DOWN
RHOD	ras homolog family member D	TRG	Hs00205854_m1	0.28	DOWN
RHOG	ras homolog family member G	TRG	Hs00750922_s1	0.12	DOWN
RND3	Rho family GTPase 3	TRG	Hs00170603_m1	0.03	DOWN
RRAS	related RAS viral (r-ras) oncogene homolog	TRG	Hs00196699_m1	0.47	DOWN
RRAS2	related RAS viral (r-ras) oncogene homolog 2	TRG	Hs00273367_m1	0.05	DOWN
SHC1	SHC adaptor protein 1	TRG	Hs00427539_m1	1.05	ND
SHC3	SHC adaptor protein 3	TRG	Hs00375042_m1	NA	NA
SOS1	SOS Ras/Rac guanine nucleotide exchange factor 1	TRG	Hs00362308_m1	0.03	DOWN
SOS2	SOS Ras/Rho guanine nucleotide exchange factor 2	TRG	Hs00183311_m1	0.25	DOWN
SRC	SRC proto-oncogene, non-receptor tyrosine kinase	TRG	Hs00178494_m1	0.24	DOWN
STAT1	signal transducer and activator of transcription 1	TRG	Hs01013989_m1	0.05	DOWN
STAT3	signal transducer and activator of transcription 3	TRG	Hs00374280_m1	8.89	UP
VAV1	vav guanine nucleotide exchange fator 1	TRG	Hs00232108_m1	NA	NA
VAV2	vav guanine nucleotide exchange fator 2	TRG	Hs00610104_m1	0.11	DOWN
VAV3	vav guanine nucleotide exchange fator 3	TRG	Hs00196125_m1	0.05	DOWN

REF - endogenous controls; TRG - target gene; * endogenous controls used in the analysis; NA - not analyzed due no amplification or bad amplification curve; ND - no statistical difference compared with control

ARTIGO 2

Phenotypic cellular heterogeneity among triple negative breast cancer cell lines and breast cancer stem cells subpopulation promote differential sensibility at standard chemotherapy

Phenotypic cellular heterogeneity among triple-negative breast cancer cell lines and breast cancer stem cells subpopulation promote differential sensibility at standard chemotherapy

Milene Pereira Moreira[1,2], Eliza Pereira Franco[1], Letícia da Conceição Braga[1], Geovanni Dantas Cassali[2], Luciana Maria Silva[1*]

[1]Serviço de Biologia Celular, Diretoria de Pesquisa e Desenvolvimento, Fundação Ezequiel Dias - Rua Conde Pereira Carneiro 80, Gameleira, Belo Horizonte, Minas Gerais, Brasil, 30510-010.

[2]Laboratório de Patologia Comparada, Departamento de Patologia Geral, Instituto de Ciências Biológicas, Universidade Federal de Minas Gerais - Avenida Presidente Antônio Carlos 6627, Pampulha, Belo Horizonte, Minas Gerais, Brasil, 31270-901.

*Corresponding author

luciana.silva@funed.mg.gov.br

(55) 31 3314-4746

ORCID: 0000-0002-2038-0405

Abstract

Purpose Triple negative breast cancer is a heterogeneous disease. A multitude of different cell types were identified within the tumor microenvironment carrying distinct roles, contributing to their heterotypic nature. Thereby, efforts have been done to discover cellular and molecular markers present in the tumor. We aimed to characterize distinct cell subpopulations for better understanding the cellular heterogeneity related to the biological mechanisms of chemoresistance.

Methods BT-549, Hs 578T and HMT-3522 S1 were cultivated in monolayer and under tumorspheres (TS) model (breast cancer stem cells (BCSCs)-enriched culture). The cells were evaluated by flow cytometry and further treated with paclitaxel (PTX) and doxorubicin (DOX) by MTT assay.

Results The cellular heterogeneity was observed among and within the cells in term of morphology, phenotyping and drug response. For BT-549, we suggested that the plasticity properties of $CD44^+/CD24^+/CD146^+$ hybrid cells and $CD44^-/CD24^+/CD146^+$ epithelial cells enable the phenotypic conversion into the $CD44^+/CD24^-/CD146^-$ epithelial-mesenchymal transition/EMT-like BCSCs. Further these non-BCSCs may generate $ALDH^+$ epithelial-like BCSCs. The enriched BCSCs may undergo differentiation into $CD44^-/CD24^-/CD146^-$ cells and self-renewal. Our cytotoxicity data showed that BT-549 was the only one more resistant to PTX instead of DOX, which appears to be associated to $CD24^+$ cells. In contrast, under TS model, the BT-549 TS were extremely resistance to DOX probably due the enrichment of BCSCs ($CD44^+/CD24^-$/ $CD146^-$ and $ALDH^+$).

Conclusions BT-549 was highly heterogeneous, completely altering the cell subsets under BCSCs enrichment culture demonstrating elevated phenotypic plasticity when undergoing EMT. Further this finding seems to play a major role in DOX-resistance.

Keywords: Breast cancer; cancer stem cell; cellular heterogeneity; chemotherapy; three-dimensional culture

Introduction

Breast cancer is a highly heterogeneous disease classified in distinct molecular subtypes, each one with a unique biology features that lead to differences in response patterns to current therapies and clinical outcomes [1], [2]. In clinical practice, three main types of receptor are used to subtyping of breast cancer: estrogen receptor (ER), progesterone receptor (PR) and the human epidermal growth factor receptor 2 (HER-2) [3]. Tumors that are hormonal receptor positive or HER-2 positive can benefit from anti-hormonal and HER-2 targeted therapies, respectively [4]. Conversely, tumors that are negative for these receptors, named triple-negative breast cancer (TNBC), cannot benefit for target-therapies available nowadays, therefore chemotherapy is the only systemic therapy option [5]. Overall, patients with TNBC tend to have higher rates of relapse and shorter overall survival within 3-5 years after diagnosis compared to other types of breast cancer [6].

The TNBC, accounting for 10-20% of all breast cancer, is a disease with inter- and intra-tumor heterogeneity [7], [8]. Gene expression analysis identified four TNBC molecular subtypes (basal-like 1, basal-like 2, mesenchymal and luminal androgen receptor subtype), displaying unique biological features that significantly have an impact in chemotherapy responses [9], [10]. The cellular heterogeneity of individual tumors, refers as the intra-tumor heterogeneity, can be described in terms of functional differences and distinct phenotype [11] and has been supported by cancer stem cells (CSCs) theory [12].

The CSCs concept proposes a hierarchical cellular organization within the tumors in which CSCs are at the highest level [13] able to self-renew and generate a varied of progeny of highly proliferative cells forming the bulk of the tumor [14]. The CSCs are an aggressive small subpopulation of cancer stem-like cells implicated in chemoresistance, metastatic spread and disease relapse [13], [15]. TNBC aggressive behavior is likely driven by these chemotherapy-resistant cells well-known as breast cancer stem cells (BCSCs). Three markers (CD44, CD24, and ALDH) are commonly used for the identification of putative BCSCs since the $CD44^{+}/CD24^{-/low}$ cells and $ALDH^{+}$ cells were reported to be the BCSCs [16], [17]. The CD44 cell surface marker acts primarily as a receptor for hyaluronic acid, a component of the extracellular matrix regulating cell migration and invasion [18]. In contrast, CD24 leads to an inhibition of cell migration [19]. The aldehyde dehydrogenase 1 (ALDH1) is an enzyme responsible for the oxidation of intracellular aldehydes and seems to play a role in the BCSCs differentiation through the oxidation of retinol to retinoic acid [20]. TNBC shows a high mortality rate due to the development of metastatic disease and resistance to current therapies. CD146 has been implicated in the tumor progression of many cancers and recent work has shown that this molecule promotes breast cancer progression by epithelial-mesenchymal transition (EMT) induction being considered a therapeutic target for TNBC [21].

A model to study the BCSCs is the stem/progenitor cell-enriched assay, a three-dimensional (3D) spherical culture system that allows these cells to grow as multicellular non-adherent spheres named tumorspheres (TS) [22]. This assay attempts to reproduce tumor cellular hierarchy encompassing by tumorigenic CSCs and their differentiated progeny (non-tumorigenic) [23]. TS model is a promising platform for screening potential anti-CSCs drugs [24] and to assess the effects of the currently used drugs on this cell subpopulation.

In the present study, we evaluated the immunophenotype of two TNBC cell lines (BT-549 and Hs 578T) and the TS obtained from these cells using BCSCs markers (CD44, CD24 and ALDH) and EMT marker (CD146). Further, the cells were exposed to doxorubicin (DOX) and paclitaxel (PTX) to determine the half maximal inhibitory concentration IC50. We intended to characterize distinct cell subpopulations for better understanding the cell heterogeneity related to the biological mechanisms of chemoresistance to PTX and DOX.

Materials and methods

Cell culture

BT-549 (ATCC®, HTB-122™) and Hs 578T (ATCC®, HTB-126™) TNBC cell lines and the HMT-3522 S1 (ECACC, 98102210), a non-malignant breast cell line, were propagated in monolayer according to the manufacturer's instructions. For tumorspheres (TS) culture, stem/progenitor cell-enriched assay was performed as described by Moreira et al. [25].

Immunophenotyping analysis

After seven days of suspension culture, the BT-549 TS, Hs 578T TS and HMT-3522 S1 TS were collected, washed with PBS and incubated with Trypsin-EDTA (0.25%/0.5 mM) for two minutes at 37°C to dissociate the cells.

BT-549, Hs 578T and HMT-3522 S1 and the cells dissociated from the TS was washed with PBS and resuspended in labeling buffer (PBS 1X, 0.1% sodium azide and 1% fetal bovine serum). The cells were incubated with the antibodies anti-human CD44 (APC; Immunotools, Friesoythe, Germany), CD24 (FITC; Invitrogen, Carlsbad, CA, EUA), and CD146 (PE; BD Biosciences, San Jose, CA, USA) at the concentration recommended by the manufacturer. The antibodies were incubated protected from light for 20 min at 4°C. Isotype controls were used to set up the threshold for positivity.

ALDEFLUOR™ stem cell identification (Stem Cell Technologies, Vancouver, BC, Canada) was performed to identify $ALDH^+$ cells, according manufacturer's instructions. 1 x 10^6 cells/mL were incubated for 40 minutes at 37°C according to the manufacturer's instructions.

The experiments were performed on the FACSCanto II flow cytometer (BD Bioscience, San Jose, CA, USA) and data were analyzed using FACSDiva 6.1.3 software (BD Bioscience, San Jose, CA, USA).

Cell survival analysis

The effect of DOX and PTX on cell viability was evaluated by MTT (Thiazolyl Blue Tetrazolium Bromide) colorimetric assay. To titrate the IC50 of the chemotherapeutic drugs, the cell lines propagated as monolayer and TS were exposed to a range of drug concentrations (0.1562 µM to 80.0 µM), increasing the concentration by 2-fold between each point. Untreated cells served as controls. The drug was prepared freshly for each experiment and incubated for 48h. The formazan crystals, MTT product, were solubilized with 100 µL of DMSO (Sigma, St. Louis, Missouri, USA) for monolayer culture and 100 µL of isopropanol/0.04 M HCl (Merck, Darmstadt, Germany) for TS culture at room temperature for one hour under agitation. The colorimetric reaction was measured using SpectraMax M5e Microplate Reader (Molecular Devices, Sunnyvale, CA, USA) at 550 nm. The assays were performed in triplicate in at least two independent experiments.

The selectivity index (SI) of PTX and DOX was determined in order to investigate whether the cytotoxic activity was specific to cancer cells. The SI was defined as the ratio of IC50 value on HMT-3522 S1 to BT-549 or Hs 578T. The SI was calculated separately considering the type of culture (monolayer and TS). SI value higher than three were considered to have high selectivity towards cancer cells [26].

Data analysis

IC50 DOX and PTX concentration was estimated by Dr Fit, version 1.042 [27] and statistical analysis was performed in SPSS software, version 18.0 (SPSS Inc., Chicago, Illinois, USA). The statistical significance was assessed at $p<0.05$.

Results

Immunophenotyping analysis

The percentage of positive cells obtained on the immunophenotyping of BT-549, Hs 578T and HMT-3522 S1 cultured as monolayer and TS are showed in Table 1. $CD44^+/CD24^+/CD146^+$ cells were detected on a majority of cells on BT-549. The others subsets found represented minor and restrict cell subpopulations. On the other hand, the main subpopulation on Hs 578T were $CD44^+/CD24^-/CD146^+$ cells follow by $CD44^+/CD24^-/CD146^-$ cells and the majority of cells on HMT-3522 S1 were $CD44^+/CD24^-/$ $CD146^-$ cells. The others subsets represented only restrict cells subpopulations or were not expressed.

Under culture of the cell lines in TS medium, a condition favoring expansion of BCSCs subpopulations, the $CD44^+/CD24^-/CD146^-$ and $CD44^-/CD24^-/CD146^-$ cells were highly enriched on BT-549 TS. Notably the main subpopulation presented in BT-549 disappeared in BT-549 TS. In Hs 578T TS it was observed an enrichment of $CD44^+/CD24^-/CD146^-$ and $CD44^-/CD24^-/CD146^-$ cells and a decrease of $CD44^+/CD24^-/$ $CD146^+$ cells. The subpopulations observed on HMT-3522 S1 TS remains the same as those observed in HMT-3522 S1.

$ALDH^+$ cells were founded in BT-549, BT-549 TS, Hs 578T TS, HMT-3522 S1 and HMT-3522 S1 TS (Table 1), however, only BT-549 TS and HMT-3522 S1 showed a high ALDH activity as indicated by ALDEFLUOR™ assay.

Regarding the individual expression of the markers the majority of cells were $CD24^-$, except for BT-549; $CD44^+$ for all cells; CD146-, except for BT-549 and Hs 578T.

Our analysis revealed broad variation among a majority of the cell subpopulations between monolayer and TS culture on each TNBC cell lines. Likewise, the cell heterogeneity is observed within and among the cell lines and TS. In general, it was observed that the cell subpopulations composing each cell line had more similarity between the BT-549 TS and Hs 578T TS that between the parental cell lines.

Table 1 Immunophenotyping of the cell lines and their tumorspheres (TS)

Phenotype[a]	BT-549	BT-549 TS	Hs 578T	Hs 578T TS	HMT-3522 S1	HMT-3522 S1 TS
$ALDH^+$	0.1	6.2	0.0	0.4	3.0	0.1
$CD44^+/CD24^-/CD146^-$	1.2	45.5	40.7	61.8	90.07	92.50
$CD44^+/CD24^-/CD146^+$	13.0	11.3	50.5	5.6	9.56	5.70
$CD44^+/CD24^+/CD146^-$	0.5	0.1	0.5	0.2	0.02	0.91
$CD44^+/CD24^+/CD146^+$	75.4	0.0	1.2	0.0	0.01	0.03
$CD44^-/CD24^-/CD146^-$	1.2	37.4	7.0	32.3	0.33	0.79
$CD44^-/CD24^-/CD146^+$	3.4	5.5	0.0	0.0	0.0	0.0
$CD44^-/CD24^+/CD146^-$	0.1	0.1	0.0	0.1	0.0	0.06
$CD44^-/CD24^+/CD146^+$	5.3	0.0	0.0	0.0	0.01	0.01
$CD24^+$	87.9	1.6	1.2	0.3	0.0	1.8
$CD24^-$	12.1	98.4	98.8	99.7	100.0	98.2
$CD44^+$	90.4	53.1	92.5	57.7	99.5	98.9
$CD44^-$	9.6	46.9	7.5	42.3	0.5	1.1
$CD146^+$	98.1	35.3	58.1	8.0	9.7	3.9
$CD146^-$	1.9	64.7	41.9	92.0	90.3	96.1

Cell survival analysis

Our results showed statistically different responses to each investigated drugs (PTX and DOX) between the types of culture (monolayer vs. TS) for BT-549, Hs 578T and HMT-3522 S1 (Fig. 1a-f). Exceptions were observed for BT-549 treated with PTX (Fig. 1a) and for HMT-3522 S1 treated with DOX (Fig. 1f).

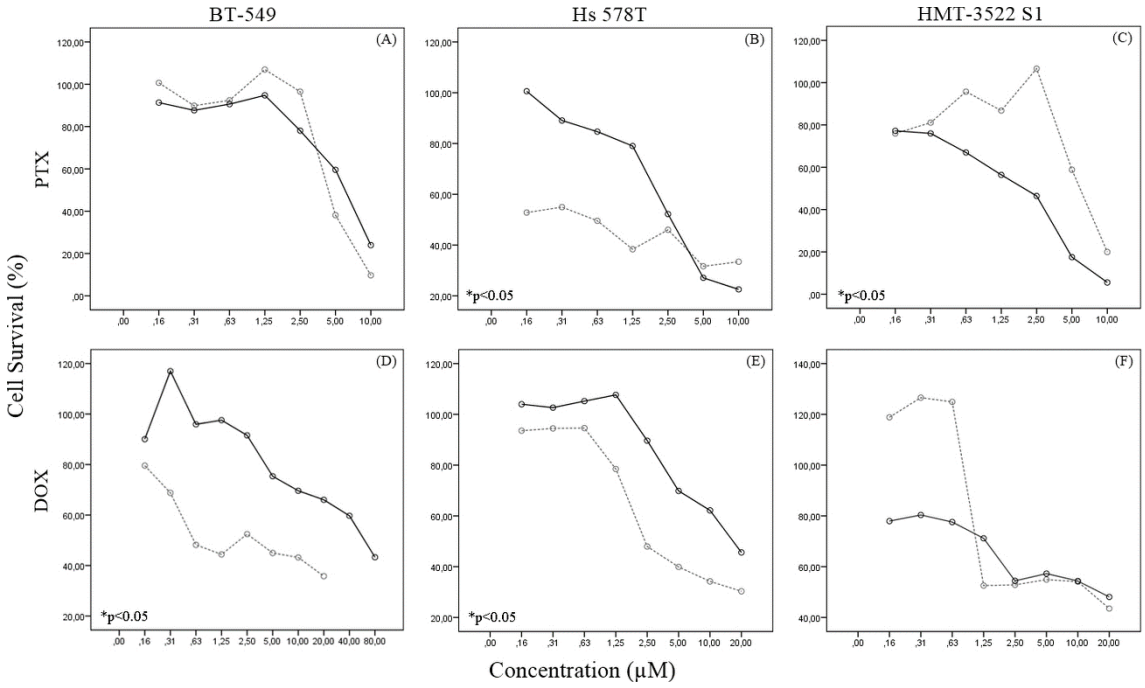

Fig. 1 Cell survival analysis of BT-549, Hs 578T and HMT-3522 S1 cultured in monolayer and as TS after treatment with PTX and DOX. Cells treated with PTX: (a) BT-549; (b) Hs 578T; (c) HMT-3522 S1. Cells treated with DOX: (d)

BT-549; (e) Hs 578T; (f) HMT-3522 S1. Monolayer culture is represented by grey dotted line and TS culture by black line. *Significant differences between monolayer and TS culture. Statistical significance was indicated by $p < 0.05$ using ANOVA

Based on the cell survival curve analysis, the IC50 value of PTX and DOX were estimated by Dr Fit software [27]. IC50 values are showed in Table 2. Statistical analysis revealed significant difference between the types of culture (monolayer vs. TS) only for BT-549 treated with DOX (Table 2)

Table 2 IC50 of paclitaxel and doxorubicin and the selectivity index

CELL LINES	**PTX**		**DOX**	
	IC50[a]	**SI[b]**	**IC50[a]**	**SI[b]**
BT-549	4.22	1.45	0.572*	32.37
BT-549 TS	5.36	0.47	55.7*	0.16
Hs 578T	0.347	22.43	2.39	8.52
Hs 578T TS	2.19	1.16	15.9	3.00
HMT-3522 S1	5.97	-	18.8	-
HMT-3522 S1 TS	2.4	-	12.7	-

[a]IC50 (μM) mean

[b]Selectivity index mean calculated by means of HMT-3522 S1and HMT-3522 S1 TS

*Significant differences between the types of culture (monolayer vs. TS). Statistical significance was indicated by $p < 0.05$ using ANOVA post hoc LSD method (n = 3).

Analysis of drug selectivity demonstrated that DOX exhibits higher selectivity towards BT-549 and Hs 578T as well as PTX towards Hs 578T indicated by SI value greater than 3 (Table 2). The SI obtained for BT-549 treated with DOX and Hs 578T treated with PTX showed significant statistical difference between monolayer and TS culture (Fig. 2). However, the IC50 of DOX and PTX used in TS culture were highly toxic to HMT-3522 S1 TS (Table 2).

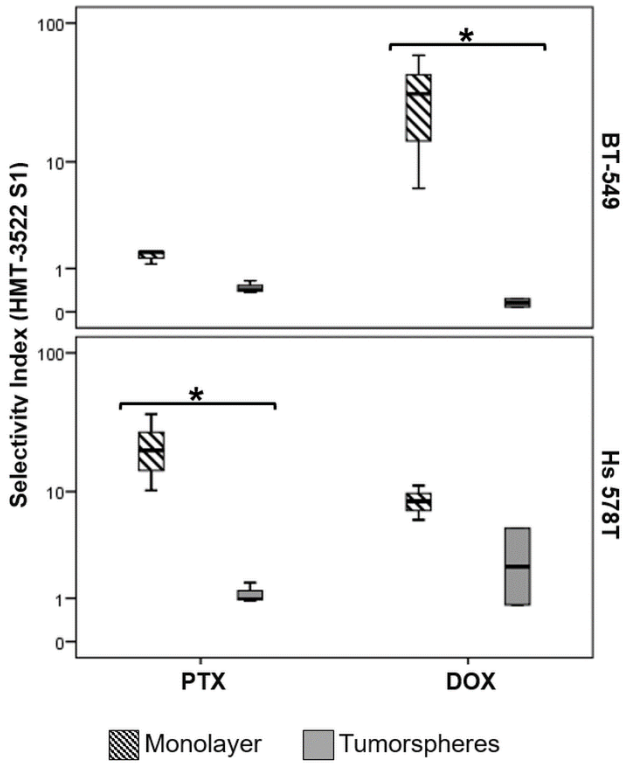

Fig. 2 Statistical box plot analysis of selectivity index of PTX and DOX for BT-549 and Hs 578T. Monolayer culture is represented in diagonal black lines and TS culture in grey. *Significant differences between the types of culture (monolayer vs. TS). Statistical significance was indicated by $p < 0.05$ using ANOVA post hoc LSD method (n = 3)

Discussion

The study and treatment of cancer is complicated by diversity in biological properties such as cellular morphology, proliferation index, cell motility, genetic alterations and metabolism within and between tumors [28]. The presence of BCSCs accounts for breast tumor phenotypic and functional heterogeneity [29] being these cells the main player in chemoresistance, metastasis and disease recurrence [30].

BCSCs possess stem cell-like features such as self-renewal and differentiation abilities generating breast tumors which recapitulate the heterogeneity of the parental tumor [16], [17]. It is well-known that residual BC tumors are enriched for BCSCs after chemotherapy [31]–[33], being that multiple mechanisms confer this resistance, among them quiescence cells, apoptosis evasion, drug efflux mechanisms, DNA repair, self-renewal, hypoxic and inflammatory microenvironment [15]. Liu et al. [34] showed that BCSCs exist in two phenotypic states: (i) the mesenchymal-like characterized as $CD44^+/CD24^-$ cells, mainly quiescent with high invasive capacity and (ii) the epithelial-like identified by highly proliferative $ALDH^+$ cells. BCSCs display a plasticity that allows them to transit between the two states, thus supporting metastatic colonization. In contrast, the $CD44^-/CD24^+$ cells are associated with epithelial cells and are largely present in distant metastases [35], [36]. Further Grosse-Wilde et al. [37] identified that $CD44^+/CD24^+$ cells had mesenchymal and epithelial features demonstrated by the expression of genes representative of each phenotype being therefore plastic and able to self-renewal.

BT-549 and Hs 578T TNBC cell lines are classified as claudin-low, a BC subtype characterized by high enrichment for epithelial-mesenchymal transition (EMT) markers, immune response genes and cancer stem cell features [38]. EMT is a reversible process by which epithelial cells lose their characteristics to acquire mesenchymal properties providing

migratory ability to the cells [39]. Metastatic disease is the leading cause of death among BC patients [40] and almost all patients with TNBC die of this disease [6]. EMT endows epithelial cells with stem cell features, providing a close association between EMT, BCSCs and drug resistance [13], [41]. The reverse process, known as mesenchymal-epithelial transition (MET), trigger the cessation of cell migration inducing cell adhesion and proliferation at the secondary site for metastatic colonization [42].

As observed the breast cancer cells are heterogeneous considering the cell surface markers CD44 and CD24 expression. However their relation to CD146, an EMT marker [21], has not yet been evaluated to our knowledge. Then in order to characterize the BCSCs, we evaluated the CD44, CD24 and CD146 by flow cytometry. Beyond that, the ALDH functional expression was also evaluated. Our immunophenotyping results highlights the cell heterogeneity between the TNBC cell lines being the $CD44^+/CD24^+/CD146^+$ hybrid tumor cells the main population presented in BT-549 whereas in Hs 578T were the $CD44^-/CD24^-/CD146^-$ tumor cells and in HMT-3522 S1 were $CD44^+/CD24^-/CD146^-$ BCSCs EMT-like cells. This data reinforces the EMT characteristic of BT-549, since the majority of cells expressed CD146 and they did not express E-cadherin according our microscopy fluorescence data (data not show). We designed a schematic representation of tumor heterogeneity based on the profile of cell subpopulations obtained by immunophenotyping (Fig. 3a). This model is useful to better understanding the differences within and among the cells.

The stem/progenitor cell-enriched assay performed by us was successful as showed by the highly increase of BCSCs subpopulation ($CD44^+/CD24^-$) and the ability to form non-adherent multicellular spheres. However, the enriched BCSCs was associated with $CD146^-$ subset once the BCSCs $CD146^+$ showed decreases or remained unchanged. Notably, for BT-549 TS it was observed an enrichment of the $CD44^-/CD24^-/CD146^-$ tumor cells.

Grosse-Wilde et al. [37] showed a nearly complete phenotypic conversion from $CD44^-/CD24^+$ epithelial cells, sorted from a normal human mammary epithelial immortalized, to $CD44^+/CD24^-$ mesenchymal cells under stem/progenitor cell-enriched assay. Such plasticity was not observed in $CD44^+/CD24^-$ mesenchymal cells, however it was highly enriched in the culture indicating a self-renewal capacity [37]. Indeed, [41] demonstrated that the $CD44^-/CD24^+$ epithelial cells is unable to survive in non-adherent condition, nonetheless in monolayer culture this cells can be originate from the $CD44^+/CD24^-$ mesenchymal cells. Our results for BT-549 under the stem/progenitor cell-enriched assay showed remarkable phenotypic change as described by [37], but this only occurred when either $CD44^-/CD24^+$ and $CD44^+/CD24^+$ cells were $CD146^+$ reinforcing the EMT features of this cell line. We suggest that $CD44^-/CD24^+/CD146^+$ epithelial tumor cells can undergo EMT and therefore, have potential to become BCSC, since it is known that this process can trigger the transformation of non-BCSC into BCSC. CD146 promoted cell motility, invasion and generate BCSC through EMT supporting breast cancer progression [21], [43], [44].

BT-549 TS was the only one with high ALDH activity, thus the presence of BCSCs ($CD44^+/CD24^-$ and $ALDH^+$) suggests a greatest tumor-initiating, aggressive and invasive capacity of this cell line [17], [34]. Grosse-Wilde et al. [37] showed that $CD44^+/CD24^+$ hybrid tumor cells and $CD44^-/CD24^+$ epithelial tumor cells produced 7.0% and 5.7% $ALDH1^+$ progenies, respectively. We propose that these two cells are capable to convert into $CD44^+/CD24^-/CD146^-$ EMT-like BCSCs and generate $ALDH^+$ epithelial-like BCSCs, that can self-renewal and differentiate into non-BCSC such as $CD44^-/CD24^-/CD146^-$ tumor cells (Fig. 3b). This is in agreement with [45] that showed cleavage of CD146 from the cell surface induced by CD44 leading to an increase in soluble CD146 and subsequently invasion of breast cancer cells. Further, according to ATCC®, the tumor tissue that originates BT-549 cell line had locoregional metastasis. In contrast, the minor subpopulations of $CD44^+/CD24^+$ and $CD44^-/CD24^+$ cells present in the Hs 578T, in additional to the lack of ALDH expression may led to the smaller enrichment of $CD44^+/CD24^-/CD146^-$ EMT-like

BCSCs and ALDH$^+$ epithelial-like BCSCs observed in the Hs 578T TS compared to BT-549. Or yet the phenotypic change related to CD44/CD24 has already occurred in the parental cell line Hs 578T.

Tumor cell heterogeneity have an impact on drug response and so we evaluable the effect of DOX and PTX, commonly used drugs in chemotherapy of TNBC patients [46]. PTX had a high toxicity against HMT-3522 S1, a non-malignant cell line used as control, and DOX was only toxic when used the IC50 estimated for BT-549 TS. BT-549 cells had a predominant population of CD24$^+$ cells whereas all the others were mainly CD24$^-$. Our cytotoxicity data showed that BT-549 was the only one more resistant to PTX instead of DOX, according to the IC50 value. This is in accordance with the previous findings showing that the CD24$^+$ cells are more resistant to docetaxel, a taxane drug like PTX, and the CD24$^-$ cells are more resistant to DOX [47]. Our results demonstrated significant statistical difference between the types of culture (monolayer vs. TS) only for BT-549 treated with DOX, which were 97.4X more sensitive to DOX compared to BT-549 TS. Nonetheless, although the cells showed different sensitivity to drugs, what they have in common is that they have a high proportion CD44$^+$/CD24$^-$/CD146$^-$ BCSC EMT-like, except for BT-549. Beyond that, recently, our group suggested that *STAT3* gene upregulation is related to DOX-resistance in BT-549 TS, since this gene showed an increase of 8.89-fold in its expression after DOX treatment [25].

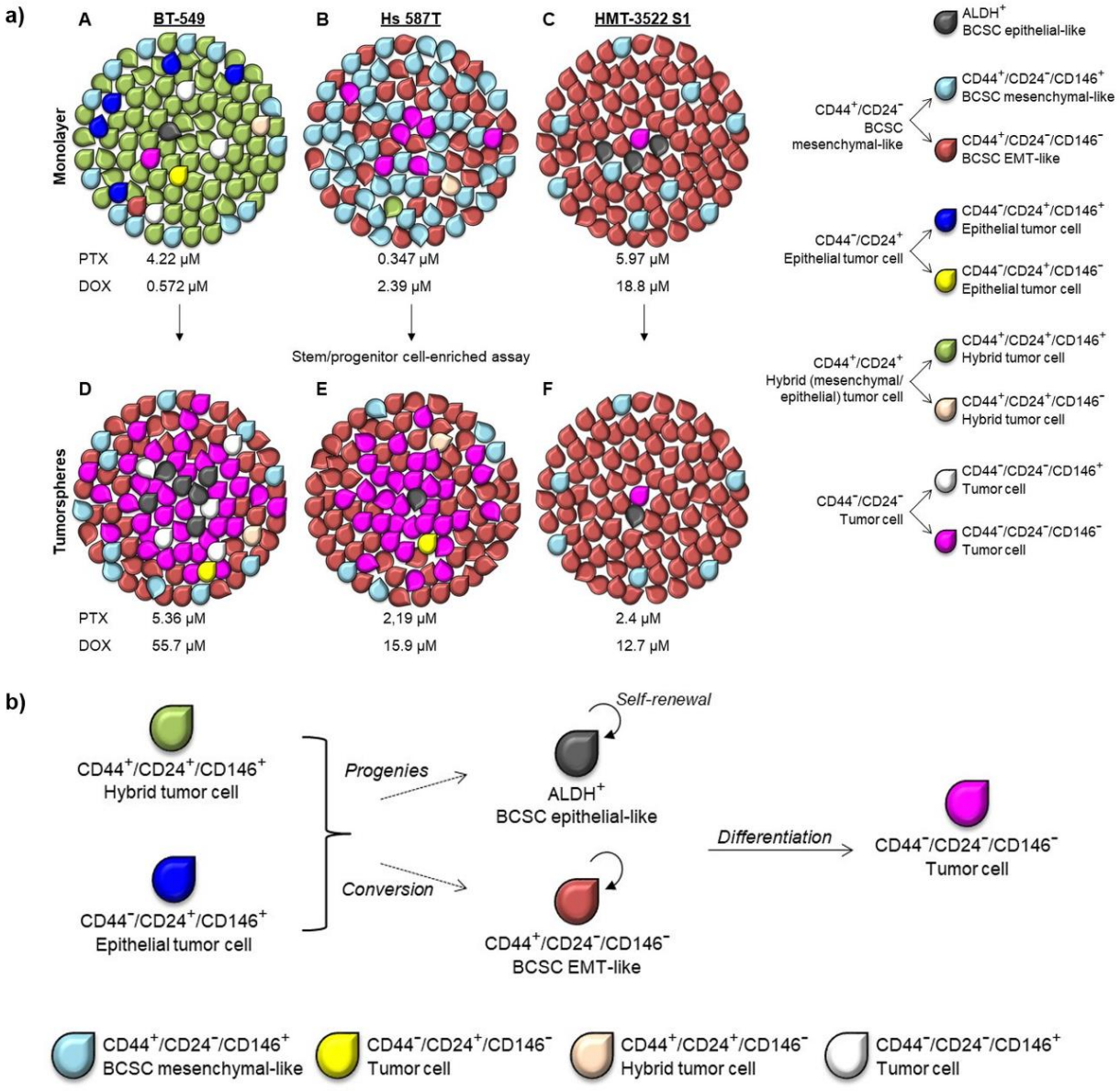

Fig. 3 Breast cancer cell heterogeneity model. **a)** Schematic representation of tumor cell heterogeneity. (a) BT-549, (b) Hs 578T (c) HMT-3522 S1, (d) BT-549 TS, (e) Hs 578T TS, (f) HMT-3522 S1 TS immunophenotyping for BCSCs markers (CD44, CD24, ALDH) and EMT marker (CD146). Each color represents a cell phenotype (see key on right of figure). The BCSCs characterized as mesenchymal-like and epithelial-like were identified by $CD44^{+}/CD24^{-}$ and $ALDH^{+}$ subsets, respectively. The non-BCSCs were named tumor cell ($CD44^{-}/CD24^{-}$ subset), epithelial tumor cell ($CD44^{-}/CD24^{+}$ subset) and the hybrid tumor cell defined by the presence of mesenchymal and epithelial features ($CD44^{+}/CD24^{+}$ subset). The presence of CD44 and absence of CD146 on cell surface was considered an indicator that cell underwent EMT. **b)** Model of cell subpopulations transition dynamics under BCSCs-enriched assay in BT-549. The plasticity properties of $CD44^{+}/CD24^{+}/CD146^{+}$ hybrid tumor cell and $CD44^{-}/CD24^{+}/CD146^{+}$ epithelial tumor cell presented in the parental cell line enable the phenotypic conversion into $CD44^{+}/CD24^{-}/CD146^{-}$ EMT-like BCSCs. Further these non-BCSCs can generate $ALDH^{+}$ epithelial-like BCSCs. The enriched BCSCs undergo differentiation into $CD44^{-}/CD24^{-}/CD146^{-}$ tumor cell and self-renewal

Considering all the characteristics studied by us that are associated at aggressive cancer cells and the fact of the cellular heterogeneity present in tumors is not taken into account by most studies, they indicate the necessity of more studies to elucidate the behavior of cell subpopulation in clinical assay and your distribution within tumor mass as predictive indicator of chemoresistance.

Conclusion

For TNBC treatment until now no actionable targets were identified, most likely due the vast heterogeneous disease. In this way, cytotoxic chemotherapy remains the mainstay treatment for TNBC patients resulting in poor survival. An aggravating in chemoresistance is the drug-induced phenotypic plasticity, wherein BCSCs arise from the conversion of non-BCSCs conferring resistance to the treatment. Recently most study evaluates the cells that form the tumor as one unit. However, this does not faithfully represent the role played by each cell, as demonstrated by us. Our result demonstrates the cellular heterogeneity among and within BT-549 and HS 578T TNBC cell lines in term of morphology, phenotyping and drug response. In additional, BT-549 was highly heterogeneous, completely changing the cell subsets under BCSCs enrichment culture condition, demonstrating elevated phenotypic plasticity when undergoing EMT. Further this finding seems to play a major role in DOX-resistance. Thus, understanding tumor heterogeneity and how BCSCs resist chemotherapy via single cell analysis could lead to the development of more efficient cancer treatments improving survival in patients with TNBC.

Conflicts of interest

The authors declare that they have no conflict of interest.

Acknowledgments

Not applicable

Funding

This work was financially supported through grants from Fundação de Amparo à Pesquisa do Estado de Minas Gerais (FAPEMIG) [grant number CBB-APQ-00054-12], Coordenação de Aperfeiçoamento de Pessoal de Nível Superior (CAPES) and Conselho Nacional de Desenvolvimento Científico e Tecnológico (CNPq).

References

[1] C. M. *+ Perou *et al.*, "Molecular portraits of human breast tumours. [Letter]," *Nature*, vol. 406, no. august, pp. 747–752, 2000.

[2] T. Sorlie *et al.*, "Gene expression patterns of breast carcinomas distinguish tumor subclasses with clinical implications," *Proc. Natl. Acad. Sci.*, vol. 98, no. 19, pp. 10869–10874, 2001.

[3] D. C. Allred, "Issues and updates: Evaluating estrogen receptor-α, progesterone receptor, and HER2 in breast cancer," *Mod. Pathol.*, vol. 23, no. SUPPL. 2, pp. S52–S59, 2010.

[4] S. J. L. Payne, R. L. Bowen, J. L. Jones, and C. A. Wells, "Predictive markers in breast cancer - The present," *Histopathology*, vol. 52, no. 1, pp. 82–90, 2008.

[5] B. D. Lehmann and J. A. Pietenpol, "Clinical implications of molecular heterogeneity in triple negative breast cancer Brian," *Breast*, vol. 24, no. 02: S36-S40, pp. 1–11, 2015.

[6] R. Dent *et al.*, "Triple-negative breast cancer: Clinical features and patterns of recurrence," *Clin. Cancer Res.*, vol. 13, no. 15, pp. 4429–4434, 2007.

[7] V. G. Abramson, B. D. Lehmann, and T. J. Ballinger, "Subtyping of triple-negative breast cancer: implications for therapy," *Cancer*, vol. 121, no. 1, pp. 8–16, 2015.

[8] G. Palma *et al.*, "Triple negative breast cancer: looking for the missing link between biology and treatments," *Oncotarget*, vol. 6, no. 29, pp. 26560–26574, 2015.

[9] B. D. Lehmann *et al.*, "Refinement of Triple-Negative Breast Cancer Molecular Subtypes: Implications for Neoadjuvant Chemotherapy Selection," *PLoS One*, vol. 11, no. 6, p. e0157368, 2016.

[10] B. D. B. Lehmann *et al.*, "Identification of human triple-negative breast cancer subtypes and preclinical models for selection of targeted therapies," *J. Clin. Invest.*, vol. 121, no. 7, pp. 2750–2767, 2011.

[11] M. Tellez-Gabriel, B. Ory, F. Lamoureux, M. F. Heymann, and D. Heymann, "Tumour heterogeneity: The key advantages of single-cell analysis," *Int. J. Mol. Sci.*, vol. 17, no. 12, 2016.

[12] N. A. Fonseca, A. Filipa, V. Moura, S. Simões, and J. Nuno, "The cancer stem cell phenotype as a determinant factor of the heterotypic nature of breast tumors," *Crit. Rev. Oncol. / Hematol.*, vol. 113, pp. 111–121, 2017.

[13] A. Carnero, Y. Garcia-Mayea, C. Mir, J. Lorente, I. T. Rubio, and M. E. LLeonart, "The cancer stem-cell signaling network and resistance to therapy," *Cancer Treat. Rev.*, vol. 49, pp. 25–36, 2016.

[14] D. R. Pattabimaran and R. A. Weinberg, "Tackling the cancer stem cells – what challenges do they pose?," *Nat Rev Drug Discov*, vol. 13, no. 7, pp. 497–512, 2014.

[15] J. Zhao, "Cancer stem cells and chemoresistance: The smartest survives the raid," *Pharmacol. Ther.*, vol. 160, pp. 145–158, 2016.

[16] M. Al-Hajj, M. S. Wicha, A. Benito-Hernandez, S. J. Morrison, and M. F. Clarke, "Prospective identification of tumorigenic breast cancer cells.," *Proc. Natl. Acad. Sci. U. S. A.*, vol. 100, no. 7, pp. 3983–8, 2003.

[17] C. Ginestier *et al.*, "ALDH1 is a marker of normal and malignant human mammary stem cells and a predictor of poor clinical outcome," *Cell Stem Cell*, vol. 1, no. 5, pp. 555–567, 2007.

[18] T. Chanmee, P. Ontong, K. Kimata, and N. Itano, "Key Roles of Hyaluronan and Its CD44 Receptor in the Stemness and Survival of Cancer Stem Cells," *Front. Oncol.*, vol. 5, no. August, pp. 1–11, 2015.

[19] H. Schabath, "CD24 affects CXCR4 function in pre-B lymphocytes and breast carcinoma cells," *J. Cell Sci.*, vol. 119, no. 2, pp. 314–325, 2006.

[20] C. Ginestier *et al.*, "Retinoid signaling regulates breast cancer stem cell differentiation," *Cell Cycle*, vol. 8, no. 20, pp. 3297–3302, 2009.

[21] Q. Zeng *et al.*, "CD146, an epithelial-mesenchymal transition inducer, is associated with triple-negative breast cancer," *Proc. Natl. Acad. Sci.*, vol. 109, no. 4, pp. 1127–1132, 2012.

[22] D. Ponti *et al.*, "Isolation and In vitro Propagation of Tumorigenic Breast Cancer Cells with Stem / Progenitor Cell Properties," no. 13, pp. 5506–5512, 2005.

[23] T. Ishiguro, H. Ohata, A. Sato, K. Yamawaki, T. Enomoto, and K. Okamoto, "Tumor-derived spheroids: Relevance to cancer stem cells and clinical applications," *Cancer Sci.*, vol. 108, no. 3, pp. 283–289, 2017.

[24] C.-H. Lee, C.-C. Yu, B.-Y. Wang, and W.-W. Chang, "Tumorsphere as an effective *in vitro* platform for screening anti-cancer stem cell drugs," *Oncotarget*, vol. 7, no. 2, pp. 1215–1226, 2016.

[25] M. P. Moreira, L. da Conceição Braga, G. D. Cassali, and L. M. Silva, "STAT3 as a promising chemoresistance biomarker associated with the CD44+/high/CD24-/low/ALDH+ BCSCs-like subset of the triple-negative breast cancer (TNBC) cell line," *Exp. Cell Res.*, vol. 363, no. 2, pp. 283–290, 2018.

[26] W. Mahavorasirikul, V. Viyanant, W. Chaijaroenkul, A. Itharat, and K. Na-Bangchang, "Cytotoxic activity of Thai medicinal plants against human cholangiocarcinoma, laryngeal and hepatocarcinoma cells in vitro," *BMC Complement. Altern. Med.*, vol. 10, no. 55, pp. 2–8, 2010.

[27] G. Y. Di Veroli *et al.*, "An automated fitting procedure and software for dose-response curves with multiphasic features," *Sci. Rep.*, vol. 5, pp. 1–11, 2015.

[28] V. Almendro, A. Marusyk, and K. Polyak, "Cellular Heterogeneity and Molecular Evolution in Cancer," *Annu. Rev. Pathol. Mech. Dis.*, vol. 8, no. 1, pp. 277–302, 2013.

[29] J. E. Visvader and G. J. Lindeman, "Cancer stem cells: Current status and evolving complexities," *Cell Stem Cell*, vol. 10, no. 6, pp. 717–728, 2012.

[30] M. Luo, M. Brooke, and M. S. Wicha, "Epithelial-Mesenchymal Plasticity of Breast Cancer Stem Cells: Implications for Metastasis and Therapeutic Resistance," *Curr. Pharm. Des.*, vol. 21, no. 10, pp. 1301–1310, 2015.

[31] C. J. Creighton *et al.*, "Residual breast cancers after conventional therapy display mesenchymal as well as tumor-initiating features," *Proc. Natl. Acad. Sci. U. S. A.*, vol. 106, no. 33, pp. 13820–13825, 2009.

[32] D. Jia *et al.*, "Cardamonin reduces chemotherapy-enriched breast cancer stem-like cells in vitro and in vivo," vol. 7, no. 1, pp. 2015–2016, 2015.

[33] R. Sun *et al.*, "Nanoparticle-facilitated autophagy inhibition promotes the efficacy of chemotherapeutics against breast cancer stem cells," *Biomaterials*, vol. 103, pp. 44–55, 2016.

[34] S. Liu *et al.*, "Breast cancer stem cells transition between epithelial and mesenchymal states reflective of their normal counterparts," *Stem Cell Reports*, vol. 2, no. 1, pp. 78–91, 2014.

[35] M. Shipitsin *et al.*, "Molecular Definition of Breast Tumor Heterogeneity," *Cancer Cell*, vol. 11, no. 3, pp. 259–273, 2007.

[36] S. Y. Park, H. E. Lee, H. Li, M. Shipitsin, R. Gelman, and K. Polyak, "Heterogeneity for stem cell-related markers according to tumor subtype and histologic stage in breast cancer," *Clin. Cancer Res.*, vol. 16, no. 3, pp. 876–887, 2010.

[37] A. Grosse-Wilde *et al.*, "Stemness of the hybrid epithelial/mesenchymal state in breast cancer and its association with poor survival," *PLoS One*, vol. 10, no. 5, pp. 1–28, 2015.

[38] A. Prat *et al.*, "Phenotypic and molecular characterization of the claudin-low intrinsic subtype of breast cancer," *Breast cancer Res.*, vol. 12, no. 5, p. R68, 2010.

[39] S. Lamouille, J. Xu, and R. Derynck, "Molecular mechanisms of epithelial-mesenchymal transition.," *Natl. Rev. Mol. Cell Biol.*, vol. 15, no. 3, pp. 178–196, 2014.

[40] P. Mallini, T. Lennard, J. Kirby, and A. Meeson, "Epithelial-to-mesenchymal transition: What is the impact on breast cancer stem cells and drug resistance," *Cancer Treat. Rev.*, vol. 40, no. 3, pp. 341–348, 2014.

[41] S. A. Mani *et al.*, "The Epithelial-Mesenchymal Transition Generates Cells with Properties of Stem Cells," *Cell*, vol. 133, no. 4, pp. 704–715, 2008.

[42] N. P. A. D. Gunasinghe, A. Wells, E. W. Thompson, and H. J. Hugo, "Mesenchymal-epithelial transition (MET) as a mechanism for metastatic colonisation in breast cancer," *Cancer Metastasis Rev.*, vol. 31, no. 3–4, pp. 469–478, 2012.

[43] A.-M. Imbert, C. Garulli, E. Choquet, M. Koubi, M. Aurrand-Lions, and C. Chabannon, "CD146 Expression in Human Breast Cancer Cell Lines Induces Phenotypic and Functional Changes Observed in Epithelial to Mesenchymal Transition," *PLoS One*, vol. 7, no. 8, p. e43752, 2012.

[44] G. Zabouo *et al.*, "CD146 expression is associated with a poor prognosis in human breast tumors and with enhanced motility in breast cancer cell lines," *Breast Cancer Res.*, vol. 11, no. 1, p. R1, 2009.

[45] A. Ouhtit, M. E. Abdraboh, A. D. Hollenbach, H. Zayed, and M. H. G. Raj, "CD146, a novel target of CD44-signaling, suppresses breast tumor cell invasion," *Cell Commun. Signal.*, vol. 15, no. 1, pp. 1–10, 2017.

[46] A. S. Coates *et al.*, "Tailoring therapies - improving the management of early breast cancer: St GallenInternational Expert Consensus on the Primary Therapy of Early Breast Cancer 2015.," *Ann. Oncol.*, vol. 26, no. 8, pp. 1533–46, 2015.

[47] X. Deng *et al.*, "CD24 Expression and differential resistance to chemotherapy in triple-negative breast cancer," *Oncotarget*, vol. 8, no. 24, pp. 38294–38308, 2017.

ARTIGO 3

Phenotypic, structural and ultrastructural analysis of triple-negative breast cancer cell lines and breast cancer stem cells subpopulation

Phenotypic, structural and ultrastructural analysis of triple-negative breast cancer cell lines and breast cancer stem cells subpopulation

Milene Pereira Moreira[1,3], Fábio André Brayner [2], Luiz Carlos Alves [2], Geovanni Dantas Cassali[3], Luciana Maria Silva[1*]

[1]Serviço de Biologia Celular, Diretoria de Pesquisa e Desenvolvimento, Fundação Ezequiel Dias - Rua Conde Pereira Carneiro 80, Gameleira, Belo Horizonte, Minas Gerais, Brasil, 30510-010.

[2]Laboratório de Imunopatologia Keizo Asami/LIKA-UFPE, Instituto Aggeu Magalhães, Fundação Oswaldo Cruz (IAM/FIOCRUZ) - Campus Universidade Federal de Pernambuco UFPE, Avenida Professor Moraes Rêgo s/n, Cidade Universitária, Recife, Pernambuco, Brasil, 50670-420.

[3]Laboratório de Patologia Comparada, Departamento de Patologia Geral, Instituto de Ciências Biológicas, Universidade Federal de Minas Gerais - Avenida Presidente Antônio Carlos 6627, Pampulha, Belo Horizonte, Minas Gerais, Brasil, 31270-901.

*Corresponding author luciana.silva@funed.mg.gov.br

(55) 31 3314-4746 ORCID: 0000-0002-2038-0405

Abstract

Triple negative breast cancer (TNBC) is a highly heterogeneous disease, which influences the therapeutic response and it makes difficult the discovery of effective targets. This heterogeneity is attributed to the presence of breast cancer stem cells (BCSCs), which determines resistance to chemotherapy and subsequently disease recurrence and metastasis. In this context, this work aimed to evaluate the morphological and phenotypic cellular heterogeneity of two TNBC cell lines cultured in monolayer and tumorspheres (TS) model by fluorescence and electron microscopy and flow cytometry. The BT-549 and Hs 578T analysis demonstrated large phenotypic and morphological heterogeneity between these cell lines, as well as between the cell subpopulations that compose them. BT-549 and Hs 578T are heterogeneous considering the cell surface markers CD44 and CD24 expression, characterizing BCSCs mesenchymal-like cells ($CD44^+/CD24^-$), epithelial cells ($CD44^-/CD24^+$), hybrid cells with mesenchymal and epithelial features ($CD44^+/CD24^+$) and $CD44^-/CD24^-$ cells. BCSCs epithelial-like cells ($ALDH^+$) were founded in BT-549, BT-549 TS and Hs 578T TS, however, only BT-549 TS showed a high ALDH activity. Ultrastructural characterization showed the heterogeneity within and among BT-549 and Hs 578T in monolayer and TS model being formed by more than one cellular type. Further, the mesenchymal characteristic of these cells is demonstrated by E-cadherin absence and filopodia. It is well known that tumor cells heterogeneity can influence survival, therapy responses and in the rate of tumor growth. Thus, molecular understanding of this heterogeneity is essential for the identification of potential therapeutic options and vulnerabilities of oncological patients.

Keywords: cancer stem cell**;** cell line; cellular heterogeneity; triple negative breast cancer

1 Introduction

Breast cancer is the second more common type of cancer worldwide (Bray et al., 2018). This is a highly heterogeneous disease which has great impact on treatment response and clinical outcome (Perou et al., 2000; Sorlie et al., 2001). Triple negative breast cancer (TNBC) comprises approximately 15% of breast cancers that lack expression of estrogen receptor (ER), progesterone receptor (PR) and human epidermal growth factor receptor 2 (HER2). This type of breast cancer is characterized with the higher rates of relapse and shorter overall survival in the metastatic setting compared to other subtypes of breast cancer (Abramson et al., 2015).

Cytotoxic chemotherapy is currently the mainly treatment option for TNBC. The vast disease heterogeneity (inter and intra-tumoral) is responsible for the lack of effective molecular therapeutic targets for this type of cancer (Abramson et al., 2015). Cell heterogeneity has been supported by cancer stem cells (CSCs) (Fonseca et al., 2017). Putative breast cancer stem cells (BCSCs) are identified as $CD44^{+}/CD24^{-/low}$ cells and $ALDH^{+}$ (M. Al-Hajj et al., 2003; Ginestier et al., 2007) and are implicate in disease recurrence, metastasis and drug resistance (Luo et al., 2015). In this way, it is important to better understand the biology of TNBC and for the development of better therapies.

Cancer cell lines are often used as a model for the study of cancer biology. Multicellular tumor spheroid is a three-dimensional (3D) culture model capable to reproduce in vivo characteristics of tumors by recapitulating cell-cell and cell-microenvironment interactions more reliably than conventional two-dimensional (2D) (Laurent et al., 2013; Riffle et al., 2017; Riffle and Hegde, 2017). In this context, the transposition of *in vitro* findings into 3D models for clinical practice enhances the success of anticancer treatment (Lee et al., 2015; Tellez-Gabriel et al., 2016). In addition, they are less expensive compared to *in vivo* models and attenuate the ethical issues involved in these studies (Huber et al., 2016).

3D culture models that promote *in vitro* enrichment of stem/progenitor cells are widely used in the study of CSCs, allowing of these cells to growth as non-adherent multicellular spheres (tumorspheres - TS) (Weiswald et al., 2015). The use of this culture model can provide invaluable clues in cancer therapy (Ishiguro et al., 2017).

In the present study, we evaluated structural and ultrastructural morphology of BT-549 and Hs 578T, an established TNBC cell lines and the TS obtained from these cells. Further we applied immunophenotyping using BCSCs markers (CD44, CD24 and ALDH) to characterize distinct cell subpopulations for better understanding the cell heterogeneity.

2 Materials and Methods

2.1 Cell culture

BT-549 (ATCC®, HTB-122™) and Hs 578T (ATCC, HTB-126™) TNBC breast cancer cell lines were propagated in monolayer according to the manufacturer's instructions.

For tumorspheres (TS) culture, stem/progenitor cell-enriched assay was performed as described by (Moreira et al., 2018).

For Matrigel™ (BD Bioscience) culture, the whole TS obtained after seven day of suspension culture was cultured in three-dimensional (3D) on-top system according with (Lee et al., 2007). These cultures were incubated for three days in a 5% CO_2 incubator at 37°C.

2.2 Database cellular characteristics

Information regarding the TNBC cell lines was obtained from the American Type Culture Collection (ATCC; http://www.atcc.org; accessed December 5, 2017) and scientific publications. In addition, the mutational status of known cancer genes was obtained from and the Catalogue of Somatic Mutations in Cancer database (COSMIC, version 87; http://cancer.sanger.ac.uk/cell_lines; accessed February 22, 2019).

2.3 Morphological characterization

2.3.1 Fluorescence

Cells were labeled with Image-iT™ LIVE Plasma Membrane and Nuclear Labeling kit (Invitrogen), Phalloidin Alexa Fluor® 488 (Molecular Probes) and the nuclei were counterstained with 4,6-diaminidino-2-phenylindole (DAPI; Molecular Probes) according to the manufacturer's instructions. Image acquisition was performed using AxioVert 200 microscope (Zeiss).

2.3.2 Immunofluorescence

Cells were fixed with formaldehyde 4% for 1h at room temperature and washed 3 times with PBS. Then the cells were pre-incubated in blocking solution (10% fetal bovine serum, 1% bovine serum albumin) for 1h at room temperature. The cells were stained with anti-E-Cadherin (BD Bioscience) at room temperature for 45 min. After incubation, cells were washed 3 times with PBS and incubated with secondary antibody anti-mouse IgG (Fab especific) - FITC (Sigma) for 30 min. The nuclei were counterstained with DAPI 300nM for 5 min. Image acquisition was performed using AxioVert 200 microscope (Zeiss).

2.3.3 Scanning electron microscopy (SEM)

Cells were overnight fixed in a solution containing 2.5% glutaraldehyde and 4% formaldehyde in 0.1M sodium cacodylate buffer (pH 7.2) and post-fixation was performed on 1% osmium tetroxide

in 0.1M phosphate buffer for 90 min. Then, three washes were carried out in 0.1M phosphate buffer for further dehydration, using a growing series of 30%, 50%, 70%, 90% and 100% ethanol for 10 min each step. After dehydration, the critical point for the substitution of ethanol with carbon dioxide was obtained, drying the material for assembling the material in metallic stubs using a double carbon tape. The metallization was then performed by covering the material with a thin layer of gold for visualization and analysis on the scanning electron microscope JEOL JSM-5600 LV.

2.3.4 Transmission electron microscopy (TEM)

Cells were overnight fixed in a solution containing 2.5% glutaraldehyde and 4% formaldehyde in 0.1M sodium cacodylate buffer (pH 7.2) and post-fixed for two hours in a solution containing 1% tetroxide of osmium (OsO4) in sodium cacodylate buffer. Then they were dehydrated in increasing series of acetone, infiltrated and embedded in Epon resin. The sections obtained by ultramicrotomy were contrasted with lead citrate and uranyl acetate, and visualized on the Transmission Electron Microscope Tecnai G2 Spirit BioTWIN, FEI Company.

2.4 Flow cytometry analysis of TNBC cell lines

After seven days of suspension culture, the BT-549 TS and Hs 578T TS were collected, washed with PBS and incubated with Trypsin-EDTA (0.25%/0.5 mM) for two minutes at 37°C to dissociate the cells.

BT-549, Hs 578T and the cells dissociated from the TS was washed with PBS and resuspended in labeling buffer (PBS, 0.1% sodium azide and 1% fetal bovine serum). The cells were incubated with the antibodies anti-human CD44 (APC; Immunotools, Friesoythe, Germany), CD24 (FITC; Invitrogen, Carlsbad, CA, EUA) at the concentration recommended by the manufacturer. The antibodies were incubated protected from light for 20 min at 4°C. Isotype controls were used to set up the threshold for positivity.

ALDEFLUOR™ stem cell identification (Stem Cell Technologies, Vancouver, BC, Canada) was performed to identify $ALDH^+$ cells, according manufacturer's instructions. 1 x 10^6 cells/mL were incubated for 40 minutes at 37°C according to the manufacturer's instructions.

The experiments were performed on the FACSCanto II flow cytometer (BD Bioscience, San Jose, CA, USA) and data were analyzed using FACSDiva 6.1.3 software (BD Bioscience, San Jose, CA, USA).

3 Results and Discuss

3.1 Cell lines characteristics

We have compiled the currently available data (Table 1) and carried out further analyses to better characterize BT-549 and Hs 578T TNBC cell lines. The cells are morphologically and molecularly very similar, although they are distinct regarding mutant genes, being only *TP53* mutated in both cells.

Table 1 TNBC breast cell lines characteristics

Cell line	BT-549 (HTB-122™)	Hs 578T (HTB-126™)
Source[a]	Primary breast	Primary breast
Tumor type[a]	Ductal carcinoma	Carcinoma
Molecular Classification		
BC Subtype[b,c]	Basal B Claudin-low	Basal B Claudin-low
TNBC Subtype[d]	Mesenchymal	Mesenchymal stem-like
Mutant Gene (Cancer Gene Census)[e]	*PTEN, TERT, TP53, RB1*	*HNFIA, NF1, PIK3R1, TP53, MED12*
Morphology		
2D model[a]	Epithelial	Epithelial
3D model[f]	Stellate	Stellate
Tumorigenicity[g]	Yes	Yes
Invasive/ Metastatic[h]	Yes	Yes

Source and tumor ATCC®[a]
Molecular classification: [b](Neve et al., 2006)[c] (Aleix Prat et al., 2010); [d] (Lehmann et al., 2011)
Mutant Gene[e]: mutation related to known cancer gene from COSMIC database
Morphology: [a]ATCC® ; [f](Kenny et al., 2007)
Tumorigenicity[g]: (Daniel et al., 2011; Tate et al., 2012)
Invasive/Metastatic[h]: (Bischoff et al., 2014; Ferrari-Amorotti et al., 2014; Kenny et al., 2007; Kim et al., 2015; Rhodes et al., 2015; Zhang et al., 2014; Ziperstein et al., 2015)

3.2 Flow cytometry analysis of TNBC cell lines

The percentage of positive cells obtained on the immunophenotyping of BT-549, Hs 578T cultured as monolayer and TS are showed in Table 2. $CD44^{+}/CD24^{+}$ cells were detected on a majority of cells on BT-549. The others subsets found represented minor cell subpopulations. On the other hand, the main subpopulation on Hs 578T were $CD44^{+}/CD24^{-/low}$ cells. The others subsets represented only restrict cells subpopulations or were not expressed.

Under culture of the cell lines in TS medium, a condition favoring expansion of BCSCs subpopulations, the $CD44^{+}/CD24^{-/low}$ cells were highly enriched on BT-549 TS. Notably the main subpopulation presented in BT-549 almost disappeared in BT-549 TS. The main subpopulation on Hs 578T TS were $CD44^{+}/CD24^{-/low}$ cells, however it showed a decreased compared to Hs 578T. The $CD44^{-}/CD24^{-}$ showed an increased in both TS compared to monolayer cells. The $CD44^{-}/CD24^{+}$

cells on BT-549 TS and Hs 578T TS and the $CD44^+/CD24^+$ on Hs 578T TS presented only little changes in their expression.

$ALDH^+$ cells were founded in BT-549, BT-549 TS and Hs 578T TS (Table 2), however, only BT-549 TS showed a high ALDH activity as indicated by ALDEFLUOR™ assay.

This results showed that BT-549 TS and HS 578T TS presents the BCSCs-like subset determined by $CD44^+/CD24^{-/low}$ cells. Further, BT-549 TS is highly enriched of BCSCs-like determined by $ALDH^+$ cells.

Table 2 Immunophenotyping of the cell lines and their tumorspheres

Phenotype	**Cells subpopulations (%)**			
	BT-549	**BT-549 TS**	**Hs 578T**	**Hs 578T TS**
$ALDH^+$	0.1	6.2	0.0	0.4
$CD44^+/CD24^{-/low}$ (BCSCs)	8.9	52.1	91.3	57.5
$CD44^+/CD24^+$	81.5	1.0	1.2	0.2
$CD44^-/CD24^+$	6.4	0.6	0.0	0.1
$CD44^-/CD24^-$	3.2	46.2	7.4	42.3

BCSCs possess stem cell-like features such as self-renewal and differentiation abilities generating breast tumors which recapitulate the heterogeneity of the parental tumor (Muhammad Al-Hajj et al., 2003; Ginestier et al., 2007). Further, residual breast cancer tumors are enriched for BCSCs after chemotherapy (Creighton et al., 2009; Jia et al., 2015; Sun et al., 2016). Breast cancer cells are heterogeneous considering the cell surface markers CD44 and CD24 expression: (i) the $CD44^+/CD24^-$ cells characterized the BCSCs mesenchymal-like phenotype with cells mainly quiescent and highly invasive, (ii) the $CD44^-/CD24^+$ cells are associated with epithelial cells and are largely present in distant metastases (Park et al., 2010; Shipitsin et al., 2007), (iii) the $CD44^+/CD24^+$ cells had mesenchymal and epithelial features confirmed by the expression of genes representative of each phenotype being therefore plastic and able to self-renewal (Grosse-Wilde et al., 2015). Beyond that, the $ALDH^+$ cells characterized the highly proliferative BCSCs epithelial-like phenotype. In this way, BCSCs display a plasticity that allows them to transit between the states mesenchymal-like and epithelial-like, thus supporting metastatic colonization (Liu et al., 2014).

3.3 Structural and ultrastructural characterization of TNBC cell lines

BT-549 and Hs 578T grew as adherent epithelial-like monolayer cells in a disorganized manner, appearing to be overlapping one under the other as typical of cancer cells due to the loss contact-

dependent growth inhibition. Hs 578T presents a nucleus-cytoplasm ratio greater than the BT-549 (Fig. 1-I A-D; M-P). The expression of E-cadherin was not observed in the two cell lines (Fig. 1-I E, F, Q, R).

Under stem/progenitor cell-enriched assay, the BT-549 TS (Fig. 1-I G-L) and Hs 578T TS (Fig. 1-I S-Z) grew into 3D non-adherent multicellular spheroids indicated by the quantity of visualized nucleus (Fig. 1-I H, J, L, T, V, Z) and with a diffuse distribution of actin filaments (Fig. 1-I G, H, S, T). Hs 578T TS are twice the size, structurally more dense and the cell surface is better delineated compared to BT549 TS. BT-549 TS and Hs 578T TS presented no expression of E-cadherin (Fig. 1-I K, L, X, Z). In Figure 1-II is possible to visualized the tumorsphere formation during the seven days of culture.

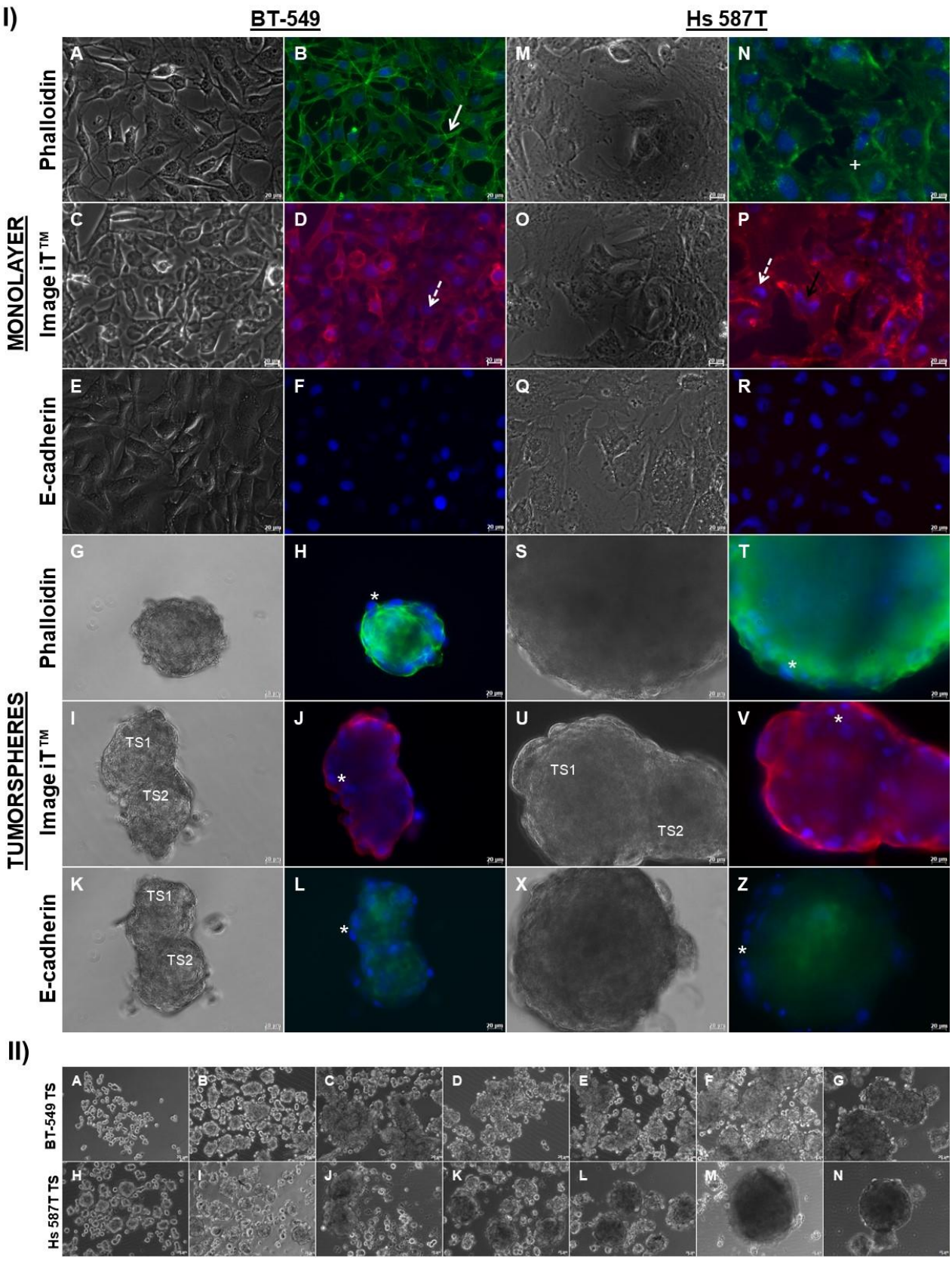

Fig. 1. BT-549 and Hs 578T cell lines growing as monolayer and as tumorspheres (TS). I) Cells were stained with Phalloidin/DAPI (green/blue), Image iT™ LIVE Plasma Membrane and Nuclear Labeling kit (red/blue) and E-cadherin/DAPI (green/blue). BT-549 (A-F) and Hs 578T (M-R) cell lines cultivated in monolayer**.** The phase contrast images are represented in A, C, E for BT-549 and M, O, Q for Hs 578T. Actin stained in

cytoplasmic projections (white arrow) and peripherally to the plasmatic membrane (cross). Small and spherical nuclei of BT-549 cell (white dotted arrow) and polymorphic nuclei of Hs 578T cell (spherical -with dotted arrow; reniform - black arrow). It is observed no expression of E-cadherin in the plasma membrane for both cell lines. BT-549 TS (G-L) and Hs 578T TS (S-Z) grew as tumorspheres. The phase contrast images are represented in G, I, H for BT-549 TS and S, U, X for Hs 578T TS. Multicellular structures are observed, demonstrated by several nuclei presented (asterisk) and actin filaments had homogeneous distribution. Both cell lines are E-cadherin negative. II) Tumorspheres culture showing the day 1 (A, H) to day 7 (G, N), respectively for BT-549 TS and Hs 578T TS. Hs 578T TS are observed since the day 1 (asterisk) and during the period of culture there were a decrease in the number of tumorspheres.

BT-549 and Hs 578T TNBC cell lines are classified as claudin-low, a BC subtype characterized by high enrichment for epithelial-mesenchymal transition (EMT) markers, immune response genes and cancer stem cell features (A Prat et al., 2010). EMT is a reversible process by which epithelial cells lose their characteristics to acquire mesenchymal properties providing migratory ability to the cells (Lamouille et al., 2014). E-cadherin loss is the main marker of EMT, thus the lack of expression of this adhesion molecule in BT-549 and Hs 578T showed by us endorse the mesenchymal features of these cells. Additionally, several authors demonstrated that these cells express mesenchymal markers (N-cadherin and vimentin) (Ferrari-Amorotti et al., 2014; Kim et al., 2015; Zhang et al., 2014; Ziperstein et al., 2015). Furthermore, the absence of E-cadherin is also sustained in the BT-549 TS and Hs 578T TS.

The whole tumorspheres, after seven day of culture under stem/progenitor cell-enriched assay, were plated in Matrigel™ for three days (Figure 2-I). The tumorspheres attach to the Matrigel™ and it was possible to visualize cells migration from the tumorspheres with an invasive aspect. The morphology can also be visualized through the stained with Phalloidin/DAPI and Image iT™. The tumorspheres presented a higher expression of actin filaments than the migrated cells. BT-549 TS and Hs 578T TS presented no expression of E-cadherin in Matrigel™ culture (Figure 2-II).

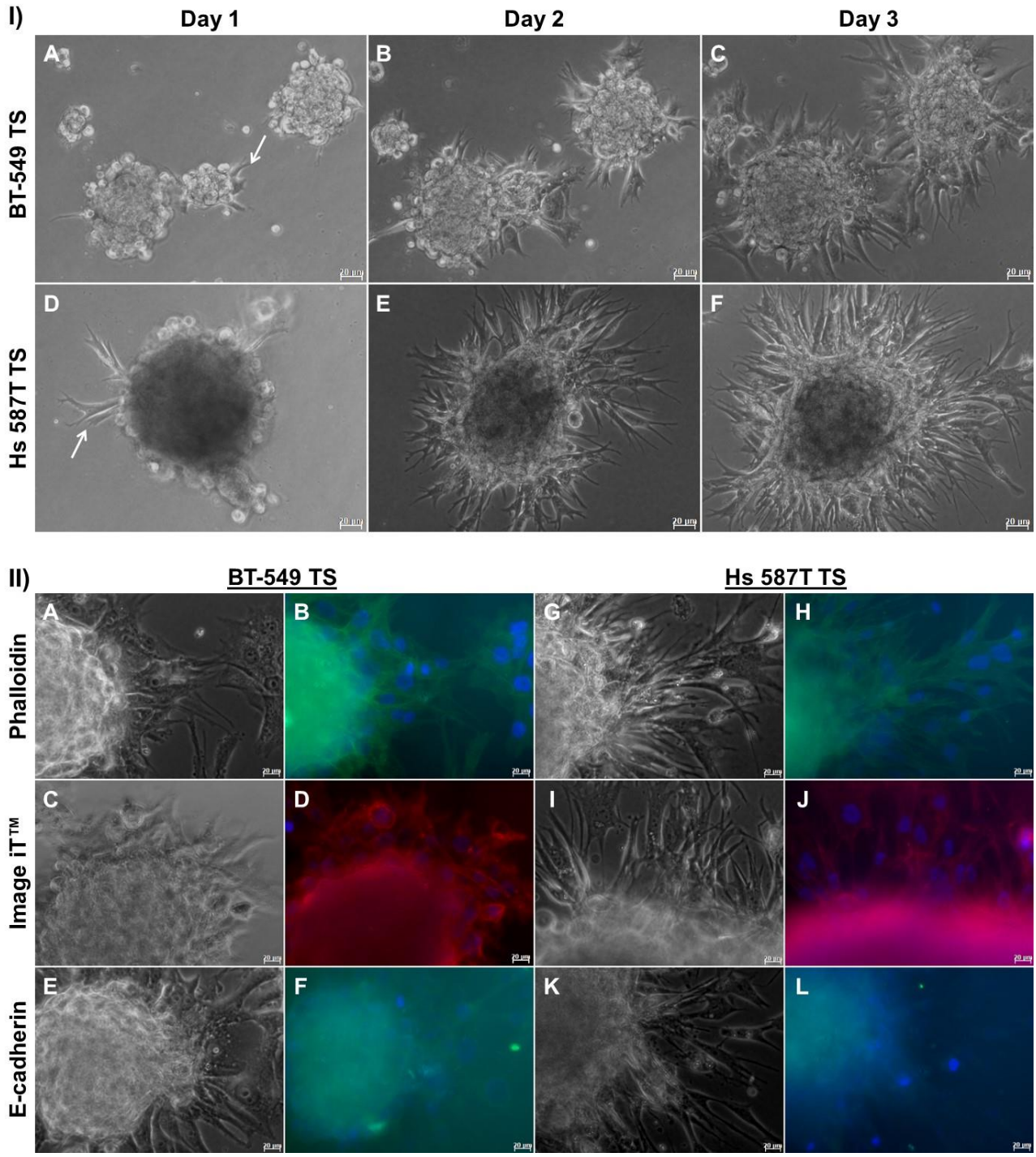

Fig. 2. BT-549 and Hs 578T tumorsphere cultured in Matrigel™ for three days. I) It is possible to visualize cells migration from the tumorspheres since the day 1 (arrow). II) In the third day of culture the cells were labeled with Phalloidin/DAPI (green/blue) and Image iT™ (red/blue), E-cadherin (green/blue). The differential interference contrast (DIC) images are represented in A, C, E for BT-549 and G, I, K for Hs 578T. Actin filaments had homogeneous distribution in TS and in migrated cells. Both TS are E-cadherin negative.

The ability of cancer cells to migrate is one of the hallmarks of metastatic cancer, the major cause of cancer-related deaths (Hanahan and Weinberg, 2011). Matrigel™ is a complex protein mixture

obtained from the extracellular matrix extracted from the Engelbreth-Holm-Swarm mouse sarcoma, a tumor rich in extracellular matrix proteins such as laminin, type IV collagen, fibronectin, growth factor. Due to these properties, Matrigel™ is widely used in cancer culture models to simulate the environment of a basement membrane in the studies of cell morphogenesis, differentiation and tumor growth (Kleinman and Martin, 2005). Matrigel™ facilitates migration, most probably by providing a supportive and growth factor retaining environment (Anguiano et al., 2017). It is highly representative of the tumor microenvironment and useful to evaluate the efficacy of drug to inhibit cell invasion.

To characterize the ultrastructural morphology of cells cultured as monolayer and TS we performed SEM. In both models the cell lines presented more than one cellular type that differs in the surface features (rough and smooth) (Fig. 2A-H). It also observed the connection between the cells and presence of filopodia (Fig. 2A, B, D, E, F, G). On two-dimensional culture, cells use organelles to explore and move into the surrounding environment, such as filopodia (Yilmaz and Christofori, 2009). Filopodia are actin-rich plasma membrane protrusions that extend out from the cell edge involved in cell motility (Jacquemet et al., 2015) and this structure has been directly observed in invasive and metastatic cancer cells (Caswell and Zech, 2018).

Cells ultrastructural characterization by TEM analysis shows amorphous nucleus, visible nucleoli and organelle-poor cytoplasm. There are numerous secretion vesicles of variable size. Some are filled with electron-dense granules (dense-core vesicles) and others with electron-lucent granules (clear-core vesicles) surrounded by a membrane (Fig. 3A-L and 4A-L). The cells are releasing their secretion products to the outside via exocytosis (Fig. 3D, I and Fig. 4J, L).

The organelles visualized in BT-549 are mitochondria and lysosomes (Fig. 3C, E, F). For BT-549 TS it is possible to observe an increase in the number of mitochondria compared to BT-549 (Fig. 3E, F, G, I). TS are multicellular spheroids and consistent with that our data demonstrate a cohesive interaction with focal adhesion structures between the cells that form BT-549 TS. Two type of cell are visualized in BT-549 TS, one presents more mitochondria (Fig. 3G, I, L) and the other more secretory vesicles (Fig. 3K, L). BT-549 presents filopodia (Figure 3B, E) and apparently this membrane protrusion is loss in BT-549 TS.

Hs 578T have nucleus/nucleolus bigger compared with BT-549 and the nucleolus presents granular shape (Fig. 4A-L). The organelles visualized in Hs 578T and Hs 578T TS are mitochondria (Fig. 4B, G), rough endoplasmic reticulum (Fig. 4C, H) and Golgi complex (Fig. 4D, E), being the last present only in Hs 578T. The cytoplasm is extremely vacuolated, especially in Hs 578T TS (Fig. 4E, G, I, J). Hs 578T seem to have two type of cell one more vacuolated than the other. Apparently Hs 578T TS present a more secretory phenotype (Fig. 4H, J, L) than BT-549 and BT-549 TS (Fig.

3D, H). Furthermore, the plasmatic membrane of Hs 578T and Hs 578T TS (Fig. 4D, G, I) seems to be more continues than BT-549 and BT-549 TS (Fig. 3A, D, E, H, I, J).

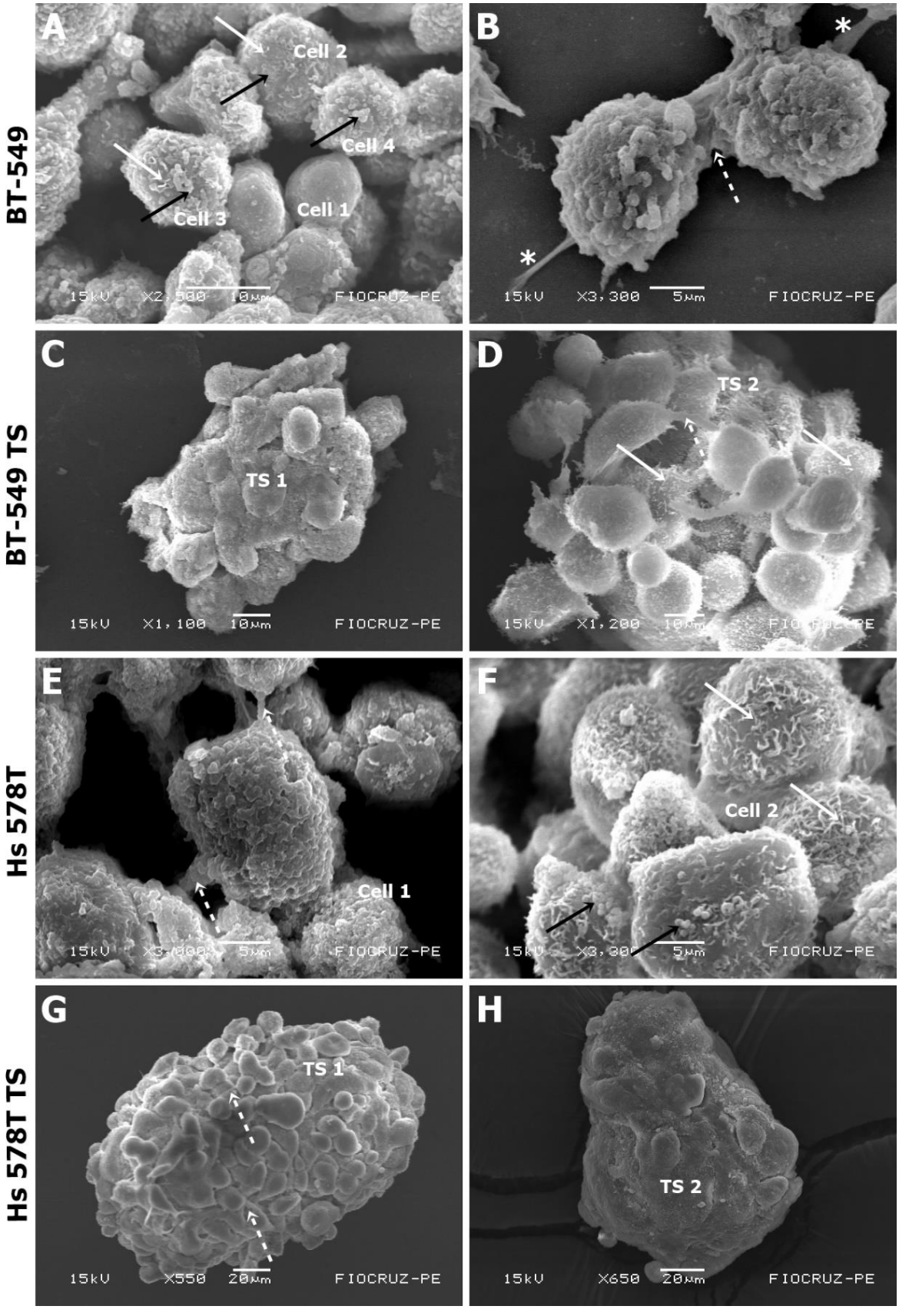

Fig. 3. Scanning electron microscope (SEM) images of BT-549 and Hs 578T and their tumorspheres (TS). BT-549: (**A**) Presence of four cell type that present differences in surface roughness with little or no secretion and presence of filopodia (white arrow). (**B**) Two interconnected cells (dotted white arrow) with cytoplasmic projections (asterisk). BT-549 TS: (**C**) One type (TS 1) with a rough surface and a compacted structure. (**D**) Interconnected cells (dotted white arrow) and several filopodia (white arrow). Hs 578T: (**E**) Interconnected cells (dotted white arrow) and rough surface (Cell 1). (**F**) Smooth surface with secretion (black arrow) and filopodia (white arrow) (Cell 2). Hs 578T TS: (**G**) Interconnected cells (dotted white arrow) (TS 1). (**H**) Tumorspheres very compacted with individual cells indistinguishable (TS 2)

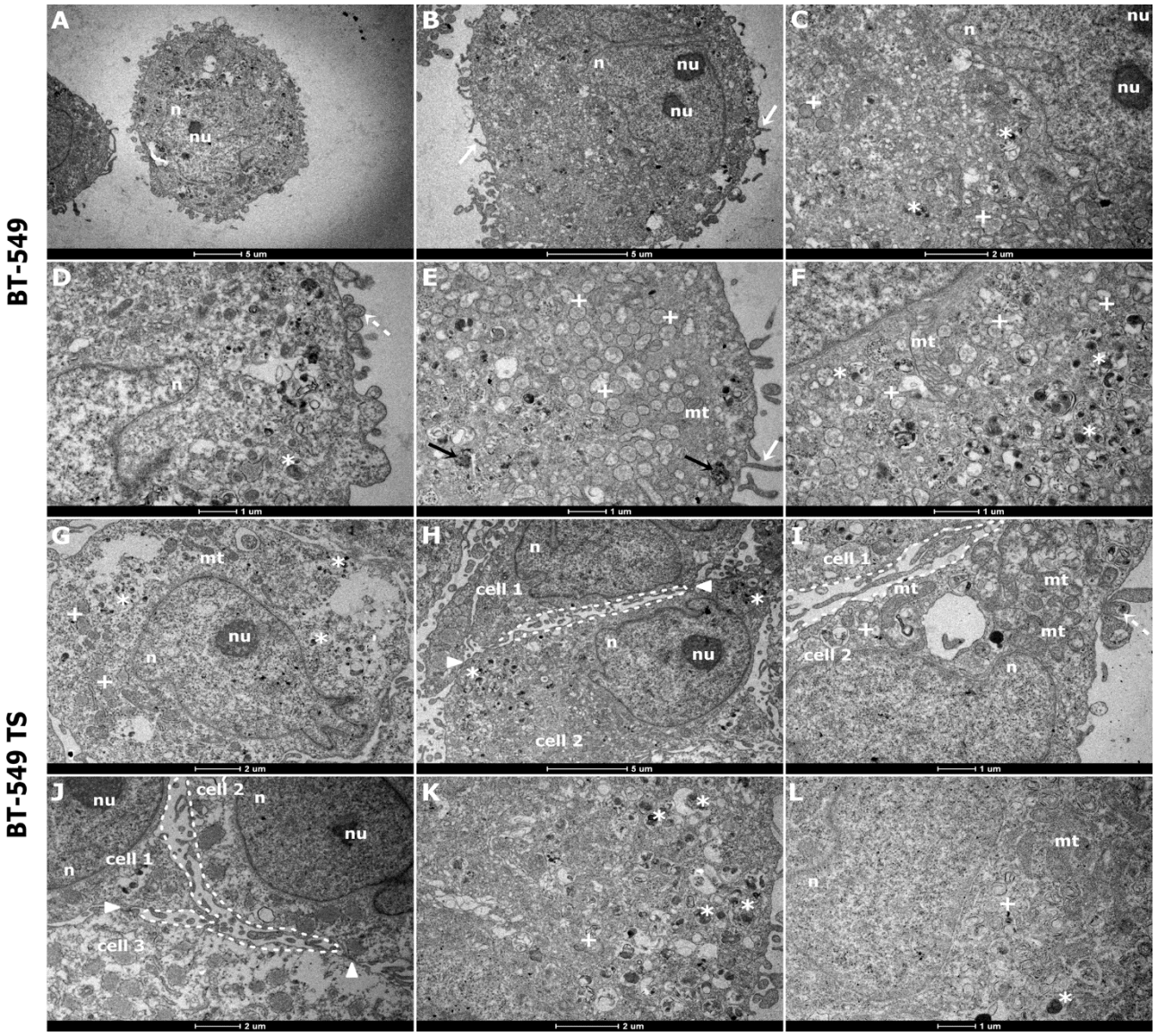

Fig. 4. Transmission electron microscopy (TEM) images of BT-549 and BT-549 TS. BT-549: (**A**) Cell overview (**B**) Cell with an amorphous nucleus (n) and two nucleoli (nu). Presence of filopodia (white arrow). (**C**) Clear-core (cross) and dense-core (asterisk) secretion vesicles. (**D**) Exocytosis vesicles (dotted white arrow). (**E**) Clear-core (cross) and dense-core (asterisk) secretion vesicles, lysosomes (black arrow) and mitochondria (mt). (**F**) Mitochondria (mt) and clear-core (cross) and dense-core (asterisk) secretion vesicles.

BT-549 TS: (**G**) Cell with an amorphous nucleus (n), clear-core (cross) and dense-core (asterisk) secretion vesicles and mitochondria (mt). (**H**) Intercellular space with vesicles between two cells (dashed outline), dense-core secretion vesicles (asterisk) and focal adhesion points (arrowhead). (**I**) Exocytosis vesicle (dotted arrow) and several mitochondria (mt). (**J**) Intercellular space with vesicles between three cells (dashed outline) and focal adhesion points (arrowhead). (**K**) Dense-core secretion vesicles (asterisk). (**L**) Mitochondria and clear-core (cross) and dense-core (asterisk) secretion vesicles

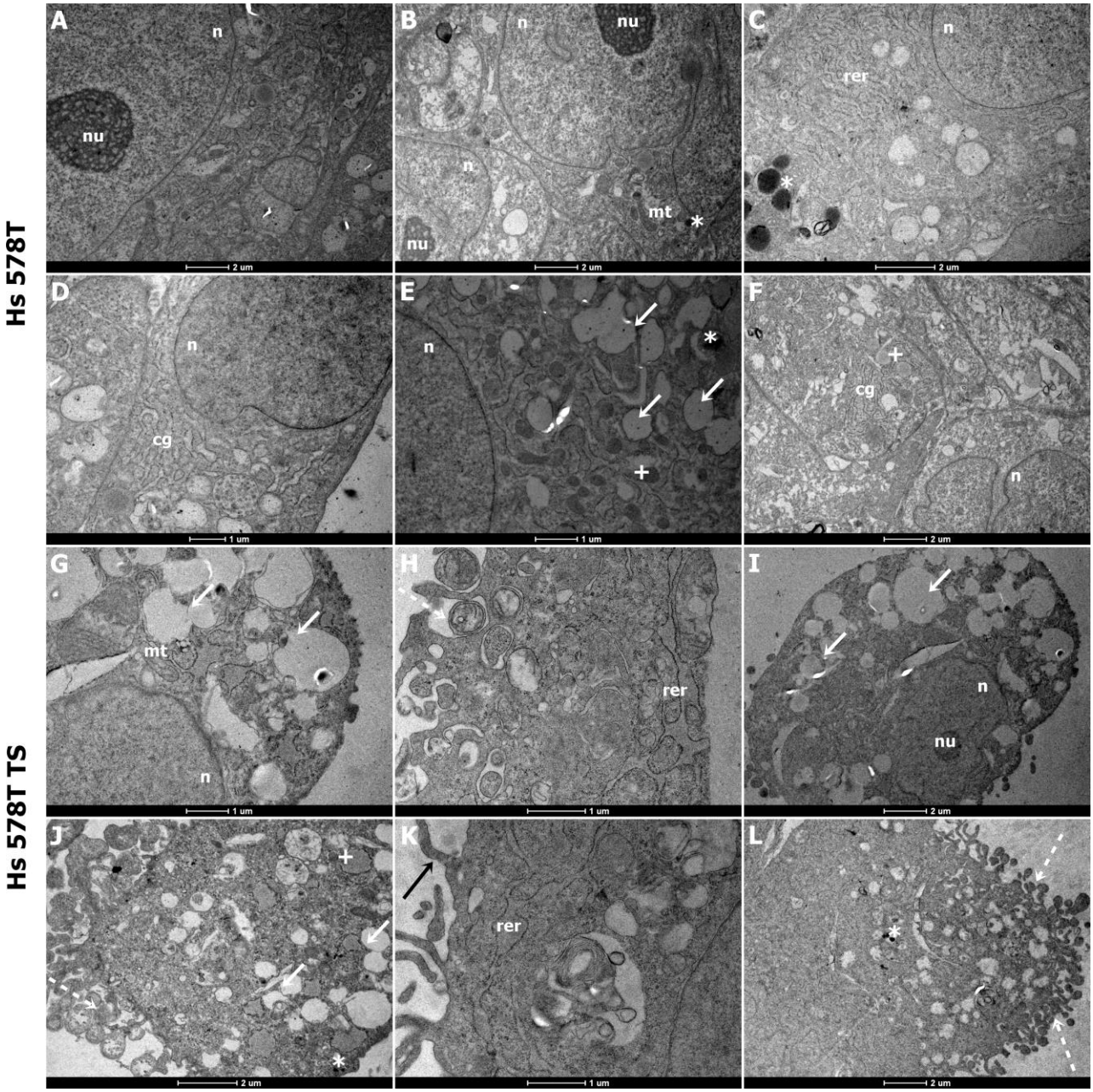

Fig. 5. Transmission electron microscopy (TEM) images Hs 578T and Hs 578T TS. Hs 578T: (**A**) Granular nucleolus (nu). (**B**) Mitochondria (mt), clear-core (cross) and dense-core (asterisk) secretion vesicles and cytoplasmic vacuoles (arrow). (**C**) Cell with an amorphous nucleus (n), rough endoplasmic reticulum (rer), clear-core (cross) and dense-core (asterisk) secretion vesicles. (**D**) Golgi complex (cg) and clear-core secretion vesicles (cross). (**E**) Clear-core (cross) and dense-core (asterisk) secretion vesicles and several

vacuoles in the cytoplasm (arrow). (**F**) Golgi complex (cg) and clear-core secretion vesicles (cross). Hs 578T TS: (**G**) Vacuolated cytoplasm (arrow) and presence of mitochondria (mt). (**H**) Rough endoplasmic reticulum (rer) and exocytosis vesicles (dotted arrow). (**I**) Vacuolated cytoplasm (arrow). (**J**) clear-core (cross) and dense-core (asterisk) secretion vesicles, cytoplasmic vacuoles (arrow) and exocytosis vesicle (dotted arrow). (**K**) filopodia (black arrow) and rough endoplasmic reticulum (rer). (**L**) Dense-core secretion vesicles (asterisk) and several exocytosis vesicles (dashed arrow).

In addition to the heterogeneous cell phenotype shown by us, ultrastructural characterization also showed the heterogeneity within and among BT-549 and Hs 578T cultured in monolayer as well as TS, having been identified two or four cell types. The cell lines are formed by cells with differences regarding the cell surface, especially BT-549. It was also possible to visualized filopodia, a mesenchymal cell characteristic and focal adhesion points representing the communication among cells in tumorspheres. Moreover, the cell lines formed distinct spheroids being Hs 578T TS more compact and bigger compared to BT-549 TS.

5 Conclusion

Spheroid models mimic various parameters present in the tumors involved in tumor resistance to the treatment adding value to studies of development and efficacy of new drugs. The cell tridimensional arrangement is of great importance since it can influence the drug response (de Lima et al., 2017). The authors showed that a marine alkaloid analog (3-alkylpyridine) has no action in TNBC cell line cultured in monolayer model, but in the TS model, the BCSCs and non-BCSCs subpopulations were decreased after treatment. Further, (Moreira et al., 2018) showed the high chemoresistance of BCSCs-like subset related to *STAT3* gene up-regulation compared to monolayer culture. BCSCs-like subset were after doxorubicin treatment, 97.4x more resistance than the monolayer model with an increase in *STAT3* expression of 8.7-fold change. Therefore, STAT3 is a promising chemoresistance biomarker in the BCSCs-like subset related to doxorubicin resistance. Our work demonstrated large morphological and phenotypic heterogeneity between TNBC cell lines as well the cell subpopulations. It is well known that tumor cells heterogeneity can influence survival, therapy responses and in the rate of tumor growth (Haynes et al., 2017). Thus, molecular understanding of this heterogeneity is essential for the identification of potential therapeutic options and vulnerabilities of oncological patients.

Conflicts of interest

None

Acknowledgments

Not applicable

Funding

This work was financially supported through grants from Fundação de Amparo à Pesquisa do Estado de Minas Gerais (FAPEMIG) [grant number CBB-APQ-00054-12], Coordenação de Aperfeiçoamento de Pessoal de Nível Superior (CAPES) and Conselho Nacional de Desenvolvimento Científico e Tecnológico (CNPq).

References

Abramson, V.G., Lehmann, B.D., Ballinger, T.J., 2015. Subtyping of triple-negative breast cancer: implications for therapy. Cancer 121, 8–16. https://doi.org/10.1002/cncr.28914.Subtyping

Al-Hajj, M., Wicha, M.S., Benito-Hernandez, A., Morrison, S.J., Clarke, M.F., 2003. Prospective identification of tumorigenic breast cancer cells. Proc. Natl. Acad. Sci. 100, 3983–3988. https://doi.org/10.1073/pnas.0530291100

Anguiano, M., Castilla, C., Maška, M., Ederra, C., Peláez, R., Morales, X., Muñoz-Arrieta, G., Mujika, M., Kozubek, M., Muñoz-Barrutia, A., Rouzaut, A., Arana, S., Garcia-Aznar, J.M., Ortiz-de-Solorzano, C., 2017. Characterization of three-dimensional cancer cell migration in mixed collagen-Matrigel scaffolds using microfluidics and image analysis. PLoS One 12. https://doi.org/10.1371/journal.pone.0171417

Bischoff, A., Huck, B., Keller, B., Strotbek, M., Schmid, S., Boerries, M., Busch, H., Müller, D., Olayioye, M.A., 2014. MiR149 functions as a tumor suppressor by controlling breast epithelial cell migration and invasion. Cancer Res. 74, 5256–5265. https://doi.org/10.1158/0008-5472.CAN-13-3319

Bray, F., Ferlay, J., Soerjomataram, I., Siegel, R.L., Torre, L.A., Jemal, A., 2018. Global cancer statistics 2018: GLOBOCAN estimates of incidence and mortality worldwide for 36 cancers in 185 countries. CA. Cancer J. Clin. 68, 394–424. https://doi.org/10.3322/caac.21492

Caswell, P.T., Zech, T., 2018. Actin-Based Cell Protrusion in a 3D Matrix. Trends Cell Biol. 28, 823–834. https://doi.org/10.1016/j.tcb.2018.06.003

Creighton, C.J., Li, X., Landis, M., Dixon, J.M., Neumeister, V.M., Sjolund, A., Rimm, D.L., Wong, H., Rodriguez, A., Herschkowitz, J.I., Fan, C., Zhang, X., He, X., Pavlick, A., Gutierrez, M.C., Renshaw, L., Larionov, A.A., Faratian, D., Hilsenbeck, S.G., Perou, C.M., Lewis, M.T., Rosen, J.M., Chang, J.C., 2009. Residual breast cancers after conventional

therapy display mesenchymal as well as tumor-initiating features. Proc. Natl. Acad. Sci. U. S. A. 106, 13820–13825. https://doi.org/10.1073/pnas.0905718106

Daniel, J., Coulter, J., Woo, J.-H., Wilsbach, K., Gabrielson, E., 2011. High levels of the Mps1 checkpoint protein are protective of aneuploidy in breast cancer cells. Proc. Natl. Acad. Sci. 108, 5384–5389. https://doi.org/10.1073/pnas.1007645108

de Lima, A.B., Barbosa, C. de S., Gonçalves, A.M.M.N., Santos, F.V. dos, Viana, G.H.R., Varotti, F. de P., Silva, L.M., 2017. New 3-alkylpyridine marine alkaloid analogues as promising antitumor agents against the CD44+/high/CD24−/lowsubset of triple-negative breast cancer cell line. Chem. Biol. Drug Des. 90, 5–11. https://doi.org/10.1111/cbdd.12923

Ferrari-Amorotti, G., Chiodoni, C., Shen, F., Cattelani, S., Soliera, A.R., Manzotti, G., Grisendi, G., Dominici, M., Rivasi, F., Colombo, M.P., Fatatis, A., Calabretta, B., 2014. Suppression of Invasion and Metastasis of Triple-Negative Breast Cancer Lines by Pharmacological or Genetic Inhibition of Slug Activity. Neoplasia 16, 1047–1058. https://doi.org/10.1016/j.neo.2014.10.006

Fonseca, N.A., Filipa, A., Moura, V., Simões, S., Nuno, J., 2017. The cancer stem cell phenotype as a determinant factor of the heterotypic nature of breast tumors. Crit. Rev. Oncol. / Hematol. 113, 111–121. https://doi.org/10.1016/j.critrevonc.2017.03.016

Ginestier, C., Hur, M.H., Charafe-jauffret, E., Monville, F., Dutcher, J., Brown, M., Jacquemier, J., Viens, P., Kleer, C., Schott, A., Hayes, D., Birnbaum, D., Wicha, M.S., Dontu, G., 2007. ALDH1 is a marker of normal and malignant human mammary stem cells and a predictor of poor clinical outcome. Cell Stem Cell 1, 555–567.

Grosse-Wilde, A., D'Hérouël, A.F., McIntosh, E., Ertaylan, G., Skupin, A., Kuestner, R.E., Del Sol, A., Walters, K.A., Huang, S., 2015. Stemness of the hybrid epithelial/mesenchymal state in breast cancer and its association with poor survival. PLoS One 10, 1–28. https://doi.org/10.1371/journal.pone.0126522

Hanahan, D., Weinberg, R.A., 2011. Hallmarks of cancer: The next generation. Cell 144, 646–674. https://doi.org/10.1016/j.cell.2011.02.013

Haynes, B., Sarma, A., Nangia-Makker, P., Shekhar, M.P., 2017. Breast cancer complexity: implications of intratumoral heterogeneity in clinical management. Cancer Metastasis Rev. 36, 547–555. https://doi.org/10.1007/s10555-017-9684-y

Huber, J.M., Amann, A., Koeck, S., Lorenz, E., Kelm, J.M., Obexer, P., Zwierzina, H., Gamerith, G., 2016. Evaluation of assays for drug efficacy in a three-dimensional model of the lung. J. Cancer Res. Clin. Oncol. 142, 1955–1966. https://doi.org/10.1007/s00432-016-2198-0

Ishiguro, T., Ohata, H., Sato, A., Yamawaki, K., Enomoto, T., Okamoto, K., 2017. Tumor-derived spheroids: Relevance to cancer stem cells and clinical applications. Cancer Sci. 108, 283–289. https://doi.org/10.1111/cas.13155

Jacquemet, G., Hamidi, H., Ivaska, J., 2015. Filopodia in cell adhesion, 3D migration and cancer cell invasion. Curr. Opin. Cell Biol. 36, 23–31. https://doi.org/10.1016/j.ceb.2015.06.007

Jia, D., Tan, Y., Liu, H., Ooi, S., Li, L., Wright, K., Bennett, S., Addison, C.L., Wang, L., 2015. Cardamonin reduces chemotherapy-enriched breast cancer stem-like cells in vitro and in vivo 7, 2015–2016. https://doi.org/10.18632/oncotarget.5819.

Kenny, P.A., Lee, G.Y., Myers, C.A., Neve, R.M., Semeiks, J.R., Spellman, P.T., Lorenz, K., Lee, E.H., Barcellos-Hoff, M.H., Petersen, O.W., Gray, J.W., Bissell, M.J., 2007. The morphologies of breast cancer cell lines in three-dimensional assays correlate with their profiles of gene expression. Mol Oncol 1, 84–96.

Kim, R.K., Suh, Y., Yoo, K.C., Cui, Y.H., Kim, H., Kim, M.J., Kim, I.G., Lee, S.J., 2015. Activation of KRAS promotes the mesenchymal features of Basal-type breast cancer. Exp. Mol. Med. 47, e137-9. https://doi.org/10.1038/emm.2014.99

Kleinman, H.K., Martin, G.R., 2005. Matrigel: Basement membrane matrix with biological activity. Semin. Cancer Biol. 15, 378–386. https://doi.org/10.1016/j.semcancer.2005.05.004

Lamouille, S., Xu, J., Derynck, R., 2014. Molecular mechanisms of epithelial-mesenchymal transition. Natl. Rev. Mol. Cell Biol. 15, 178–196. https://doi.org/10.1038/nrm3758.Molecular

Laurent, J., Frongia, C., Cazales, M., Mondesert, O., Ducommun, B., Lobjois, V., 2013. Multicellular tumor spheroid models to explore cell cycle checkpoints in 3D. BMC Cancer 13. https://doi.org/10.1186/1471-2407-13-73

Lee, C.-H., Yu, C.-C., Wang, B.-Y., Chang, W.-W., 2015. Tumorsphere as an effective in vitro platform for screening anti-cancer stem cell drugs. Oncotarget 7, 1215–1226. https://doi.org/10.18632/oncotarget.6261

Lee, G.Y., Kenny, P.A., Lee, E.H., Bissell, M.J., 2007. Three-dimensional culture models of normal and malignant breast epithelial cells. Nat. Methods 4, 359–365. https://doi.org/10.1038/nmeth1015

Lehmann, B.D.B., Bauer, J. a J., Chen, X., Sanders, M.E., Chakravarthy, a B., Shyr, Y., Pietenpol, J. a, 2011. Identification of human triple-negative breast cancer subtypes and preclinical models for selection of targeted therapies. J. Clin. Invest. 121, 2750–2767. https://doi.org/10.1172/JCI45014DS1

Liu, S., Cong, Y., Wang, D., Sun, Y., Deng, L., Liu, Y., Martin-Trevino, R., Shang, L., McDermott,

S.P., Landis, M.D., Hong, S., Adams, A., D'Angelo, R., Ginestier, C., Charafe-Jauffret, E., Clouthier, S.G., Birnbaum, D., Wong, S.T., Zhan, M., Chang, J.C., Wicha, M.S., 2014. Breast cancer stem cells transition between epithelial and mesenchymal states reflective of their normal counterparts. Stem Cell Reports 2, 78–91. https://doi.org/10.1016/j.stemcr.2013.11.009

Luo, M., Brooke, M., Wicha, M.S., 2015. Epithelial-Mesenchymal Plasticity of Breast Cancer Stem Cells: Implications for Metastasis and Therapeutic Resistance. Curr. Pharm. Des. 21, 1301–1310.

Moreira, M.P., da Conceição Braga, L., Cassali, G.D., Silva, L.M., 2018. STAT3 as a promising chemoresistance biomarker associated with the CD44+/high/CD24-/low/ALDH+ BCSCs-like subset of the triple-negative breast cancer (TNBC) cell line. Exp. Cell Res. 363, 283–290. https://doi.org/10.1016/j.yexcr.2018.01.018

Neve, R.M., Chin, K., Fridlyand, J., Yeh, J., Frederick, L., Fevr, T., Clark, L., Bayani, N., Coppe, J., Tong, F., Speed, T., Spellman, P.T., Devries, S., Lapuk, A., Wang, N.J., Stilwell, J.L., Pinkel, D., Albertson, D.G., Waldman, F.M., Dickson, R.B., Johnson, M.D., Lippman, M., Ethier, S., Gazdar, A., Gray, J.W., Division, L.S., Berkeley, L., 2006. A collection of breast cancer cell lines for the study of functionally. Cancer Cell 10, 515–527. https://doi.org/10.1016/j.ccr.2006.10.008.A

Park, S.Y., Lee, H.E., Li, H., Shipitsin, M., Gelman, R., Polyak, K., 2010. Heterogeneity for stem cell-related markers according to tumor subtype and histologic stage in breast cancer. Clin. Cancer Res. 16, 876–887. https://doi.org/10.1158/1078-0432.CCR-09-1532

Perou, C.M.*+, Sorlie, T.+++, Eisen, M.B.*, van de Rijn, M. [S], Jeffrey, S.S.[//], Rees, C.A.*, Pollack, J.R. [curved stem paragraph sign ornament], Ross, D.T. [curved stem paragraph sign ornament], Johnsen, H.++, Akslen, L.A.#, Fluge, O. [white star], Pergamenschikov, A.*, Williams, C.*, Zhu, S.X. [S], Lonning, P.E.**, Borresen-Dale, A.-L.++, Brown, P.O. [curved stem paragraph sign ornament]++, Botstein, D.*, 2000. Molecular portraits of human breast tumours. [Letter]. Nature 406, 747–752.

Prat, A., Parker, J.S., Karginova, O., Fan, C., Livasy, C., Herschkowitz, J.I., He, X., Perou, C.M., 2010. Phenotypic and molecular characterization of the claudin-low intrinsic subtype of breast cancer. Breast Cancer Res. 12. https://doi.org/10.1186/bcr2635

Rhodes, L. V., Tate, C.R., Hoang, V.T., Burks, H.E., Gilliam, D., Martin, E.C., Elliott, S., Miller, D.B., Buechlein, A., Rusch, D., Tang, H., Nephew, K.P., Burow, M.E., Collins-Burow, B.M., 2015. Regulation of triple-negative breast cancer cell metastasis by the tumor-suppressor liver kinase B1. Oncogenesis 4, 1–8. https://doi.org/10.1038/oncsis.2015.27

Riffle, S., Hegde, R.S., 2017. Modeling tumor cell adaptations to hypoxia in multicellular tumor spheroids. J. Exp. Clin. Cancer Res. 36, 1–10. https://doi.org/10.1186/s13046-017-0570-9

Riffle, S., Pandey, R.N., Albert, M., Hegde, R.S., 2017. Linking hypoxia, DNA damage and proliferation in multicellular tumor spheroids. BMC Cancer 17, 1–12. https://doi.org/10.1186/s12885-017-3319-0

Shipitsin, M., Campbell, L.L., Argani, P., Weremowicz, S., Bloushtain-Qimron, N., Yao, J., Nikolskaya, T., Serebryiskaya, T., Beroukhim, R., Hu, M., Halushka, M.K., Sukumar, S., Parker, L.M., Anderson, K.S., Harris, L.N., Garber, J.E., Richardson, A.L., Schnitt, S.J., Nikolsky, Y., Gelman, R.S., Polyak, K., 2007. Molecular Definition of Breast Tumor Heterogeneity. Cancer Cell 11, 259–273. https://doi.org/10.1016/j.ccr.2007.01.013

Sorlie, T., Perou, C.M., Tibshirani, R., Aas, T., Geisler, S., Johnsen, H., Hastie, T., Eisen, M.B., van de Rijn, M., Jeffrey, S.S., Thorsen, T., Quist, H., Matese, J.C., Brown, P.O., Botstein, D., Lonning, P.E., Borresen-Dale, A.-L., 2001. Gene expression patterns of breast carcinomas distinguish tumor subclasses with clinical implications. Proc. Natl. Acad. Sci. 98, 10869–10874. https://doi.org/10.1073/pnas.191367098

Sun, R., Shen, S., Zhang, Y.J., Xu, C.F., Cao, Z.T., Wen, L.P., Wang, J., 2016. Nanoparticle-facilitated autophagy inhibition promotes the efficacy of chemotherapeutics against breast cancer stem cells. Biomaterials 103, 44–55. https://doi.org/10.1016/j.biomaterials.2016.06.038

Tate, C.R., Rhodes, L. V., Segar, H.C., Driver, J.L., Pounder, F.N., Burow, M.E., Collins-Burow, B.M., 2012. Targeting triple-negative breast cancer cells with the histone deacetylase inhibitor panobinostat. Breast Cancer Res. 14, R79. https://doi.org/10.1186/bcr3192

Tellez-Gabriel, M., Ory, B., Lamoureux, F., Heymann, M.F., Heymann, D., 2016. Tumour heterogeneity: The key advantages of single-cell analysis. Int. J. Mol. Sci. 17. https://doi.org/10.3390/ijms17122142

Weiswald, L.B., Bellet, D., Dangles-Marie, V., 2015. Spherical Cancer Models in Tumor Biology. Neoplasia (United States) 17, 1–15. https://doi.org/10.1016/j.neo.2014.12.004

Yilmaz, M., Christofori, G., 2009. EMT, the cytoskeleton, and cancer cell invasion. Cancer Metastasis Rev. 28, 15–33. https://doi.org/10.1007/s10555-008-9169-0

Zhang, Z., Yang, M., Chen, R., Su, W., Li, P., Chen, S., Chen, Z., Chen, A., Li, S., Hu, C., 2014. IBP regulates epithelial-to-mesenchymal transition and the motility of breast cancer cells via Rac1, RhoA and Cdc42 signaling pathways. Br. Dent. J. 217, 3374–3382. https://doi.org/10.1038/onc.2013.337

Ziperstein, M.J., Guzman, A., Kaufman, L.J., 2015. Breast cancer cell line aggregate morphology

does not predict invasive capacity. PLoS One 10, 1–17.
https://doi.org/10.1371/journal.pone.0139523

5 CONCLUSÕES

Os resultados obtidos nesse estudo permitiram concluir:

- A cultura de enriquecimento de CSCs de mama foi bem-sucedida, como indicado pela alta expressão do perfil $CD44^+/CD24^-$ e $ALDH^+$, bem como pela maior resistência ao tratamento com PTX e DOX observado na BT-549 TS e Hs 578T TS quando comparado a linhagem celular cultivada em monocamada de acordo com os valores de IC50;

- A BT-549 TS demonstrou valor de IC50 para DOX de 55,7 μM, que foi 97,4 vezes maior ao IC50 estimado para BT-549 cultivada em monocamada (0,572 μM);

- O tratamento com DOX resultou na subexpressão de 64 genes e na super-expressão de 3 genes (*STAT3*, *MAPK3* e *PRKCZ*) associados a via de sinalização *EGFR* na BT-549 TS;

- Existe uma grande heterogeneidade morfológica e fenotípica entre as linhagens BT-549 e Hs 578T;

- A BT-549 mostrou-se fenotipicamente distinta, além de possuir alta plasticidade induzida por EMT, como indicado pela regulação da expressão do marcador de superfície CD146;

- Sugere-se o seguinte modelo de transição das subpopulações celulares em cultura de enriquecimento de CSCs: a plasticidade das células tumorais híbridas $CD44^+/CD24^+/CD146^+$, caracterizadas por apresentar um fenótipo mesenquimal e epitelial, e das células tumorais epiteliais $CD44^-/CD24^+/ CD146^+$ dão origem a CSCs de mama EMT-*like* $CD44^+/CD24^-/CD146^-$ através da conversão fenotípica induzida por EMT. Além disso, estas células tumorais podem gerar a CSCs de mama identificada como $ALDH^+$ epitelial-*like*. As CSCs de mama podem se autorrenovar e diferenciar em células tumorais ($CD44^-/CD24^-/CD146^-$);

- Os dados de citotoxicidade mostraram que a BT-549 foi mais resistente ao PTX em vez de DOX, o que parece estar associado às células $CD24^+$. Em contraste, a BT-549 TS foi extremamente resistente a DOX devido ao enriquecimento de CSCs ($CD44^+/CD24^-/CD146^-$ e $ALDH^+$).

6 CONSIDERAÇÕES FINAIS

Até o momento para o tratamento de pacientes com TNBC, não foram identificados alvos terapêuticos efetivos, provavelmente devido à vasta heterogeneidade da doença. Desta forma, a quimioterapia citotóxica continua sendo a principal forma de tratamento, o que resulta no prognóstico ruim dessa doença. É sabido que CSCs são responsáveis pela heterogeneidade celular intratumoral, bem como pela resistência a morte induzida por múltiplas drogas quimioterápicas implicando na redução da eficácia do tratamento e, subsequente recorrência da doença e disseminação metastática.

Neste contexto, nós buscamos possíveis marcadores preditivos de resistência a DOX, o quimioterápico mais usado no tratamento do câncer de mama, em CSCs de mama obtidas da linhagem celular BT-549. Neste estudo, avaliamos a expressão de vários genes associados à via de sinalização *EGFR*. Observamos após o enriquecimento das CSCs de mama e tratamento com DOX um significativo aumento na expressão de *STAT3*. Isso indica uma forte relação de *STAT3* com a resistência ao tratamento com DOX atribuída a CSCs de mama, tornando este um potencial alvo terapêutico no TNBC. Sugerimos que PRKCZ e MAPK3, cujos genes também foram superexpressão após tratamento com DOX, podem atuar em conjunto contribuindo, para aumentar a ativação da via de sinalização STAT3. Em relação aos demais genes avaliados, apesar de não ter sido abordado o possível papel deles nos nossos achados, acreditamos que novos estudos envolvendo um maior número de amostras demonstre a correlação entre eles, em que a diminuição da expressão de um ou mais desses genes pode favorecer o aumento da expressão de outro(s) gene(s) e vice-versa.

Células tumorais (não-CSCs), através da conversão fenotípica induzida por EMT, dão origem as CSCs e essa plasticidade, induzida pelos próprios quimioterápicos, associada à capacidade de autorrenovação das CSCS, bem como com a resistência intrínseca dessas células aos quimioterápicos, resulta na falha do tratamento. Nossos resultados demonstram grande heterogeneidade celular presente entre duas linhagens celulares estudadas, BT-549 e HS 578T, bem como entre as células que compõem cada linhagem em termos de morfologia, fenotipagem e resposta à droga. Além disso, a BT-549 mostrou-se mais heterogênea que Hs578T, alterando completamente o fenótipo das subpopulações celulares que a compõem sob cultura de enriquecimento de CSCs de mama. O mesmo não foi observado para a Hs578T reforçando, dessa forma, a heterogeneidade existente também entre as duas células apesar de ambas serem TNBC. A elevada plasticidade fenotípica apresentada pela BT-549 foi associada à indução do processo de

EMT e este achado parece desempenhar um papel importante na resistência a DOX, uma vez que há uma forte associação entre CSCs, EMT e resistência à droga.

Estudos mostram uma relação entre o fenótipo e a resposta à droga, assim como relatado por nós, onde sugerimos que o perfil fenotípico das subpopulações celulares presente nas linhagens celulares influencia na resposta a DOX e PTX. A BT-549 que é fenotipicamente distinta apresentou maior resistência ao tratamento com PTX e maior sensibilidade a DOX, sendo observado o contrário para Hs 578T, já as tumoresferas derivadas de Hs 578T e BT-549 são, de forma geral mais semelhantes entre si. Contudo, ressalta-se que para a BT-549 após o enriquecimento de CSCs, foi necessária uma concentração de DOX 97.4X maior quando comparado ao cultivo em monocamada, reforçando o papel das CSCs da quimiorresistência.

Assim, através de uma análise individual das linhagens celulares TNBC, como um modelo experimental de estudos pré-clínicos, torna-se possível a compreensão da heterogeneidade tumoral e a forma como as CSCs de mama resistem à quimioterapia. Estes achados poderão possibilitar o desenvolvimento de tratamentos mais eficientes para o câncer de mama e, subsequente, melhora na sobrevida e/ou qualidade de vida das pacientes com TNBC. Além disso, *STAT3* destaca-se como um importante preditor de quimiorresistência em TNBC com fenótipo EMT e CSCs de mama e sua inibição pode sensibilizar as células ao tratamento. Diante desses resultados, estudos clínicos são necessários para validar o papel da via de sinalização de STAT3 na resistência à quimioterapia como marcador molecular, bem como para elucidar o comportamento das subpopulações celulares e sua distribuição dentro da massa tumoral, como indicador preditivo de resistência ao DOX.

REFERÊNCIAS

ABHOLD, E. L. et al. EGFR kinase promotes acquisition of stem cell-like properties: A potential therapeutic target in head and neck squamous cell carcinoma stem cells. **PLoS ONE**, v. 7, n. 2, 2012.

ABRAMSON, V. G.; LEHMANN, B. D.; BALLINGER, T. J. Subtyping of triple-negative breast cancer: implications for therapy. **Cancer**, v. 121, n. 1, p. 8–16, 2015.

AL-HAJJ, M. et al. Prospective identification of tumorigenic breast cancer cells. **Proceedings of the National Academy of Sciences of the United States of America**, v. 100, n. 7, p. 3983–8, 2003a.

AL-HAJJ, M. et al. Prospective identification of tumorigenic breast cancer cells. **Proceedings of the National Academy of Sciences**, v. 100, n. 7, p. 3983–3988, 2003b.

ALANAZI, I. O.; KHAN, Z. Understanding EGFR signaling in breast cancer and breast cancer stem cells: Overexpression and therapeutic implications. **Asian Pacific Journal of Cancer Prevention**, v. 17, n. 2, p. 445–453, 2016.

ALEXANDRE, J. et al. Accumulation of hydrogen peroxide is an early and crucial step for paclitaxel-induced cancer cell death both in vitro and in vivo. **International Journal of Cancer**, v. 119, n. 1, p. 41–48, 2006.

ALEXANDRE, J. et al. Novel action of paclitaxel against cancer cells: Bystander effect mediated by reactive oxygen species. **Cancer Research**, v. 67, n. 8, p. 3512–3517, 2007.

ALLRED, D. C. Issues and updates: Evaluating estrogen receptor-α, progesterone receptor, and HER2 in breast cancer. **Modern Pathology**, v. 23, n. SUPPL. 2, p. S52–S59, 2010.

ALMENDRO, V.; MARUSYK, A.; POLYAK, K. Cellular Heterogeneity and Molecular Evolution in Cancer. **Annual Review of Pathology: Mechanisms of Disease**, v. 8, n. 1, p. 277–302, 2013.

ANGUIANO, M. et al. Characterization of three-dimensional cancer cell migration in mixed collagen-Matrigel scaffolds using microfluidics and image analysis. **PLoS ONE**, v. 12, n. 2, 2017.

APOSTOLOU, P.; FOSTIRA, F. Hereditary breast cancer: the era of new susceptibility genes. **Biomed Res Int**, v. 2013, p. 747318, 2013.

BAGNARDI, V. et al. Light alcohol drinking and cancer: A meta-analysis. **Annals of Oncology**, v. 24, n. 2, p. 301–308, 2013.

BELOTTI, D. et al. The microtubule-affecting drug paclitaxel has antiangiogenic activity. **Clinical Cancer Research**, v. 2, n. November, p. 1843–1849, 1996.

BERLIN, V.; HASELTINE, W. A. Reduction of Adriamycin to a semiquinone- free radical by NADPH cytochrome P-450 reductase produlces DNA cleavage in a reaction mediated by molecular oxygen. **J. Biol. Chem.**, v. 256, n. 10, p. 4747–4756, 1981.

BISCHOFF, A. et al. MiR149 functions as a tumor suppressor by controlling breast epithelial cell migration and invasion. **Cancer Research**, v. 74, n. 18, p. 5256–5265, 2014.

BOSCH, A. et al. Triple-negative breast cancer: Molecular features, pathogenesis, treatment and current lines of research. **Cancer Treatment Reviews**, v. 36, n. 3, p. 206–215, 2010.

BOURGUIGNON, L. Y. W. et al. Hyaluronan-CD44 interaction with protein kinase Cε promotes oncogenic signaling by the stem cell marker nanog and the production of microRNA-21, leading to down-regulation of the tumor suppressor protein PDCD4, anti-apoptosis, and chemotherapy resistance . **Journal of Biological Chemistry**, v. 284, n. 39, p. 26533–26546, 2009.

BOURGUIGNON, L. Y. W. et al. Hyaluronan-CD44 interaction promotes c-Src-mediated twist signaling, microRNA-10b expression, and RhoA/RhoC up-regulation, leading to Rho-kinase-associated cytoskeleton activation and breast tumor cell invasion. **Journal of Biological Chemistry**, v. 285, n. 47, p. 36721–36735, 2010.

BRAUNSTEIN, M. et al. Downregulation of histone H2A and H2B pathways is associated with anthracycline sensitivity in breast cancer. **Breast Cancer Research**, v. 18, n. 1, p. 1–16, 2016.

BRAY, F. et al. Global cancer statistics 2018: GLOBOCAN estimates of incidence and mortality worldwide for 36 cancers in 185 countries. **CA: a cancer journal for clinicians**, v. 68, n. 6, p. 394–424, 2018.

BURGER, G. A.; DANEN, E. H. J.; BELTMAN, J. B. Deciphering Epithelial–Mesenchymal Transition Regulatory Networks in Cancer through Computational Approaches. **Frontiers in Oncology**, v. 7, n. August, 2017.

CAREY, L. A. et al. The triple negative paradox: Primary tumor chemosensitivity of breast cancer subtypes. **Clinical Cancer Research**, v. 13, n. 8, p. 2329–2334, 2007.

CARNERO, A. et al. The cancer stem-cell signaling network and resistance to therapy. **Cancer Treatment Reviews**, v. 49, p. 25–36, 2016.

CASWELL, P. T.; ZECH, T. Actin-Based Cell Protrusion in a 3D Matrix. **Trends in Cell Biology**, v. 28, n. 10, p. 823–834, 2018.

CHANMEE, T. et al. Key Roles of Hyaluronan and Its CD44 Receptor in the Stemness and Survival of Cancer Stem Cells. **Frontiers in Oncology**, v. 5, n. August, p. 1–11, 2015.

CHARAFE-JAUFFRET, E. et al. Breast cancer cell lines contain functional cancer stem sells with metastatic capacity and a distinct molecular signature. **Cancer Research**, v. 69, n. 4, p. 1302–1313, 2009.

CHEN, L.; BOURGUIGNON, L. Y. W. Hyaluronan-CD44 interaction promotes c-Jun signaling and miRNA21 expression leading to Bcl-2 expression and chemoresistance in breast cancer cells. **Molecular Cancer**, v. 13, n. 1, p. 1–13, 2014.

CHUTE, J. P. et al. Inhibition of aldehyde dehydrogenase and retinoid signaling induces the expansion of human hematopoietic stem cells. **Proceedings of the National Academy of Sciences of the United States of America**, v. 103, n. 31, p. 11707–11712, 2006.

CLARKE, M. F. et al. Cancer stem cells - Perspectives on current status and future directions: AACR workshop on cancer stem cells. **Cancer Research**, v. 66, n. 19, p. 9339–9344, 2006.

COATES, A. S. et al. Tailoring therapies - improving the management of early breast cancer: St GallenInternational Expert Consensus on the Primary Therapy of Early Breast Cancer 2015. **Annals of oncology : official journal of the European Society for Medical Oncology / ESMO**, v. 26, n. 8, p. 1533–46, 2015.

CREIGHTON, C. J. et al. Residual breast cancers after conventional therapy display mesenchymal as well as tumor-initiating features. **Proceedings of the National Academy of Sciences of the United States of America**, v. 106, n. 33, p. 13820–13825, 2009.

CROKER, A. K. et al. Differential functional roles of ALDH1A1 and ALDH1A3 in mediating metastatic behavior and therapy resistance of human breast cancer cells. **International Journal of Molecular Sciences**, v. 18, n. 10, p. 1–18, 2017.

CROKER, A. K.; ALLAN, A. L. Inhibition of aldehyde dehydrogenase (ALDH) activity reduces chemotherapy and radiation resistance of stem-like ALDHhiCD44+ human breast cancer cells. **Breast Cancer Research and Treatment**, v. 133, n. 1, p. 75–87, 2012.

CUTTS, S. M. et al. Adriamycin-induced DNA adducts inhibit the DNA interactions of transcription factors and RNA polymerase. **Journal of Biological Chemistry**, v. 271, n. 10, p. 5422–5429, 1996.

DANIEL, J. et al. High levels of the Mps1 checkpoint protein are protective of aneuploidy in breast cancer cells. **Proceedings of the National Academy of Sciences**, v. 108, n. 13, p. 5384–5389, 29 mar. 2011.

DAVE, B. et al. Epithelial-mesenchymal transition, cancer stem cells and treatment resistance. **Breast Cancer Research**, v. 14, n. 1, p. 202, 2012.

DAVIS, N. M. et al. Deregulation of the EGFR / PI3K / PTEN / Akt / mTORC1 pathway in breast cancer : possibilities for therapeutic intervention. **Oncotarget**, v. 5, n. 13, p. 4603–4650, 2014.

DE LAURENTIIS, M. et al. Treatment of triple negative breast cancer (TNBC): Current options and future perspectives. **Cancer Treatment Reviews**, v. 36, n. SUPPL. 3, p. S80–S86, 2010.

DE LIMA, A. B. et al. New 3-alkylpyridine marine alkaloid analogues as promising antitumor agents against the CD44+/high/CD24−/lowsubset of triple-negative breast cancer cell line. **Chemical Biology and Drug Design**, v. 90, n. 1, p. 5–11, 2017.

DELPY, E. et al. Doxorubicin induces slow ceramide accumulation and late apoptosis in cultured adult rat ventricular myocytes. **Cardiovascular Research**, v. 43, n. 2, p. 398–407, 1999.

DENG, X. et al. CD24 Expression and differential resistance to chemotherapy in triple-negative breast cancer. **Oncotarget**, v. 8, n. 24, p. 38294–38308, 2017.

DENT, R. et al. Triple-negative breast cancer: Clinical features and patterns of recurrence. **Clinical Cancer Research**, v. 13, n. 15, p. 4429–4434, 2007.

DESANTIS, C. et al. Breast Cancer Statistics , 2013. **CA Cancer Journal for Clinicians**, v. 64, n. 1, p. 52–62, 2013.

DI VEROLI, G. Y. et al. An automated fitting procedure and software for dose-response curves with multiphasic features. **Scientific Reports**, v. 5, p. 1–11, 2015.

DIETERICH, M. et al. Influence of lifestyle factors on breast cancer risk. **Breast Care**, v. 9, n. 6, p. 407–414, 2014.

DONTU, G. et al. In vitro propagation and transcriptional profiling of human mammary stem / progenitor cells. **Genes & Development**, v. 17, n. 10, p. 1253–1270, 2003.

DRASIN, D. J.; ROBIN, T. P.; FORD, H. L. Breast cancer epithelial-to-mesenchymal transition: Examining the functional consequences of plasticity. **Breast Cancer Research**, v. 13, n. 6, 2011.

ECCLES, S. Tumor-associated macrophages in breast cancer: distinct subets, distinct functions. **Int J Dev Biol**, v. 55, n. 7–9, p. 719–729, 2011.

EISENBERG, A. L. A.; PINTO, I. V.; KOIFMAN, S. Triple-Negative Breast Cancer in Brazilian Women without Metastasis to Axillary Lymph Nodes : Ten-Year Survival and Prognostic Factors. **British Journal of Medicine & Medical Research**, v. 3, n. 4, p. 880–896, 2013.

EROLES, P. et al. Molecular biology in breast cancer: Intrinsic subtypes and signaling pathways. **Cancer Treatment Reviews**, v. 38, n. 6, p. 698–707, 2012.

FANG, X. et al. CD24: From A to Z. **Cellular and Molecular Immunology**, v. 7, n. 2, p. 100–103, 2010.

FERRARI-AMOROTTI, G. et al. Suppression of Invasion and Metastasis of Triple-Negative Breast Cancer Lines by Pharmacological or Genetic Inhibition of Slug Activity. **Neoplasia**, v. 16, n. 12, p. 1047–1058, 2014.

FITZGERALD, T. L. et al. Roles of EGFR and KRAS and their downstream signaling pathways in pancreatic cancer and pancreatic cancer stem cells. **Advances in Biological Regulation**, v. 59, p. 65–81, 2015.

FOLEY, J. et al. EGFR Signaling in Breast Cancer : Bad to the Bone. **Semin Cell Dev Biol.**, v. 21, n. 9, p. 951–960, 2010.

FONSECA, N. A. et al. The cancer stem cell phenotype as a determinant factor of the heterotypic nature of breast tumors. **Critical Reviews in Oncology / Hematology**, v. 113, p. 111–121, 2017.

GAJEWSKI, E. et al. Oxidative DNA Base Damage in MCF-10A Breast Epithelial Cells at Clinically Achievable Concentrations of Doxorubicin. **Biochem Pharmacol.**, v. 73, n. 12, p. 1947–1956, 2007.

GEWIRTZ, D. A. Gewirtz, D. A. (1999). A critical evaluation of the mechanisms of action proposed for the antitumor effects of the anthracycline antibiotics adriamycin and daunorubicin. Biochemical Pharma- cology, 57, 727–741. v. 57, n. 98, p. 727–741, 1999.

GINESTIER, C. et al. ALDH1 is a marker of normal and malignant human mammary stem cells and a predictor of poor clinical outcome. **Cell Stem Cell**, v. 1, n. 5, p. 555–567, 2007.

GINESTIER, C. et al. Retinoid signaling regulates breast cancer stem cell differentiation. **Cell Cycle**, v. 8, n. 20, p. 3297–3302, 2009.

GROSSE-WILDE, A. et al. Stemness of the hybrid epithelial/mesenchymal state in breast cancer and its association with poor survival. **PLoS ONE**, v. 10, n. 5, p. 1–28, 2015.

GUILFOILE, P. G.; HUTCHINSON, C. R. A bacterial analog of the mdr gene of mammalian tumor cells is present in Streptomyces peucetius, the producer of daunorubicin and doxorubicin. **Proceedings of the National Academy of Sciences of the United States of America**, v. 88, n. 19, p. 8553–7, 1991.

GUNASINGHE, N. P. A. D. et al. Mesenchymal-epithelial transition (MET) as a mechanism for metastatic colonisation in breast cancer. **Cancer and Metastasis Reviews**, v. 31, n. 3–4, p. 469–478, 2012.

HANAHAN, D.; WEINBERG, R. A. Hallmarks of cancer: The next generation. **Cell**, v. 144, n. 5, p. 646–674, 2011.

HASHEMI, S. H. B.; KARIMI, S.; MAHBOOBI, H. Lifestyle changes for prevention of breast cancer. **Electronic Physician**, v. 6, n. 3, p. 894–905, 2014.

HAYNES, B. et al. Breast cancer complexity: implications of intratumoral heterogeneity in clinical management. **Cancer and Metastasis Reviews**, v. 36, n. 3, p. 547–555, 2017.

HERSCHKOWITZ, J. I. et al. Identification of conserved gene expression features between murine mammary carcinoma models and human breast tumors. **Genome Biology**, v. 8, n. 5, p. 1–17, 2007.

HINOHARA, K.; GOTOH, N. Inflammatory signaling pathways in self-renewing breast cancer stem cells. **Current Opinion in Pharmacology**, v. 10, n. 6, p. 650–654, 2010.

HONETH, G. et al. Aldehyde dehydrogenase and estrogen receptor define a hierarchy of cellular differentiation in the normal human mammary epithelium. **Breast Cancer Research**, v. 16, n. 3, p. 1–14, 2014.

HONG, I.-S.; LEE, H.-Y.; NAM, J.-S. Cancer Stem Cells: The `Achilles Heel' of Chemo-Resistant Tumors. **Recent Patents on Anti-Cancer Drug Discovery**, v. 10, n. 1, p. 2–22, 2015.

HORTOBAGYI, G. N. et al. The global breast cancer burden: Variations in epidemiology and survival. **Clinical Breast Cancer**, v. 6, n. 5, p. 391–401, 2005.

HORWITZ, S. B. Mechanism of action of taxol. **Cancer**, v. 12, p. 134–136, 1992.

HOWELL, A. et al. Risk determination and prevention of breast cancer. **Breast Cancer Research**, v. 16, n. 5, p. 1–19, 2014.

HUBER, J. M. et al. Evaluation of assays for drug efficacy in a three-dimensional model of the lung. **Journal of Cancer Research and Clinical Oncology**, v. 142, n. 9, p. 1955–1966, 2016.

ICHIKAWA, Y. et al. Cardiotoxicity of doxorubicin is mediated through mitochondrial iron accumulation. **Journal of Clinical Investigation**, v. 124, n. 2, p. 617–630, 2014.

IMBERT, A.-M. et al. CD146 Expression in Human Breast Cancer Cell Lines Induces Phenotypic and Functional Changes Observed in Epithelial to Mesenchymal Transition. **PLoS ONE**, v. 7, n. 8, p. e43752, 2012.

ISHIGURO, T. et al. Tumor-derived spheroids: Relevance to cancer stem cells and clinical applications. **Cancer Science**, v. 108, n. 3, p. 283–289, 2017.

ISLAM, F. et al. Translational potential of cancer stem cells: A review of the detection of cancer stem cells and their roles in cancer recurrence and cancer treatment. **Experimental Cell Research**, v. 335, n. 1, p. 135–147, 2015.

JACQUEMET, G.; HAMIDI, H.; IVASKA, J. Filopodia in cell adhesion, 3D migration and cancer cell invasion. **Current Opinion in Cell Biology**, v. 36, p. 23–31, 2015.

JIA, D. et al. Cardamonin reduces chemotherapy-enriched breast cancer stem-like cells in vitro and in vivo. v. 7, n. 1, p. 2015–2016, 2015.

JUNG, Y. et al. Kazinol-E is a specific inhibitor of ERK that suppresses the enrichment of a breast cancer stem-like cell population. **Biochemical and Biophysical Research Communications**, v. 470, n. 2, p. 294–299, fev. 2016.

KAWASE, M. et al. Increase of ceramide in adriamycin-induced HL-60 cell apoptosis: Detection by a novel anti-ceramide antibody. **Biochimica et Biophysica Acta - Molecular and Cell Biology of Lipids**, v. 1584, n. 2–3, p. 104–114, 2002.

KENNY, P. A. et al. The morphologies of breast cancer cell lines in three-dimensional assays correlate with their profiles of gene expression. **Mol Oncol**, v. 1, n. 1, p. 84–96, 2007.

KIM, R. K. et al. Activation of KRAS promotes the mesenchymal features of Basal-type breast cancer. **Experimental and Molecular Medicine**, v. 47, n. 1, p. e137-9, 2015.

KLEINMAN, H. K.; MARTIN, G. R. Matrigel: Basement membrane matrix with biological activity. **Seminars in Cancer Biology**, v. 15, n. 5 SPEC. ISS., p. 378–386, 2005.

KOLESNICK, R. N.; KRÖNKE, M. Regulation of Ceramide Production and Apoptosis. **Annual Review of Physiology**, v. 60, n. 1, p. 643–665, 1998.

KORKAYA, H. et al. HER2 regulates the mammary stem/progenitor cell population driving tumorigenesis and invasion. **Oncogene**, v. 27, n. 47, p. 6120–6130, 2008.

KOTIYAL, S.; BHATTACHARYA, S. Breast cancer stem cells, EMT and therapeutic targets. **Biochemical and Biophysical Research Communications**, v. 453, n. 1, p. 112–116, 2014.

LAMOUILLE, S.; XU, J.; DERYNCK, R. Molecular mechanisms of epithelial-mesenchymal transition. **National Review Molecular Cell Biology**, v. 15, n. 3, p. 178–196, 2014.

LAURENT, J. et al. Multicellular tumor spheroid models to explore cell cycle checkpoints in 3D. **BMC Cancer**, v. 13, 2013.

LEE, C.-H. et al. Tumorsphere as an effective in vitro platform for screening anti-cancer stem cell drugs. **Oncotarget**, v. 7, n. 2, p. 1215–1226, 2015.

LEE, C.-H. et al. Tumorsphere as an effective *in vitro* platform for screening anti-cancer stem cell drugs. **Oncotarget**, v. 7, n. 2, p. 1215–1226, 2016.

LEE, G. Y. et al. Three-dimensional culture models of normal and malignant breast epithelial cells. **Nature Methods**, v. 4, n. 4, p. 359–365, 1 abr. 2007.

LEHMANN, B. D. et al. Refinement of Triple-Negative Breast Cancer Molecular Subtypes: Implications for Neoadjuvant Chemotherapy Selection. **PloS one**, v. 11, n. 6, p. e0157368, 2016.

LEHMANN, B. D. B. et al. Identification of human triple-negative breast cancer subtypes and preclinical models for selection of targeted therapies. **Journal of Clinical Investigation**, v. 121, n. 7, p. 2750–2767, 2011.

LEHMANN, B. D.; PIETENPOL, J. A. Clinical implications of molecular heterogeneity in triple negative breast cancer Brian. **Breast**, v. 24, n. 02: S36-S40, p. 1–11, 2015.

LI, J. et al. Regulation of CD44 expression by tumor necrosis factor-α and its potential role in breast cancer cell migration. **Biomedicine and Pharmacotherapy**, v. 66, n. 2, p. 144–150, 2012.

LIEDTKE, C. et al. Response to neoadjuvant therapy and long-term survival in patients with triple-negative breast cancer. **Journal of Clinical Oncology**, v. 26, n. 8, p. 1275–1281, 2008.

LIND, M. Principles of Cytotoxic Chemotherapy. **Medicine**, v. 39, n. 12, p. 711=716, 2011.

LIU, S. et al. Breast cancer stem cells transition between epithelial and mesenchymal states reflective of their normal counterparts. **Stem Cell Reports**, v. 2, n. 1, p. 78–91, 2014.

LO, H. W.; HSU, S. C.; HUNG, M. C. EGFR signaling pathway in breast cancers: From traditional signal transduction to direct nuclear translocalization. **Breast Cancer Research and Treatment**, v.

95, n. 3, p. 211–218, 2006.

LUCCI, A. et al. Multidrug resistance modulators and doxorubicin synergize to elevate ceramide levels and elicit apoptosis in drug-resistant cancer cells. **Cancer**, v. 86, n. 2, p. 300–311, 1999.

LUO, M.; BROOKE, M.; WICHA, M. S. Epithelial-Mesenchymal Plasticity of Breast Cancer Stem Cells: Implications for Metastasis and Therapeutic Resistance. **Current pharmaceutical design**, v. 21, n. 10, p. 1301–1310, 2015.

MAHAVORASIRIKUL, W. et al. Cytotoxic activity of Thai medicinal plants against human cholangiocarcinoma, laryngeal and hepatocarcinoma cells in vitro. **BMC Complementary and Alternative Medicine**, v. 10, n. 55, p. 2–8, 2010.

MALHOTRA, V.; PERRY, M. C. Classical chemotherapy: mechanisms, toxicities and the therapeutic window. **Cancer biology & therapy**, v. 2, n. 4 Suppl 1, p. 4–6, 2003.

MALLINI, P. et al. Epithelial-to-mesenchymal transition: What is the impact on breast cancer stem cells and drug resistance. **Cancer Treatment Reviews**, v. 40, n. 3, p. 341–348, 2014.

MANI, S. A. et al. The Epithelial-Mesenchymal Transition Generates Cells with Properties of Stem Cells. **Cell**, v. 133, n. 4, p. 704–715, 2008.

MASUDA, H. et al. Differential response to neoadjuvant chemotherapy among 7 triple-negative breast cancer molecular subtypes. **Clinical Cancer Research**, v. 19, n. 19, p. 5533–5540, 2013.

MASUDA, H.; ZHANG, D. Role of epidermal growth factor receptor in breast cancer. **Breast cancer research …**, v. 136, n. 2, p. 1–21, 2012.

MITTAL, S. et al. Coordinate Hyperactivation of Notch1 and Ras/MAPK Pathways Correlates with Poor Patient Survival: Novel Therapeutic Strategy for Aggressive Breast Cancers. **Molecular Cancer Therapeutics**, v. 13, n. 12, p. 3198–3209, 1 dez. 2014.

MONTGOMERY, N. et al. CD44 enhances invasion of basal-like breast cancer cells by upregulating serine protease and collagen-degrading enzymatic expression and activity. **Breast Cancer Research**, v. 14, n. 3, p. R84, 2012.

MOREIRA, M. P. et al. STAT3 as a promising chemoresistance biomarker associated with the CD44+/high/CD24-/low/ALDH+ BCSCs-like subset of the triple-negative breast cancer (TNBC) cell line. **Experimental Cell Research**, v. 363, n. 2, p. 283–290, 2018.

MUTA, M. et al. Effect of low-dose paclitaxel and docetaxel on endothelial progenitor cells. **Oncology**, v. 77, n. 3–4, p. 182–191, 2009.

NAM, K. S. et al. CD44 regulates cell proliferation, migration, and invasion via modulation of c-Src transcription in human breast cancer cells. **Cellular Signalling**, v. 27, n. 9, p. 1882–1894, 2015.

NEVE, R. M. et al. A collection of breast cancer cell lines for the study of functionally. **Cancer**

Cell, v. 10, n. 6, p. 515–527, 2006.

NIETO, M. A. Epithelial plasticity: A common theme in embryonic and cancer cells. **Science**, v. 342, n. 6159, 2013.

NIETO, M. A. et al. Emt: 2016. **Cell**, v. 166, n. 1, p. 21–45, 2016.

O'REILLY, E. A. et al. The fate of chemoresistance in triple negative breast cancer (TNBC). **BBA Clinical**, v. 3, p. 257–275, 2015.

OKAZAKI, T. et al. Role of ceramide as a lipid mediator of 1 alpha,25- dihydroxyvitamin D3-induced HL-60 cell differentiation. **Journal of Biological Chemistry**, v. 265, n. 26, p. 15823–15831, 1990.

OKAZAKI, T.; BELL, R. M.; HANNUN, Y. A. Sphingomyelin turnover induced by vitamin D3 in HL-60 cells. Role in cell differentiation. **The Journal of biological chemistry**, v. 264, n. 32, p. 19076–80, 1989.

OUHTIT, A. et al. CD146, a novel target of CD44-signaling, suppresses breast tumor cell invasion. **Cell Communication and Signaling**, v. 15, n. 1, p. 1–10, 2017.

PALMA, G. et al. Triple negative breast cancer: looking for the missing link between biology and treatments. **Oncotarget**, v. 6, n. 29, p. 26560–26574, 2015.

PARK, S. Y. et al. Heterogeneity for stem cell-related markers according to tumor subtype and histologic stage in breast cancer. **Clinical Cancer Research**, v. 16, n. 3, p. 876–887, 2010.

PATTABIMARAN, D. R.; WEINBERG, R. A. Tackling the cancer stem cells – what challenges do they pose? **Nat Rev Drug Discov**, v. 13, n. 7, p. 497–512, 2014.

PAYNE, S. J. L. et al. Predictive markers in breast cancer - The present. **Histopathology**, v. 52, n. 1, p. 82–90, 2008.

PEROU, C. M. *+ et al. Molecular portraits of human breast tumours. [Letter]. **Nature**, v. 406, n. august, p. 747–752, 2000.

PIRES, B. R. B. et al. Targeting Cellular Signaling Pathways in Breast Cancer Stem Cells and its Implication for Cancer Treatment. **Anticancer Research**, v. 36, n. 11, p. 5681–5692, 2016.

POLYAK, K.; WEINBERG, R. A. Transitions between epithelial and mesenchymal states: Acquisition of malignant and stem cell traits. **Nature Reviews Cancer**, v. 9, n. 4, p. 265–273, 2009.

PONTI, D. et al. Isolation and In vitro Propagation of Tumorigenic Breast Cancer Cells with Stem / Progenitor Cell Properties. n. 13, p. 5506–5512, 2005.

PRAT, A. et al. Phenotypic and molecular characterization of the claudin-low intrinsic subtype of breast cancer. **Breast cancer research**, v. 12, n. 5, p. R68, 2010a.

PRAT, A. et al. Phenotypic and molecular characterization of the claudin-low intrinsic subtype of breast cancer. **Breast Cancer Research**, v. 12, n. 5, 2010b.

PRAT, A. et al. Response and survival of breast cancer intrinsic subtypes following multi-agent neoadjuvant chemotherapy. **BMC Medicine**, v. 13, n. 1, p. 1–11, 2015.

RHODES, L. V. et al. Regulation of triple-negative breast cancer cell metastasis by the tumor-suppressor liver kinase B1. **Oncogenesis**, v. 4, n. October 2014, p. 1–8, 2015.

RIFFLE, S. et al. Linking hypoxia, DNA damage and proliferation in multicellular tumor spheroids. **BMC Cancer**, v. 17, n. 1, p. 1–12, 2017.

RIFFLE, S.; HEGDE, R. S. Modeling tumor cell adaptations to hypoxia in multicellular tumor spheroids. **Journal of Experimental and Clinical Cancer Research**, v. 36, n. 1, p. 1–10, 2017.

RIGGS, B. L.; HARTMANN, L. C. Selective Estrogen-Receptor Modulators — Mechanisms of Action. **N Engl J Med**, v. 348, n. 12, p. 1–12, 2003.

SAKAMAKI, K. et al. Evolutionary analyses of caspase-8 and its paralogs: Deep origins of the apoptotic signaling pathways. **BioEssays**, v. 37, n. 7, p. 767–776, 2015.

SASAKI, T.; HAZEKI, K.; HAZEKI, O. Permissive effect of ceramide. **Biochem J.**, v. 834, p. 829–834, 1995.

SAVAGE, P. Chemotherapy curable malignancies and cancer stem cells: A biological review and hypothesis. **BMC Cancer**, v. 16, n. 1, p. 1–11, 2016.

SCHABATH, H. CD24 affects CXCR4 function in pre-B lymphocytes and breast carcinoma cells. **Journal of Cell Science**, v. 119, n. 2, p. 314–325, 2006.

SCHATTON, T.; FRANK, N. Y.; FRANK, M. H. Identification and targeting of cancer stem cells. **Bioassays**, v. 31, n. 10, p. 1038–1049, 2010.

SCHETTINI, F. et al. Nab-paclitaxel for the treatment of triple-negative breast cancer: Rationale, clinical data and future perspectives. **Cancer Treatment Reviews**, v. 50, p. 129–141, 2016.

SEHL, M. E. et al. Modeling of cancer stem cell state transitions predicts therapeutic response. **PLoS ONE**, v. 10, n. 9, p. 1–20, 2015.

SHIPITSIN, M. et al. Molecular Definition of Breast Tumor Heterogeneity. **Cancer Cell**, v. 11, n. 3, p. 259–273, 2007.

SIEGEL, R. et al. Cancer Statistics , 2011 The Impact of Eliminating Socioeconomic and Racial Disparities on Premature Cancer Deaths. **CA Cancer J Clin**, v. 61, p. 212–236, 2011.

SLAMON, D. J. et al. Use of Chemotherapy plus a Monoclonal Antibody against HER2 for Metastatic Breast Cancer That Overexpresses HER2. **New England Journal of Medicine**, v. 344,

n. 11, p. 783–792, 15 mar. 2001.

SMALLEY, M.; PIGGOTT, L.; CLARKSON, R. Breast cancer stem cells: Obstacles to therapy. **Cancer Letters**, v. 338, n. 1, p. 57–62, 2013.

SMITH, I. E.; DOWSETT, M. Aromatase inhibitors in breast cancer. **The new england journal of medicine**, v. 348, p. 2431–42, 2003.

SMITH, S. E. et al. Molecular characterization of breast cancer cell lines through multiple omic approaches. **Breast Cancer Research**, v. 19, n. 1, p. 1–12, 2017.

SOPHOS, N. A.; VASILIOU, V. Aldehyde dehydrogenase gene superfamily: the 2002 update. **Chem Biol Interact**, v. 143–144, p. 5–22, 2003.

SORLIE, T. et al. Gene expression patterns of breast carcinomas distinguish tumor subclasses with clinical implications. **Proceedings of the National Academy of Sciences**, v. 98, n. 19, p. 10869–10874, 2001.

SORLIE, T. et al. Repeated observation of breast tumor subtypes in independent gene expression data sets. **Proceedings of the National Academy of Sciences**, v. 100, n. 14, p. 8418–8423, 2003.

SUN, R. et al. Nanoparticle-facilitated autophagy inhibition promotes the efficacy of chemotherapeutics against breast cancer stem cells. **Biomaterials**, v. 103, p. 44–55, 2016.

SWIFT, L. P. et al. Doxorubicin-DNA adducts induce a non-topoisomerase II-mediated form of cell death. **Cancer Research**, v. 66, n. 9, p. 4863–4871, 2006.

SYMMANS, W. F. et al. Paclitaxel-induced Apoptosis and Mitotic Arrest Assessed by Serial Fine-Needle Aspiration : Implications for Early Prediction of Breast Cancer Response to Neoadjuvant Treatment Advances in Brief Paclitaxel-induced Apoptosis and Mitotic Arrest Assessed by. **Clinical Cancer Research**, v. 6, n. December, p. 4610–4617, 2000.

TANG, H. et al. AKT-ions with a TWIST between EMT and MET. **Oncotarget**, v. 7, n. 38, 2016.

TATE, C. R. et al. Targeting triple-negative breast cancer cells with the histone deacetylase inhibitor panobinostat. **Breast Cancer Research**, v. 14, n. 3, p. R79, 2012.

TELLEZ-GABRIEL, M. et al. Tumour heterogeneity: The key advantages of single-cell analysis. **International Journal of Molecular Sciences**, v. 17, n. 12, 2016.

THOMSON, C. A. et al. Cancer Risk , and Mortality in the Women â€™ s Health Initiative. **Cancer Prev Res (Phila)**, v. 7, n. 1, p. 42–53, 2014.

TSOU, S. H. et al. A critical dose of doxorubicin is required to alter the gene expression profiles in MCF-7 cells acquiring multidrug resistance. **PLoS ONE**, v. 10, n. 1, p. 1–24, 2015.

UCHINO, M. et al. Nuclear β-catenin and CD44 upregulation characterize invasive cell populations

in non-aggressive MCF-7 breast cancer cells. **BMC Cancer**, v. 10, 2010.

VAVROVA, A. et al. Catalytic Inhibitors of Topoisomerase II Differently Modulate the Toxicity of Anthracyclines in Cardiac and Cancer Cells. **PLoS ONE**, v. 8, n. 10, 2013.

VERMA, R. et al. Pathological and epidemiological factors associated with advanced stage at diagnosis of breast cancer. **British Medical Bulletin**, v. 103, n. 1, p. 129–145, 2012.

VISVADER, J. E. Cells of origin in cancer. **Nature**, v. 469, n. 7330, p. 314–322, 2011.

VISVADER, J. E.; LINDEMAN, G. J. Cancer stem cells in solid tumours: Accumulating evidence and unresolved questions. **Nature Reviews Cancer**, v. 8, n. 10, p. 755–768, 2008.

VISVADER, J. E.; LINDEMAN, G. J. Cancer stem cells: Current status and evolving complexities. **Cell Stem Cell**, v. 10, n. 6, p. 717–728, 2012.

VOGELSTEIN, B. et al. Cancer Genome Lanscapes. **Science**, v. 339, n. 6127, p. 1546–1558, 2013.

WANG, F. et al. Reciprocal interactions between 1-integrin and epidermal growth factor receptor in three-dimensional basement membrane breast cultures: A different perspective in epithelial biology. **Proceedings of the National Academy of Sciences**, v. 95, n. 25, p. 14821–14826, 1998.

WANG, Z.; YAN, X. CD146, a multi-functional molecule beyond adhesion. **Cancer Letters**, v. 330, n. 2, p. 150–162, 2013.

WEISWALD, L. B.; BELLET, D.; DANGLES-MARIE, V. Spherical Cancer Models in Tumor Biology. **Neoplasia (United States)**, v. 17, n. 1, p. 1–15, 2015.

XU, C. et al. Let-7a regulates mammosphere formation capacity through Ras/NF-κB and Ras/MAPK/ERK pathway in breast cancer stem cells. **Cell Cycle**, v. 14, n. 11, p. 1686–1697, 2015.

XU, H. et al. Enrichment of CD44 in basal-type breast cancer correlates with EMT, cancer stem cell gene profile, and prognosis. **OncoTargets and Therapy**, v. 9, p. 431–444, 2016.

YAN, W.-T. et al. Circulating tumor cell status monitors the treatment responses in breast cancer patients: a meta-analysis. **Scientific Reports**, v. 7, n. March, p. 43464, 2017.

YAN, Y.; ZUO, X.; WEI, D. Concise Review: Emerging Role of CD44 in Cancer Stem Cells: A Promising Biomarker and Therapeutic Target. **STEM CELLS Translational Medicine**, v. 4, n. 9, p. 1033–1043, 2015.

YILMAZ, M.; CHRISTOFORI, G. EMT, the cytoskeleton, and cancer cell invasion. **Cancer and Metastasis Reviews**, v. 28, n. 1–2, p. 15–33, 2009.

YU, K. DA et al. Identification of prognosis-relevant subgroups in patients with chemoresistant triple-negative breast cancer. **Clinical Cancer Research**, v. 19, n. 10, p. 2723–2733, 2013.

ZABOUO, G. et al. CD146 expression is associated with a poor prognosis in human breast tumors and with enhanced motility in breast cancer cell lines. **Breast Cancer Research**, v. 11, n. 1, p. R1, 2009.

ZENG, Q. et al. CD146, an epithelial-mesenchymal transition inducer, is associated with triple-negative breast cancer. **Proceedings of the National Academy of Sciences**, v. 109, n. 4, p. 1127–1132, 2012.

ZHANG, Y. et al. Over-Expressed Twist Associates with Markers of Epithelial Mesenchymal Transition and Predicts Poor Prognosis in Breast Cancers via ERK and Akt Activation. **Plos One**, p. 1–19, 2015.

ZHANG, Z. et al. IBP regulates epithelial-to-mesenchymal transition and the motility of breast cancer cells via Rac1, RhoA and Cdc42 signaling pathways. **British Dental Journal**, v. 217, n. 1, p. 3374–3382, 2014.

ZHAO, D. et al. Cytoplasmic p27 promotes epithelial – mesenchymal transition and tumor metastasis via STAT3-mediated Twist1 upregulation. **Oncogene**, v. 34, n. 43, p. 5447–5459, 2015.

ZHAO, J. Cancer stem cells and chemoresistance: The smartest survives the raid. **Pharmacology and Therapeutics**, v. 160, p. 145–158, 2016.

ZIPERSTEIN, M. J.; GUZMAN, A.; KAUFMAN, L. J. Breast cancer cell line aggregate morphology does not predict invasive capacity. **PLoS ONE**, v. 10, n. 9, p. 1–17, 2015.

APÊNDICES

APÊNDICE A - ORIENTAÇÕES DURANTE O PERÍODO DO DOUTORADO

1) Orientações de acadêmicos na Iniciação Científica

- Izabela Koh Guerra (2013 - 2015), Ciências Biológicas, Centro Universitário Uni-BH.

- Eliza Pereira Franco (2015 - 2017), Farmácia, Universidade Federal de Minas Gerais.

2) Coorientação de Trabalho de Conclusão de Curso (TCC)

Izabela Koh Guerra

APÊNDICE B - INFORMAÇÕES COMPLEMENTARES

1) Premiação (2016) - Egressa destaque acadêmica da 1° turma de Ciências Biológicas do Centro Universitário UNA.

2) Sócia Fundadora da CELLtype, startup criada em Junho de 2017

- 2° lugar no Biomaker Battle (Biominas), edição Belo Horizonte realizada em 23/09/2017;

- 3° lugar na Final Estadual do Desafio Científico Biomaker Battle (Biominas) realizado na Feira Internacional de Negócios, Inovação e Tecnologia (FINIT) em 03/11/2017;

- 2° lugar no Mini-Empreenda em Ação realizado na Feira Internacional de Negócios, Inovação e Tecnologia (FINIT) em 04/11/2017;

- 3° lugar no programa de pré-aceleração BioStartup Lab rodada 04/2017 (Biominas).

ANEXOS

ANEXO A - COMPROVANTE DE PUBLICAÇÃO DO ARTIGO 1

Experimental Cell Research
ISSN: 0014-4827
Fator de impacto: 3,546

Experimental Cell Research 363 (2018) 283–290

Contents lists available at ScienceDirect

Experimental Cell Research

journal homepage: www.elsevier.com/locate/yexcr

STAT3 as a promising chemoresistance biomarker associated with the $CD44^{+/high}/CD24^{-/low}/ALDH^{+}$ BCSCs-like subset of the triple-negative breast cancer (TNBC) cell line

Milene Pereira Moreira[a,d], Letícia da Conceição Braga[b,c], Geovanni Dantas Cassali[d], Luciana Maria Silva[a,*]

[a] *Serviço de Biologia Celular, Diretoria de Pesquisa e Desenvolvimento, Fundação Ezequiel Dias - Rua Conde Pereira Carneiro, 80, Gameleira, Belo Horizonte 30510-010, Minas Gerais, Brazil*
[b] *Departamento de Ginecologia e Obstetrícia, Faculdade de Medicina, Universidade Federal de Minas Gerais - Av. Prof. Alfredo Balena, 190, Santa Efigênia, Belo Horizonte 30130-100, Minas Gerais, Brazil*
[c] *Instituto de Ciências Biológicas e Saúde, Centro Universitário UNA - Rua dos Guajajaras, 175, Centro, Belo Horizonte 30180-100, Minas Gerais, Brazil*
[d] *Laboratório de Patologia Comparada, Departamento de Patologia Geral, Instituto de Ciências Biológicas, Universidade Federal de Minas Gerais - Avenida Presidente Antônio Carlos, 6627 - Pampulha, Belo Horizonte 31270-901, Minas Gerais, Brazil*

* Corresponding author.
E-mail addresses: mipmoreira@gmail.com (M.P. Moreira), braga.ltc@gmail.com (L. da Conceição Braga), geovanni.cassali@gmail.com (G.D. Cassali), luciana.silva@funed.mg.gov.br (L.M. Silva).

https://doi.org/10.1016/j.yexcr.2018.01.018
Received 2 August 2017; Received in revised form 2 January 2018; Accepted 12 January 2018
Available online 17 January 2018

ANEXO B - COMPROVANTE DE SUBMISSÃO DO ARTIGO 2

Breast Cancer Research and Treatment
ISSN: 1573-7217
Fator de impacto: 3,605

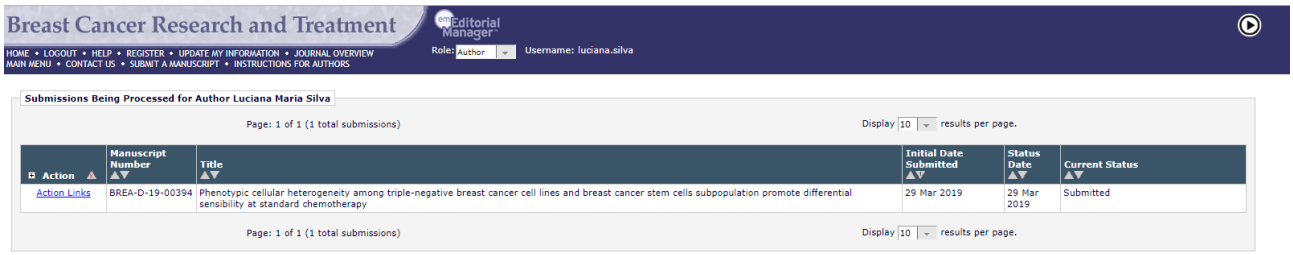

ANEXO C - COMPROVANTE DE SUBMISSÃO DO ARTIGO 3

Micron
ISSN: 0968-4328
Fator de impacto: 1,728

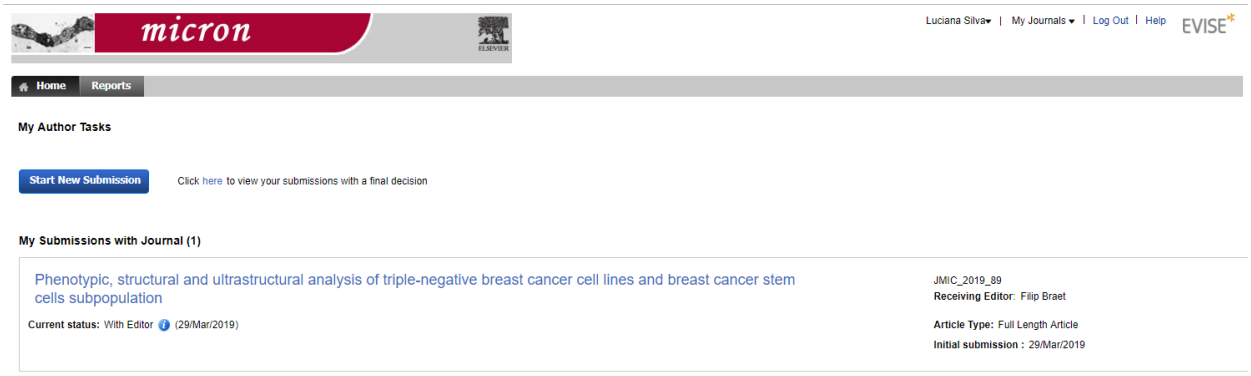

ANEXO D - PERFIL DE EXPRESSÃO DOS MARCADORES CD44, CD24 E CD146 NAS LINHAGENS CELULARES BT-549 E Hs 578T CULTIVADAS EM MODELOS MONOCAMADA E TUMORESFERAS

Perfil de expressão dos marcadores CD44 (APC), CD24 (Alexa Fluor) e CD146 (PE) para cada linhagem celular analisada. Marcação com o isotipo (painel superior) e tripla marcação com CD44/CD24/CD146 (painel inferior). Observa-se: *dot plot* FSC x SSC (1° coluna); Histograma para a marcação de CD44 (2° coluna) que foi utilizada como parâmetro para definição dos *gates* $CD44^+$ e $CD44^-$; Células $CD44^+$ analisadas com todas as possíveis combinações de CD24/CD146 (3° coluna); Células $CD44^-$ analisadas com todas as possíveis combinações de CD24/CD146 (4° coluna).

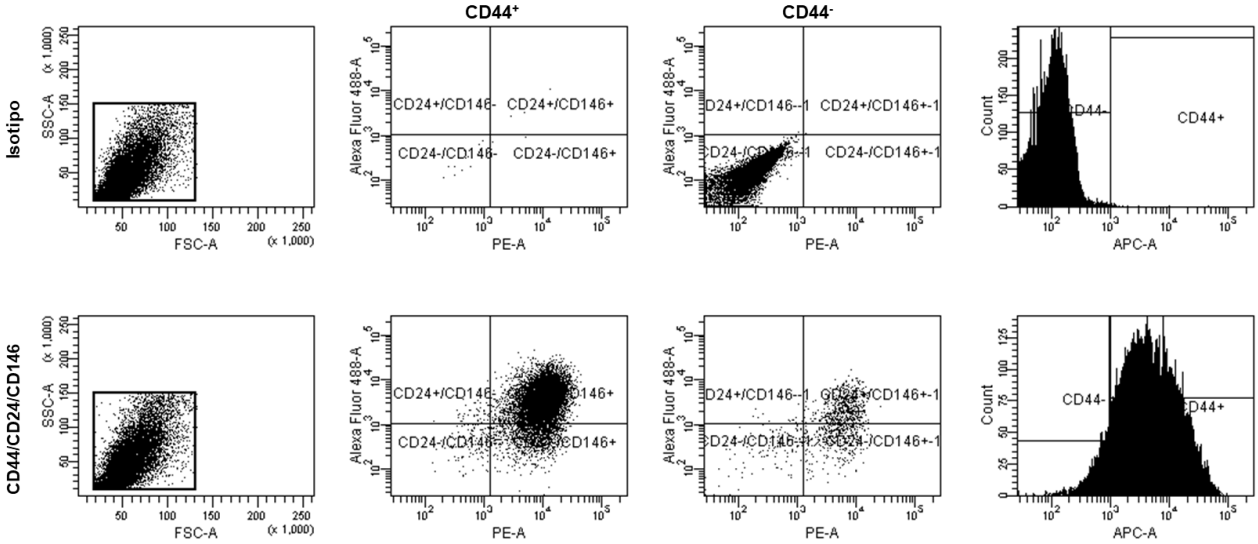

Figura 1 - Gráficos de *dot plot* e histograma representativo para a BT-549.

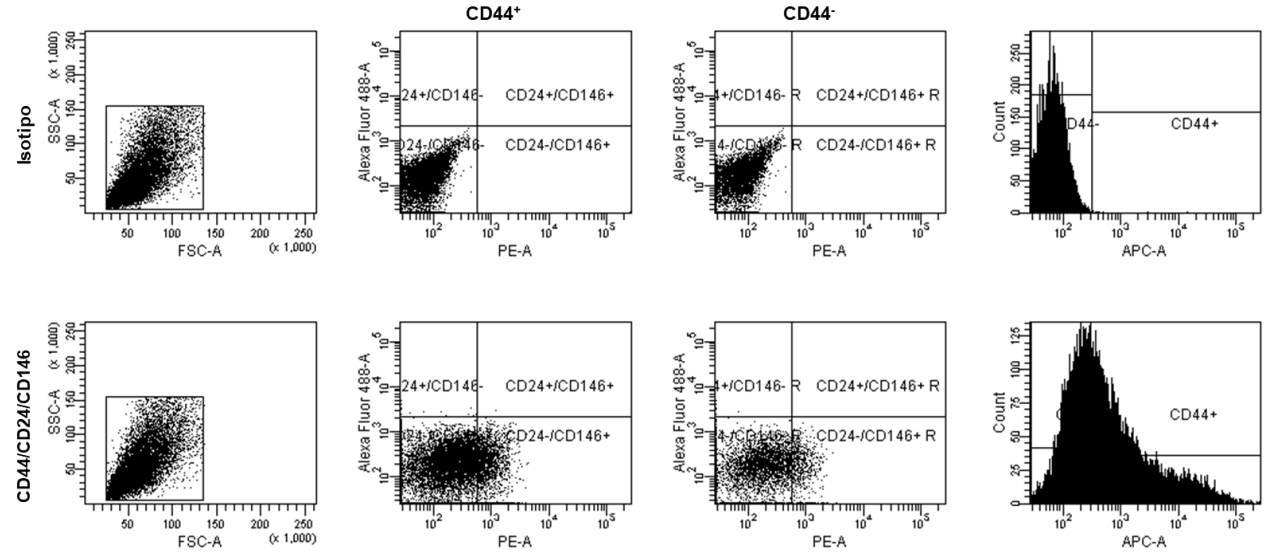

Figura 2 - Gráficos de *dot plot* e histograma representativo para a BT-549 TS.

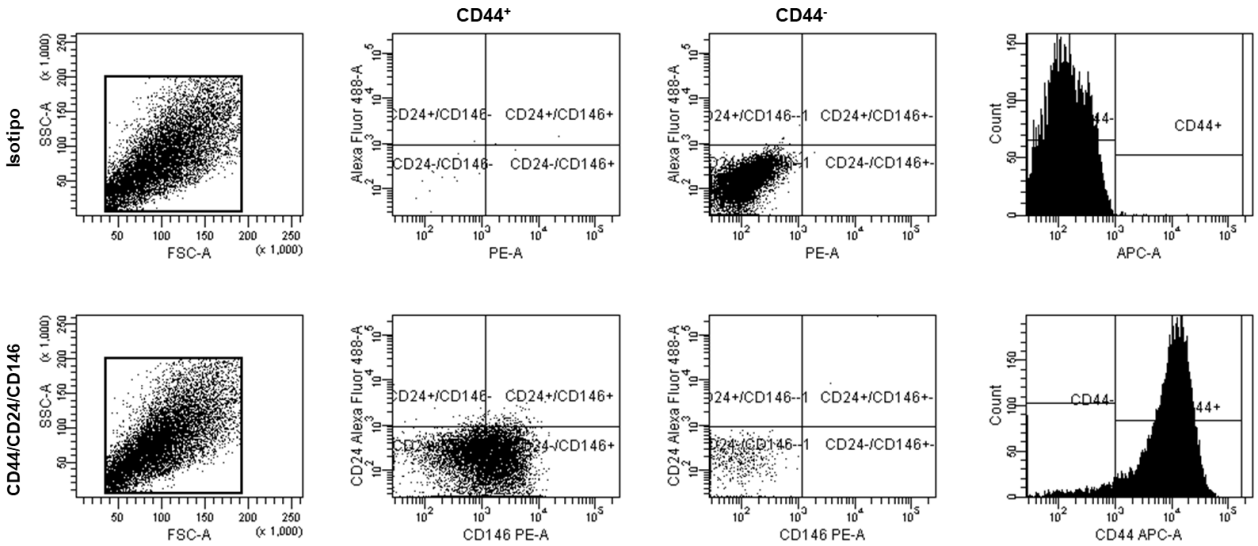

Figura 3 - Gráficos de *dot plot* e histograma representativo para a Hs 578T.

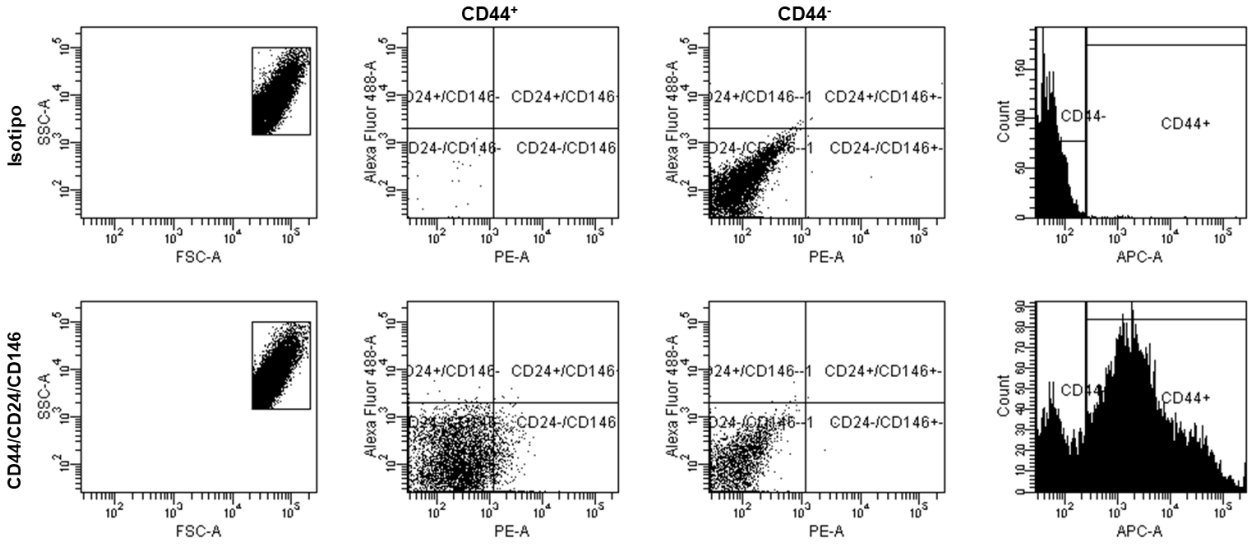

Figura 4 - Gráficos de *dot plot* e histograma representativo para a Hs 578T TS.

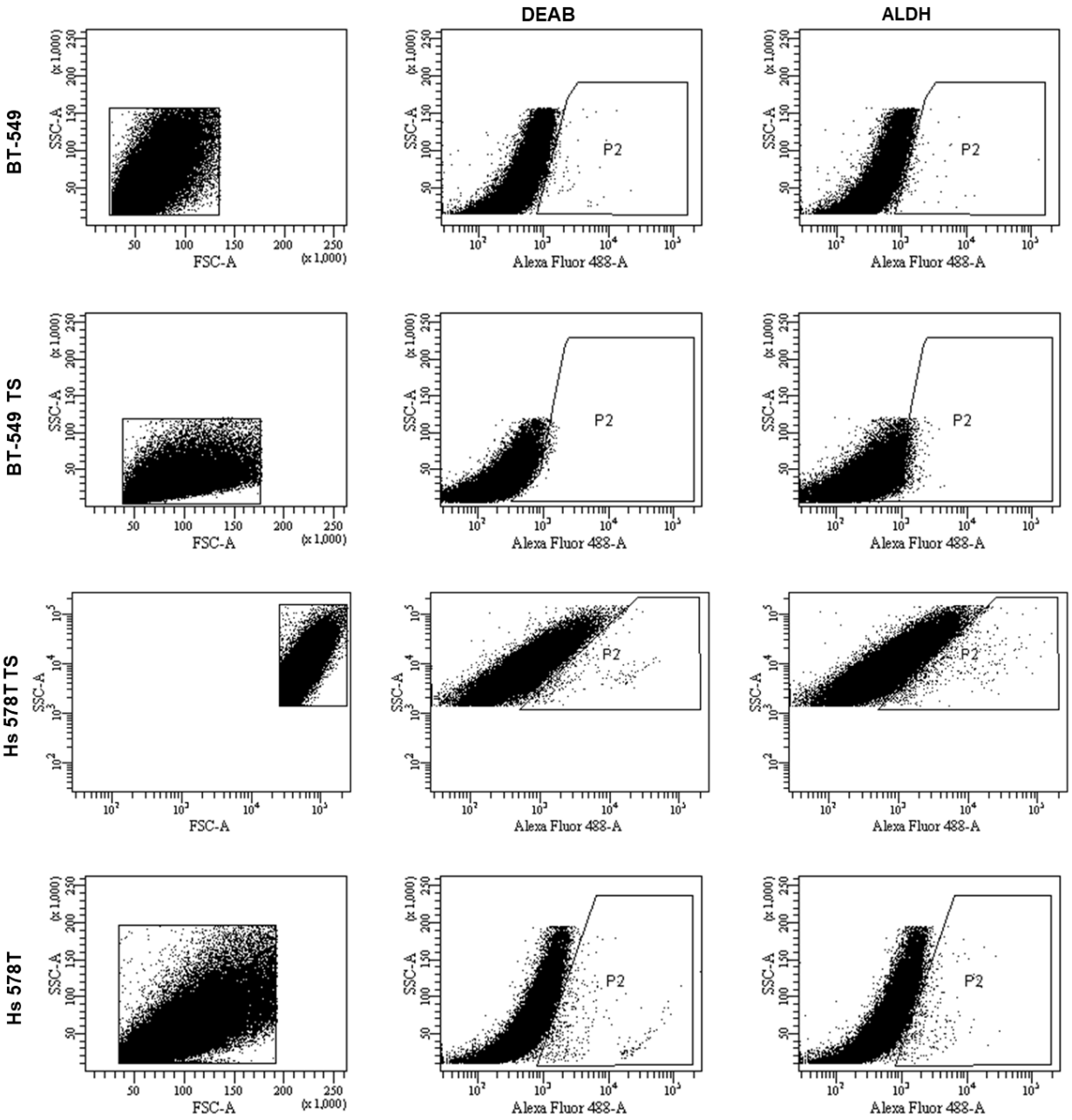

Figura 5 - Gráficos de *dot plot* representativo da população $ALDH^+$ para a BT-549, BT-549 TS, Hs 578T TS e Hs 578T. Observa-se: *dot plot* FSC x SSC (1° coluna); controle DEAB (2° coluna); marcação com ALDH (3° coluna).